

Journal Pre-proof

Epochs, events and episodes: Marking the geological impact of humans

Colin N. Waters, Mark Williams, Jan Zalasiewicz, Simon D. Turner, Anthony D. Barnosky, Martin J. Head, Scott L. Wing, Michael Wagreich, Will Steffen, Colin P. Summerhayes, Andrew B. Cundy, Jens Zinke, Barbara Fiałkiewicz-Kozieł, Reinhold Leinfelder, Peter K. Haff, J.R. McNeill, Neil L. Rose, Irka Hajdas, Francine M.G. McCarthy, Alejandro Cearreta, Agnieszka Gałuszka, Jaia Syvitski, Yongming Han, Zhisheng An, Ian J. Fairchild, Juliana A. Ivar do Sul, Catherine Jeandel



PII: S0012-8252(22)00255-0

DOI: <https://doi.org/10.1016/j.earscirev.2022.104171>

Reference: EARTH 104171

To appear in: *Earth-Science Reviews*

Received date: 8 June 2022

Revised date: 20 August 2022

Accepted date: 30 August 2022

Please cite this article as: C.N. Waters, M. Williams, J. Zalasiewicz, et al., Epochs, events and episodes: Marking the geological impact of humans, *Earth-Science Reviews* (2022), <https://doi.org/10.1016/j.earscirev.2022.104171>

This is a PDF file of an article that has undergone enhancements after acceptance, such as the addition of a cover page and metadata, and formatting for readability, but it is not yet the definitive version of record. This version will undergo additional copyediting, typesetting and review before it is published in its final form, but we are providing this version to give early visibility of the article. Please note that, during the production process, errors may be discovered which could affect the content, and all legal disclaimers that apply to the journal pertain.

Epochs, events and episodes: marking the geological impact of humans

Colin N. Waters^a, Mark Williams^a, Jan Zalasiewicz^a, Simon D. Turner^b, Anthony D. Barnosky^c, Martin. J. Head^d, Scott L. Wing^e, Michael Wagreich^f, Will Steffen^g, Colin P. Summerhayes^h, Andrew B. Cundyⁱ, Jens Zinke^a, Barbara Fiałkiewicz-Kozieł^j, Reinhold Leinfelder^k, Peter K. Haff^l, J.R. McNeill^m, Neil L. Rose^b, Irka Hajdasⁿ, Francine M.G. McCarthy^d, Alejandro Cearreta^o, Agnieszka Gałuszka^p, Jaia Syvitski^q, Yongming Han^r, Zhisheng An^r, Ian J. Fairchild^s, Juliana A. Ivar do Sul^t, and Catherine Jeandel^u.

^aSchool of Geography, Geology and the Environment, University of Leicester, University Road, Leicester LE1 7RH, UK

^bEnvironmental Change Research Centre, Department of Geography, University College London, Gower Street, London WC1E 6BT, UK

^cJasper Ridge Biological Preserve and Department of Biology, Stanford University, Stanford, CA 94305, USA

^dDepartment of Earth Sciences, Brock University, 1812 Sir Isaac Brock Way, St. Catharines, Ontario L2S 3A1, Canada

^e Department of Paleobiology, Smithsonian Museum of Natural History, 10th Street and Constitution Avenue, NW, Washington, DC 20560, USA

^fDepartment of Geology, University of Vienna, A-1090 Vienna, Austria

^gFenner School of Environment and Society, Australian National University, Canberra, ACT 0200, Australia

^hScott Polar Research Institute, Cambridge University, Lensfield Road, Cambridge CB2 1ER, UK

ⁱSchool of Ocean and Earth Science, University of Southampton, National Oceanography Centre, Southampton, UK

^jBiogeochemistry Research Unit, Institute of Geoecology and Geoinformation, Adam Mickiewicz University, Krygowskiego 10. Poznań, Poland

^kDepartment of Geological Sciences, Freie Universität Berlin, Malteserstr. 74-100/D, 12249 Berlin, Germany

^lNicholas School of the Environment, Duke University, 9 Circuit Drive, Box 90238, Durham, NC 27708, USA

^mGeorgetown University, Washington DC, USA

ⁿLaboratory of Ion Beam Physics, ETH Otto-Stern-Weg 5, 8093 Zurich, Switzerland

^oDepartamento de Geología, Facultad de Ciencia y Tecnología, Universidad del País Vasco UPV/EHU, Apartado 644, 48080 Bilbao, Spain

^pGeochemistry and the Environment Division, Institute of Chemistry, Jan Kochanowski University, 7 Uniwersytecka St, 25-406 Kielce, Poland

^qINSTAAR and CSDMS, University of Colorado, Boulder, CO, USA.

^rState Key Laboratory of Loess and Quaternary Geology, Institute of Earth Environment, Chinese Academy of Sciences, Xi'an 710061, China

^sSchool of Geography, Earth and Environmental Sciences, University of Birmingham, Birmingham B15 2TT, UK

^tLeibniz Institute for Baltic Sea Research Warnemünde (IOW), Rostock, Germany

^uLEGOS, Université de Toulouse, CNES, CNRS, IRD, UPS, 14 avenue Édouard Belin, 31400 Toulouse, France

*** Corresponding author.**

E-mail address: cw398@leicester.ac.uk (C.N. Waters).

Journal Pre-proof

Abstract

Event stratigraphy is used to help characterise the Anthropocene as a chronostratigraphic concept, based on analogous deep-time events, for which we provide a novel categorization. Events in stratigraphy are distinct from extensive, time-transgressive 'episodes' – such as the global, highly diachronous record of anthropogenic change, termed here an Anthropogenic Modification Episode (AME). Nested within the AME are many geologically correlatable events, the most notable being those of the Great Acceleration Event Array (GAEA). This isochronous array of anthropogenic signals represents brief, unique events evident in geological deposits, e.g.: onset of the radionuclide 'bomb-spike'; appearance of novel organic chemicals and fuel ash particles; marked changes in patterns of sedimentary deposition, heavy metal contents and carbon/nitrogen isotopic ratios; and ecosystem changes leaving a global fossil record; all around the mid-20th century. The GAEA reflects a fundamental transition of the Earth System to a new state in which many parameters now lie beyond the range of Holocene variability. Globally near-instantaneous events can provide robust primary guides for chronostratigraphic boundaries. Given the intensity, magnitude, planetary significance and global isochroneity of the GAEA, it provides a suitable level for recognition of the base of the Anthropocene as a series/epoch.

Keywords: Anthropocene, Anthropogenic Modification Episode, chronostratigraphy, Great Acceleration Event Array

1. Introduction

Following extensive conceptual analysis since its inauguration in 2009, the Anthropocene Working Group (AWG) of the Subcommission on Quaternary Stratigraphy (SQS), itself a constituent body of the International Commission on Stratigraphy (ICS), held a binding supermajority vote in 2019. This recommended (AWG, 2019): (1) defining the Anthropocene as an official unit within the International Chronostratigraphic Chart (ICC; Cohen et al., 2013), which serves as the basis for the international Geological Time Scale (GTS), and (2) that the primary guide for the base should be one of the stratigraphic signals around the mid-20th century (Zalasiewicz et al., 2017, 2020). Active research now proceeds on 12 reference sections, many of which are likely to be proposed as potential Global boundary Stratotype Sections and Points (GSSPs) and auxiliary sections (Waters et al., 2018; Head et al., 2021). An intrinsic feature of all Phanerozoic units in the GTS is that they are defined at their base by a GSSP that fixes a physical isochronous level for global correlation. The age assigned to any GSSP is subject to revision and refinement or fixed by agreement (Head, 2019), but its stratigraphic position is not subject to revision.

Gibbard et al. (2021, 2022) proposed that the Anthropocene be considered an informal ‘geological event’ rather than a formally defined chronostratigraphic unit within the GTS, claiming that formal definition would limit its utility across disciplines. This proposed ‘geological event’, primarily an interdisciplinary concept (Head et al., 2022a), describes a time-transgressive (diachronous) interval encompassing tens of thousands of years of progressive human cultural and societal development and impact. It contrasts starkly with the proposed formal definition of the Anthropocene marked by an isochronous array of global events that record a fundamental transition of the Earth System to a new state in which many parameters lie outside the range of Holocene variability.

But these are not mutually exclusive alternatives; rather they represent very different and potentially complementary concepts (Head et al., 2022a, in press). Formal chronostratigraphy combined with informal event stratigraphy have been used to study many intervals of Earth history. The case for a chronostratigraphic Anthropocene at the rank of series/epoch with a base defined by mid-20th century sedimentary and biological markers has already been extensively detailed (Head et al., 2021; Syvitski et al., 2020, 2022; Waters et al., 2016, 2018; Williams et al., 2022; Zalasiewicz et al., 2017, 2019a, 2020). These demonstrate overwhelming evidence for a human-generated geological epoch, an issue not the focus of this paper.

We examine here how event stratigraphy, as conventionally understood in the geological record, might help analyse changes occurring at the beginning of an Anthropocene epoch while also recognizing the gradual build-up of anthropogenic modifications to the planet that unfolded during the Pleistocene and Holocene. We examine the deep-time examples used by Gibbard et al. (2021), and also other types of phenomena. We show that what are referred to as geological ‘events’ in the literature are highly variable and often diverge from the original ‘event’ concept and from stratigraphic guidelines. We clarify this broad spectrum of ‘event’ interpretations and show how a highly resolved event concept can support, rather than oppose, a proposed Holocene–Anthropocene chronostratigraphic boundary through what we term the Great Acceleration Event Array (GAEA). In this context, we show how an extended diachronous ‘event’ *sensu* Gibbard et al. (2021, 2022), most closely corresponding to a multi-factor and multi-scalar ‘Anthropogenic Modification Episode’ (AME), relates to the recognition of an Anthropocene epoch in the geological record with an effectively traceable isochronous boundary.

2. The definition of event stratigraphy

An 'event' in geology "*expresses a happening, not an interval, either of time or of rock strata*" (Salvador, 1994, p. 73). It has no formal stratigraphic status and is not one of the hierarchical ranks of units within the ICC, which forms the basis of the GTS. Unlike formal chronostratigraphic units, which are defined at their base by a GSSP or 'golden spike', events do not have formally fixed boundaries. However, their stratigraphic expressions are typically clear enough for use in local, regional or global correlation and in general communication. Salvador (1994, p. 79) stated that "*major events...may constitute desirable points for the boundary-stratotypes of stages*", and this is of relevance to many of the examples outlined below. Events are intrinsic features of the entire geological column and are the phases of sudden change that stand out from intervals of continuity and stability; they have driven the formulation of stratigraphy from the early days of the discipline.

Ager (1973, p. 63) introduced event stratigraphy as the method "*...in which we correlate not the rocks themselves, on their intrinsic petrological characters, nor the fossils, but the events such as the Triassic transgressions...*". Salvador (1994, p. 117) reiterated this definition and noted that numerous subsequent authors have defined 'events' as used in event stratigraphy as "*...short-term phenomena – explosive volcanism, rapid tectonic movements, abrupt changes of sea level, climatic cycles, storms, distinctive sedimentologic and biologic events, and even extraterrestrial or other 'rare events' at any scale*". Event stratigraphy then refers to the stratigraphical traces left behind, which are typically brief and not significantly diachronous and can be depositional, erosional or geochemical (Rawson et al., 2002). Indeed, Ager (1973) specifically valued events because they may produce isochronous signals that transect diachronous facies boundaries (Wood et al., 2022a, in press). Events may be commonly recognised by more descriptive names, such as an 'excursion', 'crisis', 'termination' or 'reversal', but are included in this appraisal as they are consistent with the widely understood definition of an event.

Events can also range in scale from the local, such as storm events producing tempestites, to regional, such as large volcanic eruptions or glacial/interglacial transitions, to global, such as oceanic anoxic events or major bolide impacts (Fig. 1). Events also range from triggering local or regional environmental perturbations, to causing global-scale realignment of components of the Earth System. By definition, the word 'event' is singular, referring to something unusual, or of some importance (Collins English Dictionary, Merriam-Webster Dictionary, Oxford English Dictionary). However, this term has also been extended to processes that are prolonged and multi-factorial. Some of these quoted 'events' represent significant spans of time and strata, and so are better considered as 'episodes' (Fig. 1). The North American Stratigraphic Code defines 'Episode' as: "*...the unit of highest rank and greatest scope in hierarchical classification*" of diachronic units (reiterated by Salvador 1994, p. 117), and providing "*...a means of comparing the spans of time represented by stratigraphic units with diachronous boundaries at different localities...*" (NACSN, 2005, p. 1584).

An 'event' then represents a happening in time, and its stratigraphic expression forms the basis of event stratigraphy. Events have been used variably to label phenomena that unfold as a continuum in the geological record over many different time scales. We arrange them into three types (Fig. 1): Types 1 and 2 being considered 'events', and Type 3 as 'episodes':

- Type 1 phenomena are global and have onsets and/or terminations associated with rapid rates of process change over brief time intervals (effectively days to thousands of years). They represent a change of state in one or more subsystems of the Earth System to something outside the previous norm, a change with consequences that may be prolonged or essentially permanent.

- Type 2 phenomena are of brief duration (days to thousands of years), may range from local to global and do not change the functioning of the Earth System (or any of its subsystems) outside the previous bounds of variability.
- Type 3 phenomena are long-lived (tens of thousands to millions of years), global and broadly are markedly time-transgressive with slow rates of process change. These are more suitably termed ‘episodes’. However, such episodes commonly have nested within them one or more Type 1 or 2 events, which can occur internally or mark the start or end of the episode.

Table 1 gives examples (selectively described below) of important and commonly recognized ‘events’ and ‘episodes’ in the geological column. Note that most events in the geological column do not guide or define chronostratigraphic boundaries, but some examples that do are provided in this table.

3. ‘Events’ and ‘Episodes’ in the geological record and their relation to chronostratigraphy

We describe examples of event stratigraphy here categorized as Type 1 and 2 events; the former involving Earth System modifications, and the latter not. This is followed by a description of episodes, as Type 3 phenomena. The ‘events’ exemplified by Gibbard et al. (2021) — the Great Oxidation Event, the Great Ordovician Biodiversification Event, an unnamed ‘event’ of continental invasion by land plants during the Devonian, and the Quaternary ‘Anthropocene Event’ — fall outside the norms of event stratigraphy, being gradual or al and geologically protracted, with multiple causes and effects that vary widely across time and space (Table 1). They represent major, state-shifting transformations of the Earth System, here categorized as Type 3a episodes. Episodes that do not change the state of the Earth System as a whole are categorized here as Type 3b episodes.

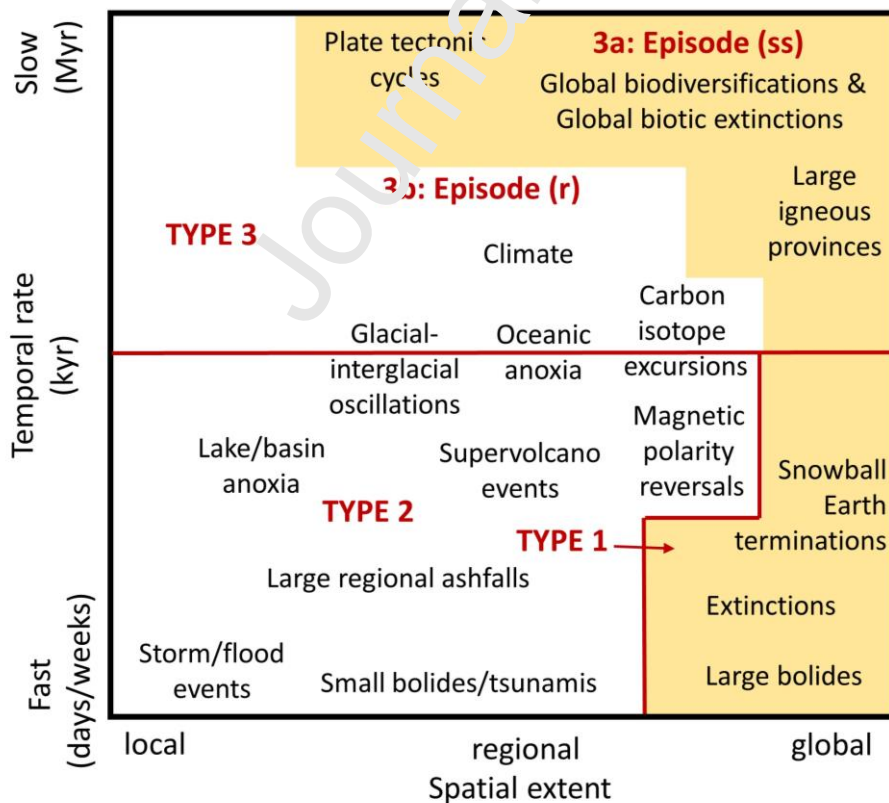


Fig. 1. Comparison of approximate spatial and temporal ranges of event (Types 1 and 2) and episode (Type 3) processes, outlined in this study. Boxes in yellow denote permanent Earth System shifts, with episodes distinguished as state-shifting (ss) or reversible (r).

Journal Pre-proof

Table 1. Examples of phenomena that illustrate distinctions between type 1 and type 2 (events) and type 3 (episodes). CIE – carbon isotope excursion.

| Selected event/episode arranged chronologically from oldest to youngest | Suggested or known causal mechanism(s) | Major geological expressions | Geological Time | Onset or geological time range | Duration | Coincident with chronostratigraphic boundary | Type | Useful references |
|---|--|------------------------------|----------------------------|--------------------------------|-----------------------|--|------|---|
| Archean – Proterozoic | | | | | | | | |
| Origin of life | Biological Oxygenic photosynthesis | Biotic Lithological/Mineral | Hadean Proterozoic | ~4.1–3.6 Ga | unknown | No | 3a | Catling and Zahnle (2020) |
| Great Oxidation/Oxygenation | | | Proterozoic | ~2.4–2.07 Ga | 100s Myr | No* ¹ | 3a | Poulton et al. (2021) |
| Lomagundi CIE | Oceanographic Tectonic/Environmental | Isotopic Lithological | Proterozoic Neoproterozoic | ~2.3–2.1 Ga | 200–300 Myr | | 3b | Prave et al. (2022) Hoffman et al. (2017); Zhou et al. (2019) |
| Sturtian panglacial termination | | | Neoproterozoic | ~659 Ma | ?1–10 kyr | Not yet defined | 1 | Hoffman et al. (2017); Zhou et al. (2019) |
| Marinoan panglacial termination | Environmental | Lithological | Neoproterozoic | ~635 Ma | ?1–10 kyr | Yes (basal Ediacaran) | 1 | Hoffman et al. (2017); Zhou et al. (2019) |
| Phanerozoic – lower Paleozoic | | | | | | | | |
| Cambrian Explosion | Biological/Environmental | Biotic/Lithological | Cambrian | ~539–509 Ma | 10s Myr | No | 3a | Servais and Harper (2018) LeRoy et al. (2021); Yang et al. (2021) |
| Drumian CIE (DICE) | Oceanographic | Isotopic Biotic/Isotopic | Cambrian | ~504.5 Ma | >4 Myr | Overlies basal Drumian | 3b | LeRoy et al. (2021) |
| Steptoean Positive CIE (SPICE) | Oceanographic | Isotopic | Cambrian | ~497–451 Ma | ~3 Myr | No | 3b | LeRoy et al. (2021) |
| Great Ordovician Biodiversification | Biological/Environmental | Biotic | Ordovician | ~491–445 Ma | 10s Myr | No | 3a | Servais et al. (2021) |
| Ireviken | } Climate/Oceanographic | Biotic/Isotopic | Silurian | ~433.5–432 Ma | ~1.5 Myr | Straddles basal Sheinwoodian | 3a | Calner (2008); Melchin et al. (2020) |
| Mulde | | | | ~428.5–426.7 Ma | ~1.8 Myr | Underlies basal Gorstian | 3a | |
| Lau | | | | ~423.8–423.3 Ma | ~0.5 Myr | No | 3a | |
| Phanerozoic – upper Paleozoic | | | | | | | | |
| Lower and Upper Kellwasser | Climate/Oceanographic | Biotic/Isotopic | Devonian | ~372.54–371.87±0.108 Ma | 86–96 and 100–130 kyr | Underlies basal Famennian | 3a | Carmichael et al. (2019) |
| Hangenberg | Climate | Biotic/Isotopic | Devonian | ~359 Ma | 100–300 kyr | Underlies and straddles basal Tournaisian | 3a | Becker et al. (2020) |
| End Permian extinction (terrestrial expression) | Volcanic | Biotic/Isotopic | Permian | ~251.9 Ma | ~1 Myr | Yes (basal Induan) | 3a | Viglietti et al. (2021) |
| End Permian extinction (marine expression) | Volcanic | Biotic/Isotopic | Permian | 251.941±0.037–251.880±0.031 Ma | 61±48 kyr | Yes (basal Induan) | 3a | Burgess et al. (2014) |
| Phanerozoic – Mesozoic | | | | | | | | |
| Tempestites in Upper Muschelkalk Limestones | Storm | Lithological | Triassic | ~240 Ma | hours/days | No | 2 | Aigner (1982) |
| End Triassic extinction | Volcanic | Biotic | Triassic | ~201.51–201.36 Ma | >200 kyr | Yes (basal Hettangian) | 3a | Lindström et al. (2017) |
| Multi-phased Pliensbachian-Toarcian extinction | Volcanic | Biotic | Jurassic | ~186–178 Ma | ~8 Myr | No | 3a | Caruthers et al. (2013) |

| | | | | | | | | |
|---|-------------------------|-----------------|------------|------------------------------------|---------------|----------------------------------|----|---|
| OAE1a positive CIE | Volcanic | Isotopic | Cretaceous | ~120.5 Ma | 2.7 Myr | Yes* ² (basal Aptian) | 3b | Beil et al. (2020) |
| OAE2 positive CIE | Volcanic | Isotopic | Cretaceous | ~94.35 Ma | ~790 kyr | Yes (basal Turonian) | 3b | Beil et al. (2020) |
| K-Pg impact/ Chicxulub | Asteroid strike | Lithological | Cretaceous | 66.043±0.043 Ma | hours/days | Yes (basal Danian) | 1 | Molina et al. (2006); Renne et al. (2013) |
| Phanerozoic – Cenozoic | | | | | | | | |
| Paleocene-Eocene Thermal Maximum (PETM) | Climate | Isotopic/biotic | Paleogene | ~56 Ma | ~100–200 kyr | Yes (basal Ypresian) | 3b | Zachos et al. (2008) |
| <i>Azolla</i> Event | Climate | Biotic | Paleogene | ~49.5 Ma | ~800 kyr | No | 3b | Brinkhuis et al. (2006) |
| Eocene-Oligocene transition (EOT) | Climate | Isotopic/biotic | Paleogene | ~34.44 Ma | 790 kyr | Stratigraphically basal Rupelian | 3a | Hutchinson et al. (2021) |
| Early Oligocene glacial maximum | Climate | Isotopic | Paleogene | ~33.65–33.26 Ma | 490 kyr | No | 3a | Hutchinson et al. (2021) |
| Mid-Miocene Climate Optimum (MMCO) | Climate | Isotopic | Neogene | ~17.0–14.7 Ma | ~2.3 Myr | No | 3b | Methner et al. (2020) |
| Mid-Piacenzian Warm Period (mPWP) | Climate | Isotopic | Neogene | ~3.264–3.025 Ma | ~20 kyr | No | 3b | Dowsett et al. (2013) |
| Kamikatsura | Magnetic | Magnetic | Quaternary | 867±2 ka | 100s–1000s yr | No | 2 | Channell et al. (2020) |
| Matuyama–Brunhes directional reversal | Magnetic | Magnetic | Quaternary | 772.9±5.4 ka | up to ~2 kyr | Close (basal Chibanian) | 2 | Head (2021) |
| Heinrich | Oceanographic | Lithological | Quaternary | last ~40 kyr | 100s–1000s yr | No | 2 | Hodell et al. (2008) |
| Late Quaternary Extinction | Human/climate | Biotic | Quaternary | ~50–7 ka | 43 kyr | No | 3a | Barnosky (2008) |
| Vedde Ash | Volcanic | Lithological | Quaternary | 12.171 ka b2k (89 yr uncertainty) | days/weeks | No | 2 | Lowe et al. (1999) |
| Saksunarvatn Ash | Volcanic | Lithological | Quaternary | 10.347 ka b2k (114 yr uncertainty) | days/weeks | No | 2 | Lowe et al. (1999) |
| 8.2 ka climate event | Climate | Isotopic | Quaternary | 8.236 ka b2k | ~400–600 yr | Yes (basal Northgrippian) | 2 | Walker et al. (2018, 2019) |
| Storegga slide | Submarine slide/tsunami | Lithological | Quaternary | ~8100±250 cal yr BP | hours | No* ³ | 2 | Haflidason et al. (2005) |
| 4.2 ka climate event | Climate | Isotopic | Quaternary | 4.250 ka b2k | ~200–300 yr | Yes (basal Meghalayan) | 2 | Walker et al. (2018, 2019) |

Event types related to their spatial impact on the Earth System:

Type 1 Event: more or less globally instantaneous, recognizable in the geological record, and clearly changed the functioning of the Earth System beyond the norm of what came before;

Type 2 Event: more or less instantaneous and recognizable in the geological record, but did not fundamentally change the Earth System;

Type 3 Episodes: global and truly time-transgressive over many tens of thousands to millions of years and state-shifting (3a) or of lower magnitude with the Earth System configuration resilient to change (3b).

*¹ But see Shields et al. (2021) on the position of the potential Skourian Period.

*² Aptian Stage has not been formalised, but maximum negative basal $\delta^{13}\text{C}$ excursion during the precursor phase of OAE1a is the likely primary marker.

*³ Note that the Storegga slide occurs within ~50 years of the 8.2 climate event.

Journal Pre-proof

3.1 Type 1 phenomena: Globally ‘rapid’, Earth System modifying events

Termination of Snowball Earth events (e.g., Sturtian and Marinoan glaciations) of the Neoproterozoic (~659 and ~635 Ma):

The Sturtian and Marinoan panglacials of the Cryogenian – so-called ‘Snowball Earth Events’ – have long durations, 58 Myr for the Sturtian and ≥ 5 Myr for the Marinoan, and hence would be consistent with our definition of Type 3a episodes. However, the termination of both are globally rapid (Hoffman et al., 2017) and these abrupt transitions from glacial diamictite to postglacial cap dolostone, modelled to be as short as 1–10 kyr, are better considered events than the prolonged glaciations themselves. The Cryogenian System is currently defined chronometrically as commencing at 720 Ma, but the aim is to replace this with a GSSP guided by the beginning of the Sturtian glaciation (Halverson et al., 2020). The base of the Ediacaran System is associated with the rapid decay of the Marinoan ice sheets, the event marker being the base of the Marinoan cap carbonate above glaciogenic deposits together with a distinctive carbon isotope signal (Knoll et al., 2006).

Cretaceous–Paleogene (K-Pg) impact event (66 Ma): This demarcates the abrupt transition from terrestrial and marine faunas of the Mesozoic Era to the succeeding ‘modern’ biota of the Cenozoic Era. It marks the fifth, and as yet most recent, global mass extinction event of the Phanerozoic. The K-Pg impact event is uniquely represented by a near-global, near-instantaneous array of event markers and was sufficiently transformative of the Earth System to justify a chronostratigraphical boundary at erathem rank.

Discovery of an iridium anomaly at the extinction level provided strong evidence of a major asteroid impact (Schulte et al., 2010). Detailed palaeontological investigations worldwide at this level, particularly of marine microfossils, indicate abrupt extinction, followed by low-diversity ‘survival’ assemblages. The iridium anomaly is commonly associated with a dark ‘Boundary Clay’ that has a basal millimetric ‘rusty layer’ showing the maximum iridium enrichments; both are interpreted as far-flung impact debris. This unit thickens toward the 200 km-diameter Chicxulub impact crater in Mexico. The timing of the impact is taken to define the age of the Mesozoic–Cenozoic boundary, with all sediments produced by the impact belonging to the base of the Danian Stage (Molina et al., 2006). This applies particularly to sites near the impact crater and even within it (Gulick et al., 2019) where material would have arrived sooner, if only by hours or days, than at the GSSP located in the El Kef section, Tunisia, placed at a level marking the initial arrival of impact debris. The K-Pg boundary impact event triggered an array of subsequent events including a mega-tsunami and palaeo-wildfires in the first hours, global cooling from dust in the first years, pioneer vegetation in the first centuries, a carbon cycle perturbation (see Fig. 8a) and an ocean surface acidification event in the first millennia, and a multi-million year episode of biotic diversification (e.g., Kring, 2007; Renne et al., 2013; Henehan et al., 2019). The initial events produced many correlatable stratigraphic signals of variable duration and isochroneity.

3.2 Type 2 phenomena: ‘rapid’ events with little long-lasting impact on the functioning of the Earth System

Matuyama–Brunhes reversal (772.9 \pm 5.4 ka) and the Kamikatsura excursion (867 \pm 2 ka) of the Quaternary:

Variations in the polarity and intensity of the Earth’s magnetic field enable precise palaeomagnetic correlation. The global reach and near-isochronous nature of magnetic variations are recorded in iron-bearing igneous rocks (e.g., lavas), clastic sedimentary deposits (e.g., hemipelagites and lacustrine mudrocks) and ice cores (using the ^{10}Be proxy), making them potentially important chronostratigraphic markers. Applying the term ‘event’ to *intervals* of normal or reversed polarity was strongly discouraged by Salvador (1994, p. 73). However, the ‘event’ persists in palaeomagnetism literature as an informal term to represent phenomena of short

duration, including polarity reversals and brief changes in the direction of the dipole field (Ogg, 2020). The Matuyama–Brunhes reversal is the most recent geomagnetic reversal and serves as the primary guide to the Lower–Middle Pleistocene Subseries boundary (Head et al., 2008). In the Chiba composite section in Japan, which hosts the Chibanian Stage and Middle Pleistocene Subseries GSSP, it has an astronomically dated directional midpoint at 772.9 ± 5.4 ka, with a duration of up to ~ 2 kyr (Head, 2021; Suganuma et al., 2021). In addition to major reversals, there are many short-lived polarity deviations for which the term *excursion* (~ 2 – 5 kyr duration) is usually used. An example is the Kamikatsura excursion, detected in lava flows in Hawaii and sediment cores from the North Atlantic (Channell et al., 2020) and representing a brief event predating the Matuyama–Brunhes reversal by about 94 kyr. However, such short excursions are not always widely documented and are also prone to being affected by diagenesis.

Late Pleistocene Climatic Events (~ 60 – 11.7 ka): A refined Upper Pleistocene regional climatic event stratigraphy (Fig. 2) is superimposed upon a hemispheric, protracted and diachronous postglacial 3°C warming over $\sim 7,000$ years from the Pleistocene to Holocene (Clark et al., 2016). For the Last Glacial interval (~ 18.0 – 11.5 cal. ka BP), a scheme applicable to the North Atlantic region was developed by Björck et al. (1998) and Walker et al. (1999) based on a $\delta^{18}\text{O}$ record from the GRIP Greenland ice core. These events represent high-amplitude cold (Greenland Stadial, GS) and warmer (Greenland Interstadial, GI) intervals, labelled from the top down as GS-1 (approximately the Younger Dryas cold event), GI-1, GS-2 and GI-2 (Fig. 2), with lower-amplitude sub- (inter)stadials being labelled GI-1a, GS-2b, etc. Based on short-lived events rather than the sharp boundaries separating them (Head, 2019), any diachroneity is considered irrelevant (Björck et al., 1998). The scheme is extended in other Greenland ice cores, providing a numbering scheme from GS-1 to GS-26 ranging from 119,140 to 12,896 years before 2000 CE (b2k) (Rasmussen et al., 2014). Corresponding Dansgaard–Oeschger (D–O) events (Fig. 2), discovered earlier in Greenland ice cores, represent decadal-scale warming events within cycles lasting some 1.5 kyr (Dansgaard et al., 1993). Related to D–O events are Heinrich events (Fig. 2), large-scale dispersals of icebergs in the North Atlantic during the collapse of northern hemisphere ice sheets (Heinrich, 1988), with deposition of extensive ice-rafted debris forming Heinrich layers, each event likely lasting some decades. Warm events in Antarctica, referred to as Antarctic (oxygen) Isotope Maximum (AIM), immediately precede the D–O warm events in Greenland; they are connected through the Atlantic Meridional Overturning Circulation, oscillations which provide a bipolar ‘seesaw’ (Pedersen et al., 2018) linking the two hemispheres mostly between 25 and 50 ka (Fig. 2).

None of these multiple inter-related events defines a chronostratigraphic boundary: they occur within the Late Pleistocene Subseries (and its equivalent, the un-named ‘fourth stage’ of the Pleistocene; Head, 2019). But they are important in providing a highly-resolved correlatory framework within this subseries, most directly applicable to northern hemisphere successions, and correspond to the concept of brief and near-synchronous events (Head et al., 2022b, in press).

Vedde and Saksunarvatn volcanic eruption events of the Quaternary (~ 12.17 and ~ 10.34 ka b2k): These ashes are tephra layers dated in Greenland ice cores at 12,171 years b2k and 10,347 years b2k respectively (Walker et al., 2009). They provide widespread isochronous stratigraphical markers across the North Atlantic region between terrestrial, marine and ice-sheet settings, helping to constrain the timing of Late Pleistocene climatic events (Lowe et al., 1999), and bracket the base of the Holocene Series.

Holocene Climatic Events (8.2 and 4.2 ka): The Holocene Series/Epoch was subdivided using climatic events at 8.2 and 4.2 ka, into the Greenlandian, Northgrippian and Meghalayan stages/ages and corresponding Lower/Early, Middle, Upper/Late subseries/subepochs. The “8.2 ka climatic event”

was a brief (~400–600 year) near-global cooling event probably triggered by a catastrophic release from glacial lakes Agassiz and Ojibway into the North Atlantic that disrupted thermohaline circulation (Walker et al., 2018, 2019). The event facilitated global correlation. The GSSP is placed at 1228.67 m depth in the NGRIP1 Greenland ice core, dated at 8,236 years b2k when abrupt cooling is marked by a conspicuous shift to more negative $\delta^{18}\text{O}$ and δD values and by reduced ice-core annual layer thickness and deuterium excess (Walker et al., 2018, 2019). More precisely, the GSSP is placed at a distinct double peak in acidity, most likely representing an eruption from an Icelandic volcano, which serves as the primary marker for the GSSP (Walker et al., 2018). This marker facilitates precise regional correlation and represents a duration of ~2 or 3 years at most (Vinther et al., 2006). The complex hemispheric “4.2 ka climatic event”, lasting for two or three centuries, links to aridification in many low- and mid-latitude regions associated with profound human cultural and societal changes, but elsewhere was evident as a wetter climate, and in high northern latitudes as cooling and glacier advance (Walker et al., 2018). The complexity of this event is illustrated by its expression in the Mediterranean, where climatic and environmental changes occurred between 4.3 ka and 3.8 ka, typically but not always associated with more arid conditions that are sometimes difficult to recognise (Bini et al., 2019). This ‘event’, at least in the Mediterranean, might also represent several important climatic oscillations rather than a single aridification event (Bini et al., 2019). The GSSP for the Meghalayan Stage/Age is placed within a brief but significant interval of heavier $\delta^{18}\text{O}$ values at the 7.45 mm depth in a Mawmluh Cave (India) speleothem record, with the boundary taken midway between the onset and intensification of the signal (Walker et al., 2018, 2019; Head, 2019). In both cases, abrupt and short-lived climatic events are used as primary global chronostratigraphic markers for the recognition of these stage/age and subseries, epoch boundaries.

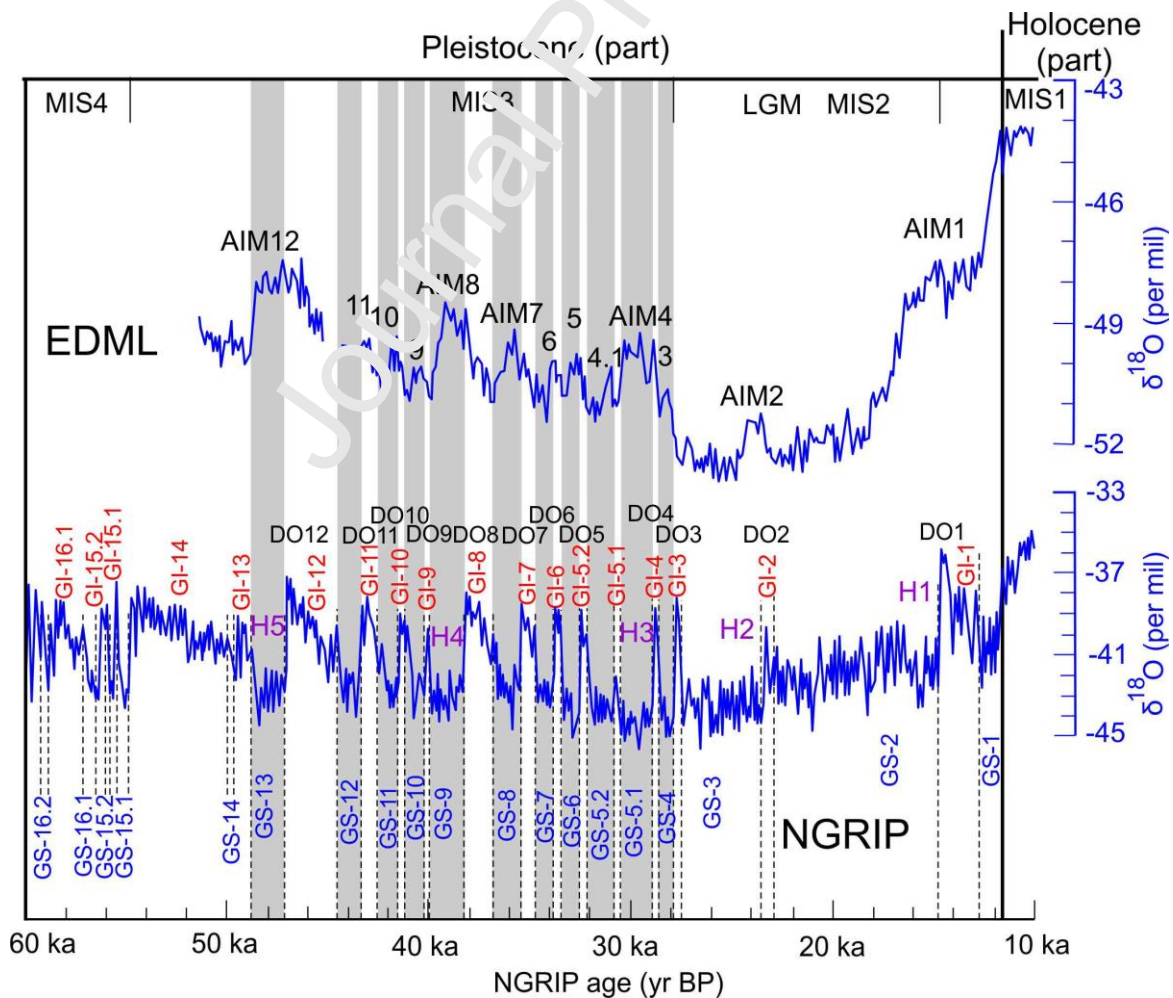


Fig. 2. Warm periods in ice cores from EPICA Dronning Maud Land (EDML) Antarctica correlate with cold periods (stadials) (grey bars) in cores from the North Greenland Ice Coring Project (NGRIP) during the last glaciation. NGRIP numbers represent Greenland Stadials (GS-1 through GS-16.2 shown) and Greenland Interstadials (GI-1 through GI-16.1 shown). Heinrich events, which coincide with cold phases of Dansgaard–Oeschger events (DO1 through DO12 events, are numbered H1 through H5. AIM1 through AIM12 are Antarctic Isotope Maxima, representing warm conditions, phased-shifted from Greenland interstadials by about a millennium. Modified from EPICA Community Members (2006, fig. 2 therein).

Storegga slide event of the Holocene (~8,100 yr BP): This submarine slide of ~2400–3200 km³ of sediments, originated on the continental slope west of southern Norway at ~8,100±250 cal. yr BP (Haflidason et al., 2005). It led to major tsunami and flood deposits that extended across the coastlines of the NE Atlantic including the North Sea. This event occurs within the range of the 8.2 ka climatic event, possibly coincidentally, with glacier advance onto the shelf-break causing rapid loading of hemipelagites and oozes, the main slide being triggered by an earthquake (Bryn et al., 2003). The Storegga slide and associated tsunami deposits are not considered a guide for the base of the Northgrippian Stage, though they help determine its level in NE Atlantic coastal successions.

3.3 Type 3a phenomena: ‘Episodes’ that permanently modify the Earth System

Great Oxidation ‘Episode’ (GOE) of the Proterozoic (~2.4–2.0 Ga): The GOE represents the transformational early introduction of free oxygen into the atmosphere, a response to the evolution of oxygenic photosynthesis. It has recently been placed outside of the standard ‘event’ nomenclature, redefined as the Great Oxidation Episode (Poulton et al., 2021; Shields et al., 2021). This reflects its complex, transitional character over ~300 Myr (Fig. 3), in which detectable atmospheric free oxygen, as shown by proxies such as the mass-independent fractionation of multiple sulfur isotopes, appeared and disappeared repeatedly after its inception at ~2.4 Ga, before finally becoming permanently established at ~2.22 Ga (Poulton et al., 2021). The stratigraphy within the GOE also reveals four glacial *episodes*: the oldest three Huronian glaciations are global, whereas the youngest has only been recorded in South Africa (Poulton et al., 2021; Bekker, 2022). A positive carbon isotope excursion (pCIE) known as the Lomagundi-Jatuli ‘Event’, often considered the largest and longest pCIE in Earth history, has been reinterpreted as facies-controlled and regional (Prave et al., 2022) and hence is interpreted here as a Type 3b episode nested within the GOE.

This re-conceptualized ‘Episode’, like its earlier ‘Event’ incarnations, is informal and independent of formal chronostratigraphy, which in the Precambrian is still largely founded upon Global Standard Stratigraphic Ages (GSSAs). Nevertheless, briefer episodes which closely coincide in time around 2.45 Ga are being explored as stratigraphic markers for a potential GSSP-based Precambrian chronostratigraphy: as a basis for a potential ‘Oxygenian Period’ mooted in Van Kranendonk et al. (2012), and the alternative ‘Skourian Period’ suggested by Shields et al. (2021). These include: the disappearance of large-scale Banded Iron Formation strata from the marine record; the disappearance of oxidizable detrital mineral grains such as pyrite and uraninite from terrestrial sediments; and the first of the global glaciations putatively resulting from oxidative loss of the greenhouse gas methane (Shields et al., 2021; see also Van Kranendonk et al., 2012). Hence, the GOE as an ‘Episode’ includes numerous distinct briefer episodes which bracket and may come to help formally define the chronostratigraphic boundary between the Archean and Proterozoic eons.

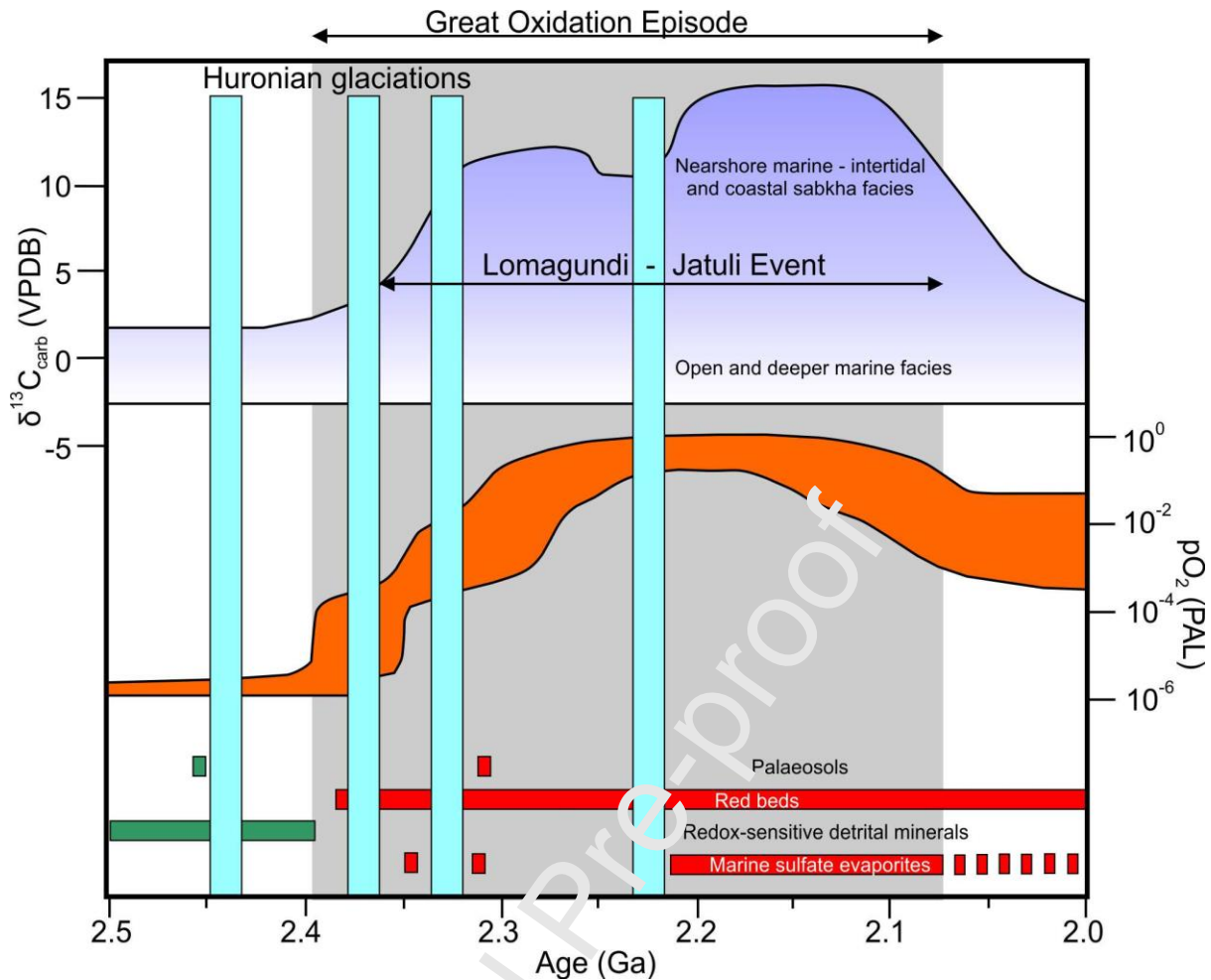


Fig. 3. Characterization of the Great Oxidation Episode through a postulated rise in atmospheric pO_2 (PAL: present atmospheric level) and carbonate C isotope ($\delta^{13}C$) trends for the Lomagundi-Jatuli 'Event' (from Prave et al., 2022, fig. 3 therein). Blue vertical bars represent the four glacial episodes. Geological indicators for the redox state of the atmosphere–ocean system are shown: green is broadly reducing ($> \sim 2.4$ Ga) and red is oxidizing (from Poulton et al., 2021, fig. 4 therein).

Great Ordovician Biodiversification 'Episode' (GOBE) (~495–445 Ma): The GOBE, first published as an event by Webby et al. (2004), encompasses at least 30 Myr with a diachronous onset (Fig. 4). However, as Servais and Harper (2018) noted, the concept behind this term is increasingly misunderstood and Servais et al. (2021) questioned whether the GOBE should be considered an event, calling this label a 'simplification'.

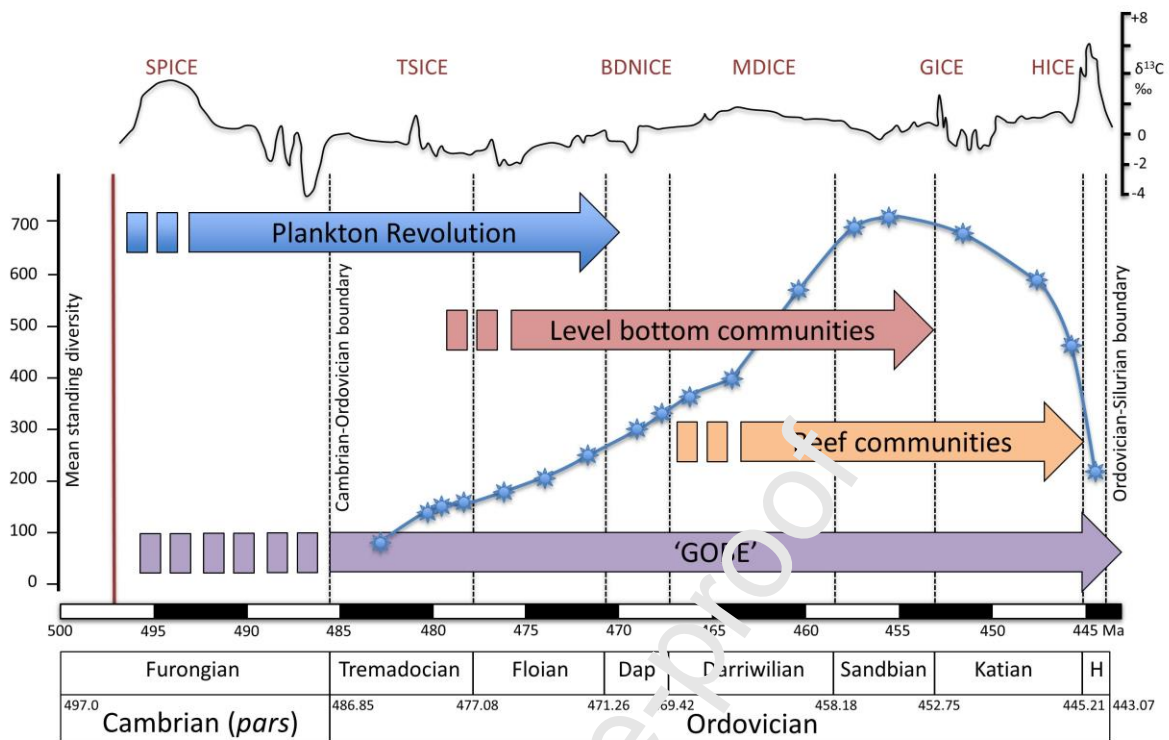


Fig. 4. The Great Ordovician Biodiversification Episode shown by a genus-level diversity trend with three distinct phases of evolutionary diversification and the position of key carbon isotopic excursions (CIEs); Steptoean Positive (SPICE), Tremadocian (TSICE), Basal Dapingian Negative (BDNICE), Middle Darriwilian (MDICE), Guttenberg (GICE) and Hirnantian (HICE) carbon isotope excursions (CIEs). Dap–Dapingian; H–Hirnantian. Modified from Servais and Harper (2018, fig. 2 therein). The carbon isotope record ($\delta^{13}\text{C}$) from marine carbonates is composited from curves in Goldman et al. (2020) and Peng et al. (2020).

The GOBE should be considered an extended episode, comprising a complex series of nested biotic episodes of varying magnitudes and temporal and spatial scales. The GOBE comprises successive phases of diversification, including those of marine plankton in the late Cambrian–Early Ordovician, of level-bottom biotas during the Early–Middle Ordovician, and of reef communities during the Middle–Late Ordovician (Fig. 4; Servais and Harper, 2018); each might be considered a diachronous ‘episode’ in its own right. Several Biotic Immigration Events (BIMEs), including the ‘Richmondian Invasion’ and ‘Boda Event’ both of late Katian age (Fig. 4), record large-scale dispersals of taxa between biogeographical areas (Servais and Harper, 2018). These BIMEs are short-lived palaeoceanographic phenomena, although spatially restricted and diachronous, and probably still better termed episodes. Superimposed upon the biodiversification episodes are global carbon isotopic excursions (CIEs), including the Steptoean pCIE (SPICE) (of the late Cambrian), and the Tremadocian CIE (TSICE), Guttenberg CIE (GICE) and Hirnantian CIE (HICE) of the Ordovician, which are more isochronous (Fig. 4, Table 1); the last of these is linked to two extinction pulses (Harper et al., 2014), each pulse effectively representing a Type 1 event. These CIEs can have durations exceeding a million years, more suitably considered episodes, but typically with abrupt onsets more characteristic of events. Although not primary markers, abrupt onsets of CIEs can help characterise

and correlate the chronostratigraphic divisions of the Ordovician, which are formally defined by the appearance of selected marker taxa at the GSSP levels. For instance, the GICE is used as a proxy for the Sandbian–Katian boundary and the onset of the HICE broadly coincides with the Katian–Hirnantian boundary (Fig. 4), each defined by first appearance datums (FADs) of graptolite species (Goldman et al., 2020).

‘Devonian’ Land Plant Radiation (~458–340 Ma): This Devonian ‘invasion’ of terrestrial plants, which to our knowledge had neither been named nor recognized as an event prior to Gibbard et al. (2021), began in the Early Ordovician with the appearance of desiccation-resistant cryptospores (Fig. 5), probably produced by charophyte ancestors of land plants (Strother and Foster, 2021). It continued with the increased abundance of land plant cryptospores in the Middle Ordovician, the first fossil sporangia of land plants (embryophytes) in the Late Ordovician, the earliest land plant macrofossils in the mid-Silurian, the earliest vascular plant macrofossils in the late Silurian (e.g., Wellman, 2010) and the continued development of larger, more complex, and deeper-rooted vascular plants in the Devonian (Pawlik et al., 2020). This came with attendant effects on rivers, landscapes, terrestrial ecosystems, and climate via sequestration of CO₂ from the atmosphere by increasing biomass and silicate weathering (e.g., Davies and Gibling, 2010; Edwards et al., 2015). This Paleozoic (not just Devonian) development of terrestrial ecosystems was a complex and prolonged process for which the term ‘event’ is surely a misnomer.

Superimposed on the protracted interval of land plant colonization are many widespread, briefer markers in marine successions (Fig. 5). These include the Late Ordovician extinction crises and associated carbon isotope excursions (CIEs), including the Hirnantian CIE (HICE), the Silurian Ireviken, Mulde and Lau extinction events, the Devonian Upper Kellwasser (Frasnian–Famennian) and Hangenberg (end-Famennian) extinction events, and the mid-Tournaisian CIE (TICE) (Table 1), in part consequent on land plant colonization phases (Dühl and Arens, 2020). Like the HICE, the Ireviken, Mulde and Lau are complex *episodes*. The latter comprises asynchronous Lau conodont and Kozlowskii graptolite events, parts of a stepwise marine extinction *episode* over some 0.5 Myr that also affected acritarchs, fish and brachiopods. The Lau-Kozlowskii extinctions are associated with progressive expansion of anoxia, part of which preceded the pCIE (Bowman et al., 2019), and the overall extinction is followed by survival and recovery phases. The short-term onsets of such extinctions, embedded within longer duration episodes, are clearly resolved and of high stratigraphic significance. The termination of the Upper Kellwasser Event coincides with the Frasnian–Famennian boundary (Upper Devonian), and is defined biostratigraphically (Becker et al., 2020). Similarly, global reappraisal of the Devonian–Carboniferous boundary recommends focus on the dramatic changes at the Hangenberg Extinction Event, which would require lowering the level of the existing chronostratigraphic boundary (Aretz and Corradini, 2021).

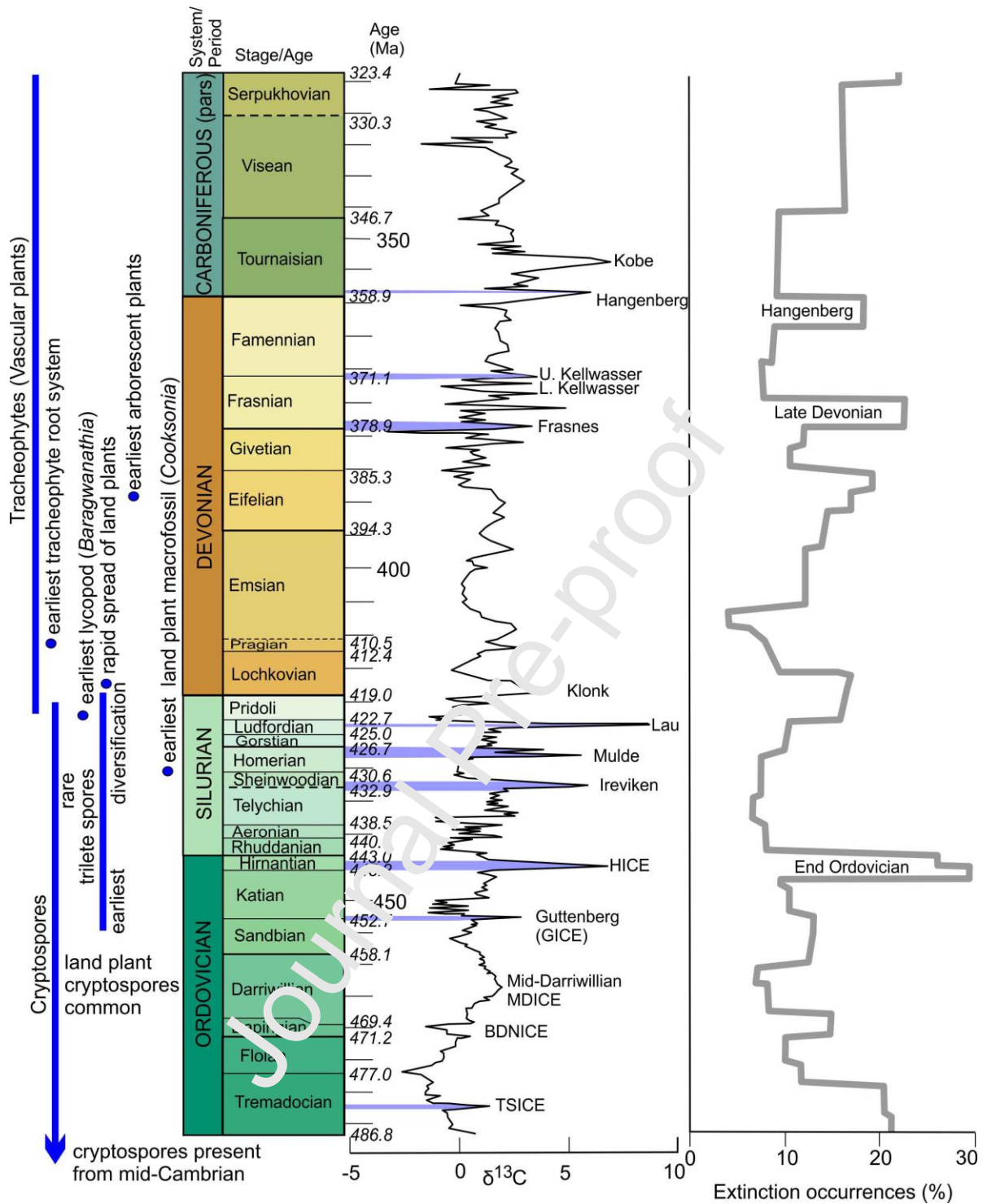


Fig. 5. The carbon isotope record ($\delta^{13}\text{C}$) from marine carbonates, with positive $\delta^{13}\text{C}$ excursions likely reflecting abrupt changes driven by plant evolution (composed from curves in Cramer and Jarvis, 2020). Details of the diversification of land plants are from Davies and Gibling (2010), Edwards et al. (2015) and Strother and Foster (2021). Apparent percentage of marine animal genera becoming extinct during any given time interval (derived from Rohde and Muller, 2005). The extinction curve is approximated against the higher resolution isotopic curve. For CIE abbreviations see Fig. 4.

Late Quaternary Extinction ‘Episode’ (LQE) (~50–7 ka): This, seemingly a component of the ‘Anthropocene Event’ of Gibbard et al. (2021), commonly referred to as an event but most closely resembles an ‘episode’. It has a highly diachronous onset and eventually comprised the demise of

about half of the world's terrestrial megafauna species, most of them mammals (extinction rates of which are shown in Fig. 6b). Globally it began with accelerated regional extinction of species about 50,000 years ago in Australia, then progressed across the planet diachronously and mostly following the arrival of modern humans in a given area (Koch and Barnosky, 2006; Sandom et al., 2014; Fig. 6). The LQE megafaunal extinctions culminated between ~20,000 and 7,000 years ago in Eurasia and the Americas (Brook and Barnosky, 2012), although mammoths lingered on Wrangel Island (Russia) until ~3700 ka. Species extinction rates then dropped, then rose slowly for a few thousand years before they began to rise as humans colonized islands. By 1500 CE, intensified human pressures dramatically accelerated species extinctions (Fig. 6b) — this time including smaller-bodied species — to levels far exceeding those of the Late Pleistocene and Early Holocene (Ceballos et al., 2015; Pimm et al., 2014; Barnosky et al., 2011). Species extinction rates have continued to accelerate from 1900 CE to the present. Even more telling is loss of populations within species: since 1970 CE, 68% of the world's wildlife has been lost (e.g., loss of populations and reduction in population density), which if unchecked presages a significant pulse of species extinctions yet to come (Ceballos et al., 2020; WWF, 2020). The lasting change in the biosphere was the replacement of many wild megafauna species with human bodies and domestic livestock (Barnosky, 2008; Smith, 2011).

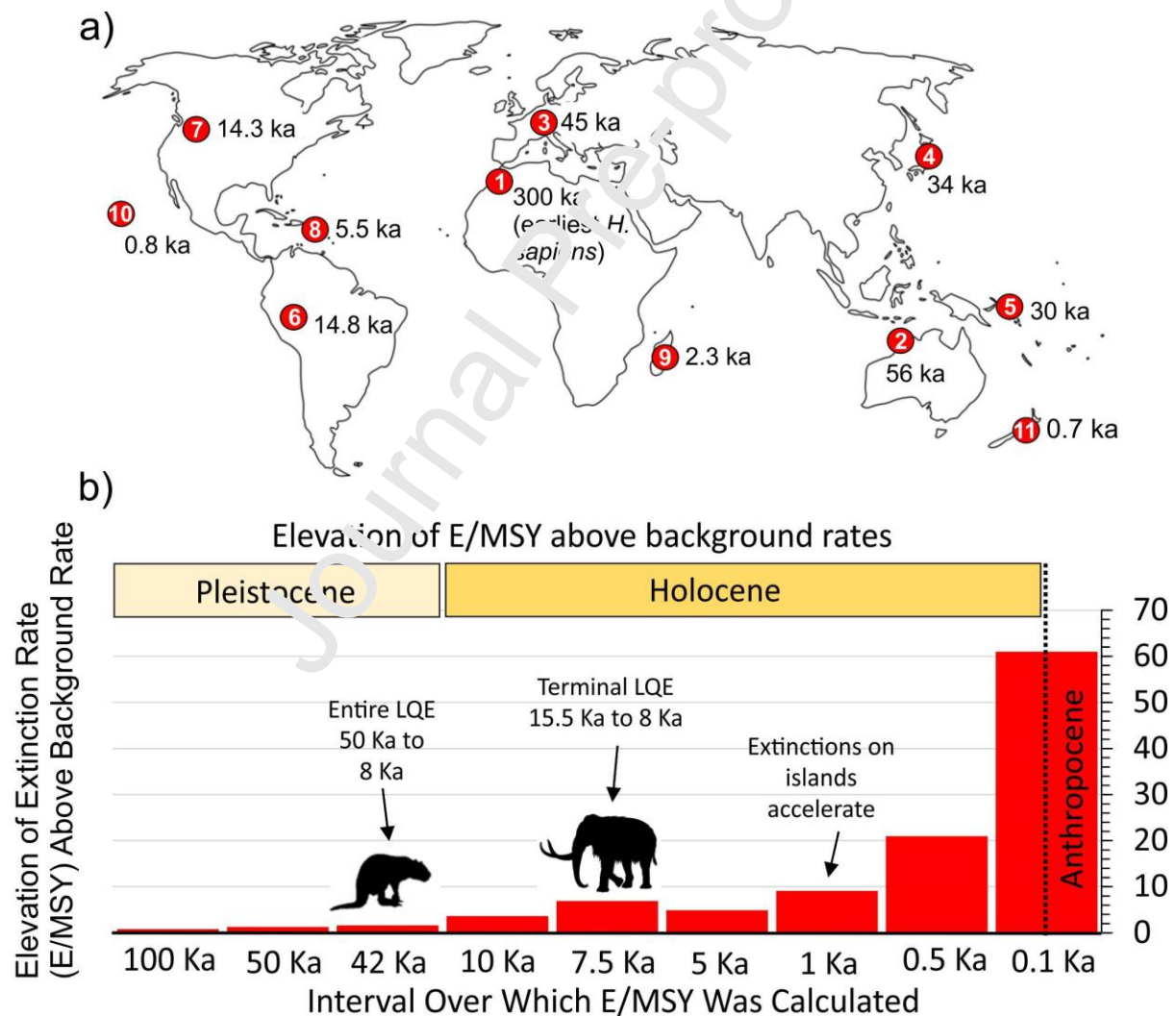


Fig. 6. a) Map indicating the timing of the first documented arrival of *Homo sapiens*, contributing to the diachronous onset of extinction pulses for the LQE; b) The rise in mammal extinction rates since 100 ka. The bars at each labelled time interval indicate the amount the extinction rate was elevated above the average background extinction rate calculated for the time interval. Except for the two

LQE bars indicated by extinct-animal icons, the intervals begin at ~2014 CE and reach back the number of years indicated on the scale. For the LQE rates marked by the animal icons, the 42 ka interval encompasses the entire LQE episode from 50 ka to 8 ka. The 7.5 ka interval encompasses the terminal LQE pulse fuelled mostly (but not entirely) by extinctions in the Americas between ~15.5 to 8 ka. The average background rate was computed for each individual time span, to account for the observation that shorter time spans are likely to show higher average extinctions per million species/year (E/MSYs) (Barnosky et al., 2011). The background E/MSYs so calculated ranged between 1.1 and 2.05 E/MSY. Expressing E/MSY for time intervals shorter than 100 years is problematic so shorter time intervals are not included. Data are from Barnosky et al. (2011) updated with information from Ceballos et al. (2015) for the 500 and 100 year intervals.

3.4 Type 3b phenomena: ‘Episodes’ without lasting impact on the Earth System

Cretaceous Ocean Anoxic Events (OAEs) (~127–94 Ma): Many ‘oceanic anoxic events’ occurred in the Mesozoic Era, especially the Cretaceous (Fig. 7), generally being relatively short-lived (<1 Myr) and commonly associated with pCIEs. Associated with some of the highest temperatures reconstructed for the Cretaceous Period, OAEs likely relate to volcanogenic CO₂ emissions from one or more Large Igneous Provinces. OAEs were initially recognized as isochronous occurrences of black shale in deep-sea drilling cores and at outcrop (Schlanger and Jenkyns, 1976), but are now considered as regional and diachronous expressions of global climatic changes and may be more suitably considered episodes. Most Cretaceous OAEs produced no substantive long-term shift in the Earth System, other than high rates of extinctions and radiations of radiolarians, planktonic foraminifera and to a lesser extent calcareous nannofossil at or near OAEs (Leckie et al., 2002), and would thus be consistent with Type 3b episodes.

The most prominent Cretaceous OAEs/CIEs are in the Early Aptian (OAE1a or Selli Event) and at the Cenomanian–Turonian boundary (OAE2 or Bonarelli Event), associated with episodes of carbonate platform drowning, transient anoxia and widespread deposition of marine organic matter across most oceans (Sano, 2003; Beil et al., 2020; Foulila et al., 2020; Gale et al., 2020). Both show a consistent pattern (Beil et al., 2020) of a precursor phase with sharp negative carbon isotope excursions (nCIEs), followed by a rapid onset phase, and more protracted peak, plateau and recovery phases (Fig. 7). Furthermore, they include short-term cooling phases possibly related to organic matter sequestration. This includes the Plenus Cold Event during the OAE2 peak phase, associated with a brief fall in $\delta^{13}\text{C}$, invasion of boreal species into the European Chalk Sea and reoxygenation of bottom water masses (Beil et al., 2020). The protracted and complex nature of the pCIEs is more typical of episodes, within which short-term events can be recognised (e.g., the precursor nCIE phase and rapid onset phase and abrupt cooling events), which are essentially Type 2 events not associated with state shifts.

The Aptian Stage has not yet been formalised. However, the maximum negative basal excursion during the precursor phase of OAE1a, coinciding with a major demise of nannoconids (Leckie et al., 2002) that is consistent with a permanent extinction (Type 1) event, will likely be chosen as its primary marker (Gale et al., 2020); this would be some 1 Myr earlier than the traditional base Aptian level. The OAE2 episode spans the Cenomanian–Turonian boundary (Fig. 7) coinciding with a high rate of turnover of calcareous nannofossils (Leckie et al., 2002) and a rudist mass-extinction (Sano, 2003), though these are not used as the primary marker for the Turonian Stage (Bengtson et al., 1996). However, the major carbon-isotope maximum associated with OAE2 occurs 0.5 m above the boundary and helped guide the choice of level (Gale et al., 2020).

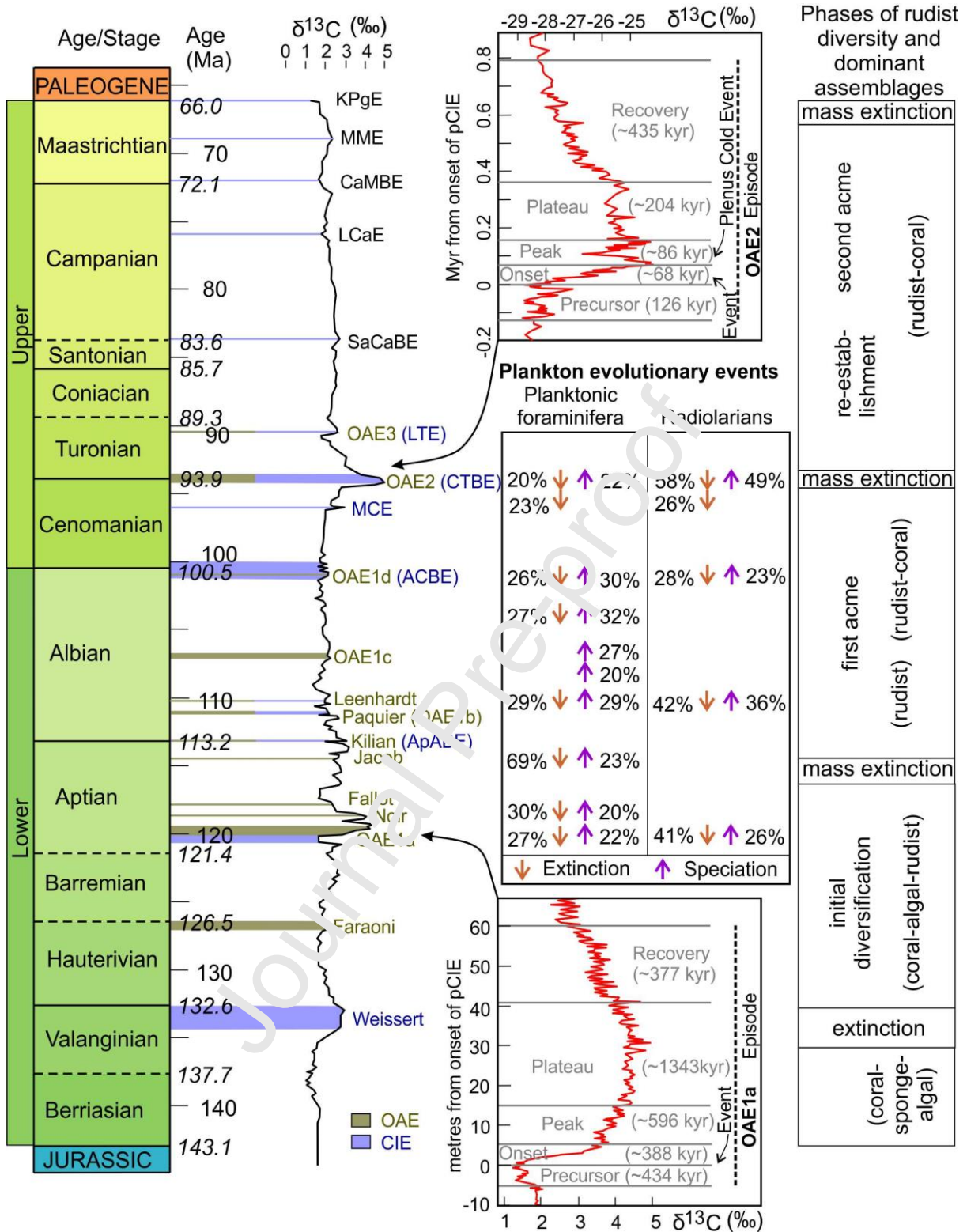


Fig. 7. Widespread Cretaceous ocean anoxic events (OAEs) with major named carbon isotope excursions (CIEs) (adapted from Gale et al. (2020) with the $\delta^{13}\text{C}$ curve derived from Cramer and Jarvis (2020, fig. 11.12 therein) and details of pCIE for OAE1a and OAE2 (adapted from Beil et al., 2020). ACBE– Albian–Cenomanian Boundary Event; ApABE– Aptian–Albian Boundary Event; CaMBE– Campanian–Maastrichtian Boundary Event; CTBE– Cenomanian–Turonian Boundary Event; KPgE– Cretaceous–Paleogene Event; LCaE– Late Campanian Event; LTE– Late Turonian Event; MCE– Mid-Cenomanian Event; MME– Mid-Maastrichtian Event; SaCaBE– Santonian–Campanian Boundary

Event. Plankton evolutionary Type 1 events after Leckie et al. (2002), showing percentage of species first appearances (speciation) or disappearances (extinction) through 1 million year increments. Phases of rudist diversity and type 1 extinction events and dominant assemblages of reef-building organisms (in brackets) after Sano (2003).

Superimposed on the pattern of OAEs (Fig. 7) is an overarching 'episode' of mid-Cretaceous rapid radiation and turnover of marine plankton, benthic foraminifera, molluscs and terrestrial plants (Leckie et al., 2002). This may be seen as a state-shift of the biosphere with, in particular, calcareous nannoplankton having their highest diversity and abundance, resulting in the typical chalk facies that spread globally in the Late Cretaceous.

Paleocene–Eocene Thermal Maximum (PETM) (~56 Ma): The Paleogene is marked throughout by numerous isotopic, biotic and climatic warming and cooling events, with the PETM being the most extreme in the context of stable carbon and oxygen isotopes (Fig. 8a). The PETM represents an array of abruptly initiating and almost coincident events, which combine to form a complex Type 3b episode that persisted over 100–200 kyr (Fig. 8b). Studying the biostratigraphy and isotopic composition of deep marine carbonates (Thomas, 1989; Kennett and Stott, 1991) revealed a Benthic Foraminiferal Extinction (BFE) and a negative carbon isotope excursion (nCIE) concurrent with rapid ocean-warming and globally with a low carbonate interval in most deep-marine cores (Zachos et al., 1993) (Fig. 8b). These occurred approximately a million years earlier than the 'classical' Paleocene–Eocene boundary recognized palaeontologically in marine strata near Ypres (Belgium) in which global correlation was complicated by miscorrelations, particularly between land and sea, of up to 1.5 Myr (Aubry et al., 2007). The nCIE allowed correlation of these oceanographic events with a rapid turnover in continental mammalian faunas, showing that the changes to climate, carbon cycle and biota were global (Koch et al., 1992).

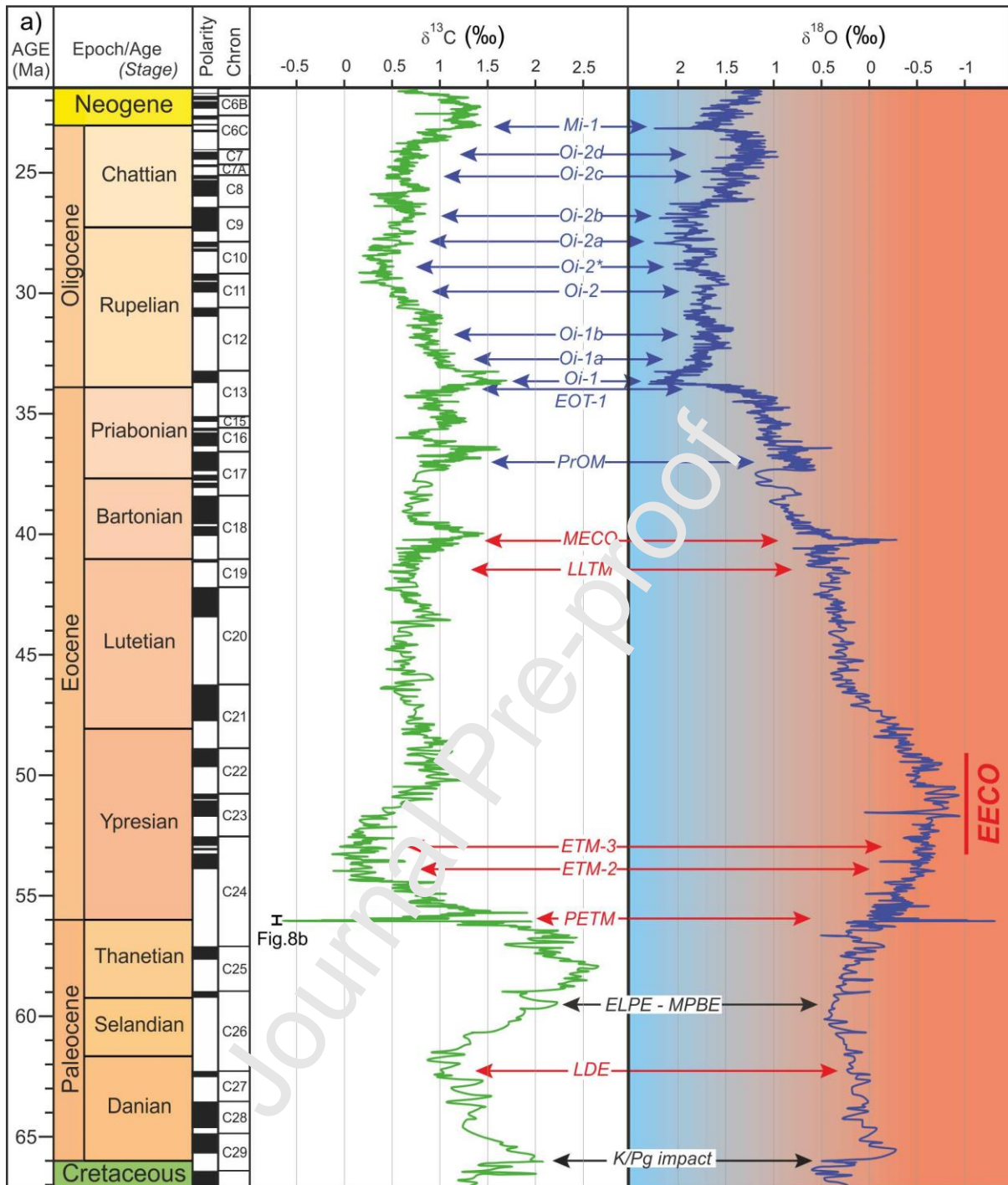


Fig. 8a. Paleogene events (reprinted from Speijer et al., 2020 with permission from Elsevier), which includes events associated with the K-Pg and PETM (discussed here), plus many more, such as the Latest Danian Event (LDE), a globally observed Paleocene warming event that correlates with land mammal fauna transitions; Early Late Paleocene Event (ELPE) or Mid-Paleocene Biotic Event (MPBE); Eocene Thermal Maximum (ETM), part of the Early Eocene Climatic Optimum (EECO); Late Lutetian Thermal Maximum (LLTM); Middle Eocene Climatic Optimum (MECO); Priabonian Oxygen Isotope Maximum event (PrOM); Eocene–Oligocene Transition (EOT1); Oligocene Oxygen Isotopic Maximum (Oi) cooling events; Miocene glaciation (Mi-1). Climatic events shown in red are hyperthermals and those in blue are cooling events/glaciations.

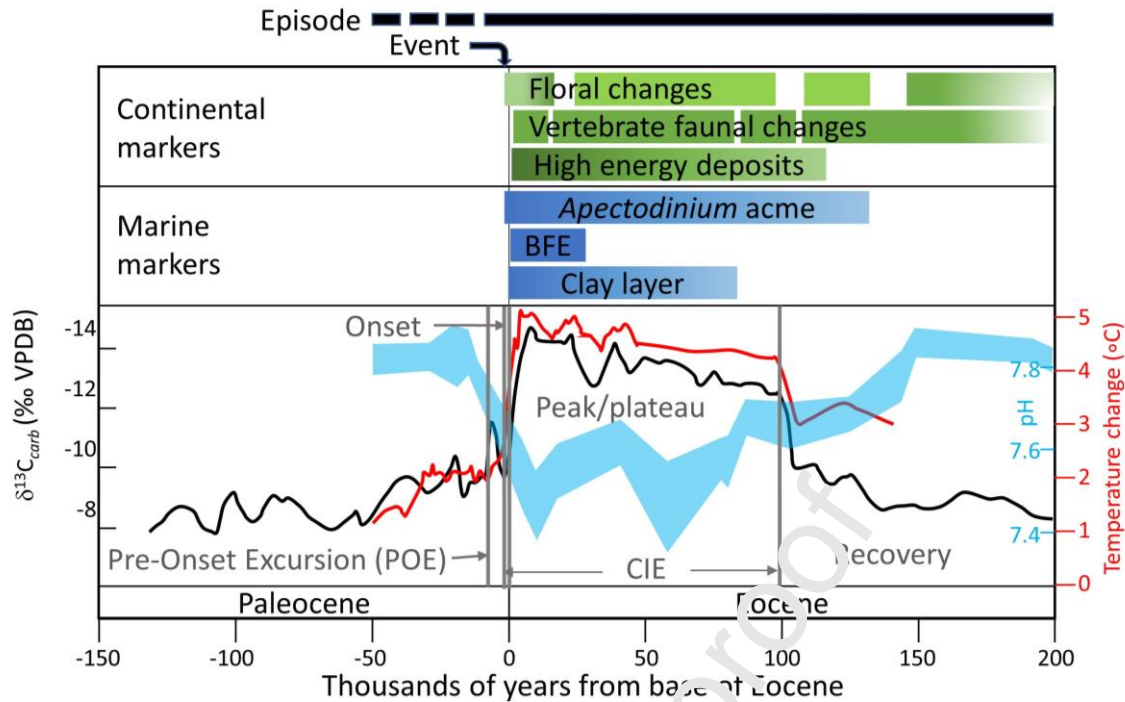


Fig. 8b. Multiple markers showing the effects of the Paleocene–Eocene Thermal Maximum: plant extinction and range changes (Wing and Currano, 2013), mammalian species turnovers (Gingerich, 2006), high-energy fluvial deposits (Schmitz and Palante, 2007), increase in abundance of the dinoflagellate *Apectodinium* (Crouch et al., 2007), benthic foraminiferal extinction (BFE; Thomas, 2003) and deep marine clay deposition (Zachos et al., 2005). Environmental changes included ocean acidification (Penman et al., 2014) and increasing global temperature (Frieling et al., 2019; Zachos et al., 2006) caused by the carbon release indicated by the nCIE (van der Meulen et al., 2020). The records are independently calibrated through cyclostratigraphy and registered at the onset of the CIE, just prior to the start of the Eocene, set at 0 in the figure.

The Working Group on the Paleocene–Eocene boundary determined that the geochemical and biostratigraphic changes associated with the PETM formed a better basis for global correlation than the classical boundary events. They recommended that the chronostratigraphic base of the Eocene (Ypresian Stage) be defined by a GSSP in a section at Dababiya, Egypt (Aubry et al., 2007; Vandenberghe et al., 2012). The GSSP was placed very near the onset of the nCIE, because of the global correlatability of this geologically sudden increase in the proportion of ^{12}C (Fig. 8a, b). The exact position of the GSSP is at the (locally) more visually apparent base of the Dababiya Quarry Member, which is slightly above the onset of the nCIE (Aubry et al., 2007). The stratotype section also preserves other signals typical of, or unique to, the base of the Eocene, with the onsets of the BFE, characteristic bioevents in calcareous nannofossils and planktonic foraminifera, changes in clay mineral composition and a low-carbonate interval coinciding with the nCIE (Aubry et al., 2007) consistent with an array of events with a nearly common level of initiation.

The source, rate, amount and mechanism for the carbon release that caused the nCIE has been intensely studied and debated (e.g., Dickens et al., 1995; Cramer and Kent, 2005; Moore and Kurtz, 2008; Zeebe et al., 2009; Kender et al., 2021). Recent estimates suggest the nCIE onset (Fig. 8b) had a duration of 3–5 kyr (Zeebe et al., 2014; Bowen et al., 2015). In the millennia immediately before the main nCIE there was at least one smaller carbon release associated with a Pre-Onset Excursion (POE) (Bowen et al., 2015; Robinson and Spivey, 2019; van der Meulen et al., 2020). During the main

nCIE associated with the PETM carbon isotope composition reached a relatively stable minimum for about 100 kyr (Zeebe et al., 2009; Frieling et al., 2016; Lyons et al., 2019). Many of the changes in physical and chemical systems appear to have persisted throughout the body of the nCIE (Röhl et al., 2007; Murphy et al., 2010). Conditions resembling those in the Late Paleocene returned during a recovery phase, probably through negative feedbacks related to productivity and silicate weathering (Bowen and Zachos, 2010; Penman and Zachos, 2018; Fig. 8b). Although recovery from the PETM varied among Earth System components (e.g., Kelly et al., 2005) the event does not appear to have shifted global climate and carbon cycle to a different state (i.e., a Type 2 event).

The biotic effects of the PETM, however, varied from transient to permanent. The benthic foraminiferal extinction (BFE; Fig. 8b), associated with loss of about 30–50% of species, represents the single, biggest evolutionary event among benthic foraminifera in the Late Cretaceous and Cenozoic (Thomas, 2003; Alegret et al., 2021). Foraminiferal extinctions commenced in the latest Paleocene, some 20–30 kyr before the main BFE and coincident with the onsets of warming and initial negative excursion of $\delta^{13}\text{C}$, probably driven by ocean acidification (Alegret et al., 2021; Fig. 8b). Some planktonic foraminifera lineages showed rapid evolutionary change during the PETM, with the appearance of short-ranging ‘excursion taxa’ (Kelly et al., 1998; Fig. 8b). Rapid evolutionary radiations among calcareous nannoplankton led to long-term change in their taxonomic composition (Gibbs et al., 2006). Other marine plankton responded with temporary range changes, such as abundance increase of the thermophilic dinoflagellate *Apectodinium* at high latitudes (Crouch et al., 2001; Denison, 2021; Fig. 8b). Intercontinental mammal migrations also had permanent consequences; mammal orders that appeared in North America during the PETM still dominate the fauna (Gingerich, 2006). Among terrestrial mammals, transient body size decreases were associated with the stable core of the nCIE (Gingerich, 2006; Secord et al., 2012). Plants demonstrate a mix of extinction, reversible intracontinental, and irreversible intercontinental range change (Wing and Curran, 2013). The global biotic changes caused by the PETM were long-lasting or permanent, hence characterising Type 1 events, and contributed to the original motivation for recognizing separate Paleocene and Eocene epochs.

Mid-Miocene Climatic Optimum (MMCO) (~17–14.7 Ma): Also known as the Miocene Climatic Optimum, it is associated with warmer global surface temperatures (Fig. 9a), elevated sea temperatures at high latitudes, reduced ice sheet extent in the Antarctic (e.g., Lewis et al., 2008; Shevenell, 2016) and species migrations and originations (e.g., Böhme, 2003; Kurschner et al., 2008). The cause may have been the eruption of the Columbia River Basalt Group in the Pacific Northwest, occurring mostly between 15.7 and 15.9 Ma, elevating atmospheric $p\text{CO}_2$ levels above 400 ppm (Kasbohm and Schoene, 2018; Fig. 9a). The MMCO occurs against the backdrop of overall Cenozoic cooling (Garzione, 2008) which led to a series of glaciations, commencing with the Oi-1 Glaciation in the Early Oligocene and was followed by the Middle Miocene Climatic Transition (MMCT), when global cooling resumed between 14.7 and 13.8 Ma (Houlbourn et al., 2005; Lewis et al., 2008; Fig. 9a). The MMCO onset, duration and the multifaceted response of the Earth System conforms to an episode, but is clearly transient (and reversible).

Mid-Piacenzian Warm Period (mPWP) (~3.264–3.025 Ma): It was a transient interval of overall warmer climate (Fig. 9a, b) associated with reduced ice sheet extent, warmer surface temperatures and higher sea levels (Dowsett et al., 2013; Burke et al., 2018). The forcing mechanisms of a warmer Pliocene climate may have been elevated levels of atmospheric CO_2 in combination with other factors such as changes in ocean heat transport, different orography, and land cover (Haywood et al., 2016). The mPWP was followed by intensification of the Cenozoic icehouse, especially the Northern Hemisphere glaciation, probably resulting from a combination of closure of low latitude

ocean gateways (Bartoli et al., 2005) and reduced levels of atmospheric CO₂ (Willeit et al., 2015). In terms of its complexity of multiple marine isotope stages (Fig. 9) and the multifaceted response of the Earth System to Pliocene warming, the mPWP represents an episode, but it was clearly transient, in that it was followed by an intensification of icehouse conditions.

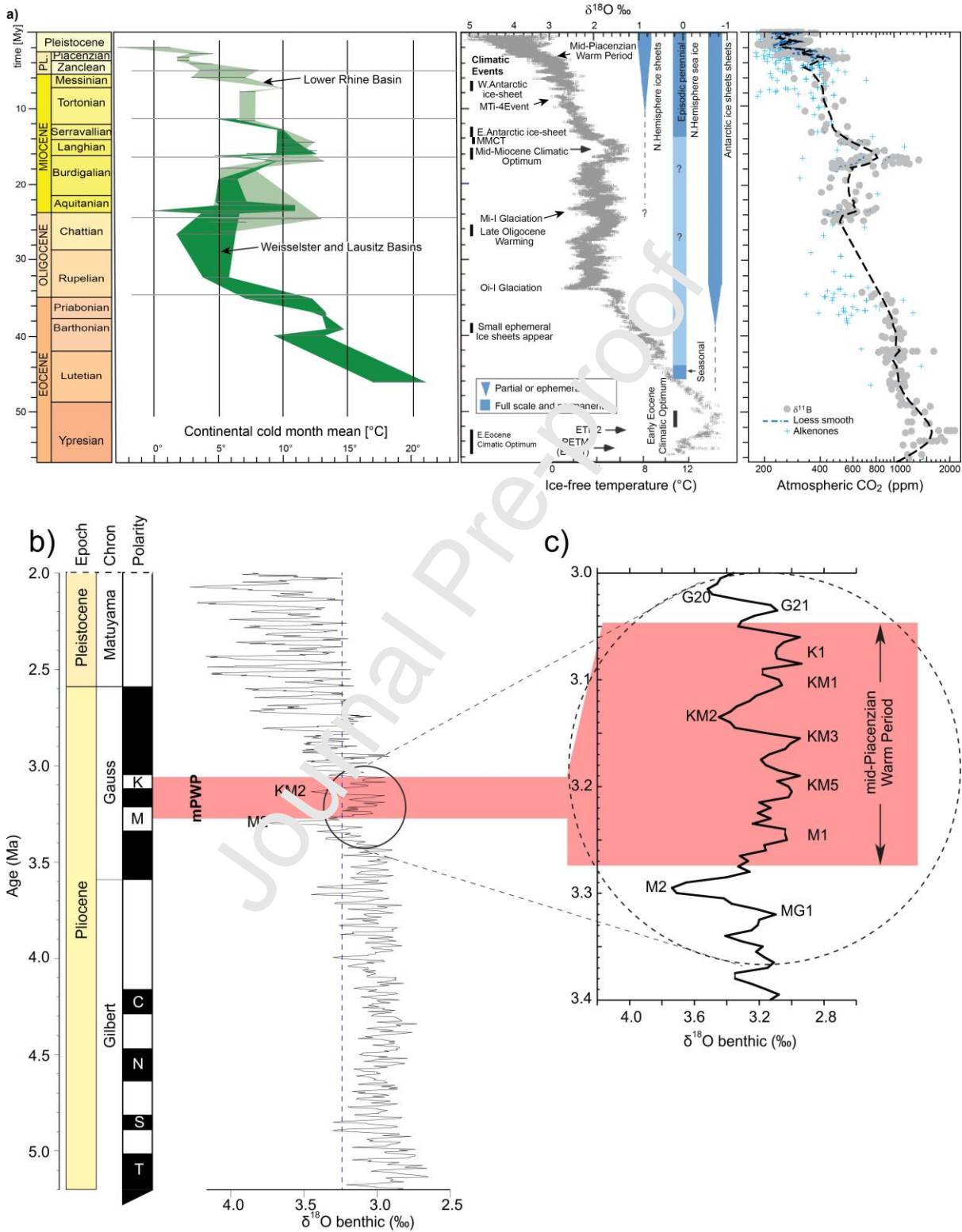


Fig. 9. (a) Palaeobotanical evidence of several Cenozoic intervals of temperature in continental Europe (left; modified from fig. 3 in Mosbrugger et al., 2005) compares well with global

temperature/sea level estimates from the benthic foraminiferal $\delta^{18}\text{O}$ record of Zachos et al. (2008) (middle) and boron isotope and alkenone-based reconstructions of atmospheric CO_2 (right; modified from fig. 5 in Rea et al., 2021). The Mid-Miocene Climatic Optimum, spanning the latest Burdigalian through Langhian stages/ages and ending with glaciation event Mi-3b, represents the last major reversal in the general cooling trend since the Early Eocene Climatic Optimum, with reconstructed $p\text{CO}_2$ concentrations ~ 800 ppm and mean global surface temperature estimated to be $5 - 6^\circ\text{C}$ warmer than today. PL. Pliocene, MMCT Mid-Miocene Climatic Transition; (b) The mid-Piacenzian Warm Period (mPWP) in relation to the long-term climate evolution of the Late Pliocene. Benthic oxygen isotope stack and timescale of Lisiecki and Raymo (2005): the vertical dashed line shows present-day benthic $\delta^{18}\text{O}$ value. The mPWP is shown by the horizontal shaded grey bar. (c) Details of timescale for the mPWP, and Marine Isotope Stages MG1, M2, M1, KM5, KM3, KM2, KM1, K1, G21 and G20 indicating significant temporal climate variation within the warm interval. Figure adapted from Haywood et al. (2016).

4. The 'Great Acceleration Event Array (GAEA)'

Abundant mid-20th century planetary-scale markers represent a profound adjustment to the Earth System in response to rapid and massive increases in human population, energy consumption and greenhouse gas emissions, industrialisation, introduction of novel technologies and globalization (Syvitski et al., 2020; Head et al., 2021). Together, these Earth System responses were named the 'Great Acceleration' by Steffen et al. (2007), based on datasets that reveal marked post-1950 CE changes in socio-economic factors and biophysical processes as well as environmental and climatic changes (Steffen et al., 2004, 2007, 2015). The scale of the Great Acceleration, seen against the wider context of the human planetary impact throughout the last 12,000 years by Syvitski et al. (2020), emphasizes the profound novelty of the changes experienced since the 1950s, establishing humans as an overwhelming Earth System force with an abrupt geological expression.

In event stratigraphic terms, the onset of the Anthropocene as conceived at the rank of series/epoch *sensu* Waters et al. (2016) is not a single event, but rather comprises an array of many near-synchronous and individually recognisable events (some of which have already ended) and their corresponding event markers, driven by overlapping sets of anthropogenic forces and coincident with the Great Acceleration. These forces include such processes as burning fossil fuels, industrial pollution, nuclear device use and testing, agriculture and deforestation, anthropogenic climate change, changes to the sediment budget, creation of new ecotypes, and biotic changes including translocations of non-native biota, expansion in numbers of domesticated species, and increased species extinctions (Table 2). The corresponding event markers are most apparent from around 1950 CE onwards, forming a diverse and ongoing array of clear signals in geological archives (Head et al., 2021). In the context of event stratigraphy this cluster of geological signals focused on the mid-20th century is termed here the Great Acceleration Event Array (GAEA). Just as the bolide impact resulted in geological evidence for the K-Pg boundary (see above), the GAEA provides the rationale behind the choice of the mid-20th century as the most pragmatic level to place the onset of the Anthropocene Epoch as a chronostratigraphic unit.

The many distinctive stratigraphic markers of the GAEA enable correlation of the Anthropocene within diverse environments across the planet. They can be categorized based upon the nature of their stratigraphic profiles, as follows:

- 1) **Markers for events with pronounced shifts following prolonged episodes of gradual change:**
Such markers comprise striking inflections following initial slow growth over centuries or

millennia. The protracted precursor phases are episodes analogous to those of the Cretaceous OAEs or the Pre-Onset Excursion of the PETM, and have been used to argue for a long-duration, informal Anthropocene (e.g., Gibbard et al., 2021, 2022). Yet, it is the sharp mid-20th century deflections of these markers, including CO₂ and CH₄ concentrations in ice records, black carbon, and stable lead isotopes, that are the stratigraphic expression of events and that represent the most robust level for stratigraphic correlation (Fig. 10).

- From the mid-20th century onwards, atmospheric CO₂ rose in this event some 100 times faster than across the Pleistocene–Holocene transition (Fig. 10a), when astronomical forcing drove the change from glacial to interglacial conditions. In contrast, anthropogenic deforestation, in part tracked by charcoal records (Fig. 10b), may have caused slow reversal from falling interglacial CO₂ concentrations (Ruddiman, 2018; but see Zalasiewicz et al., 2019a), which then rose by 25 ppm from ~8,000 yr BP to ~1750 CE (Fig. 10a) at ~0.003 ppm/yr, that is >600 times more slowly than present rates of >2 ppm/yr.
- Atmospheric CH₄ concentrations have more than doubled since 1950 CE (Waters et al., 2016; Zalasiewicz et al., 2019a; Head et al., 2021), rising at a rate of ~0.5%/yr. This contrasts with the ~100 ppb rise of anthropogenic CH₄ emissions from 5,000 years ago to 1750 CE (Fig. 10a) at a rate of <0.001%/yr, some ~500 times more slowly than during the Anthropocene.
- The rise in Pb concentrations in the 1960s – 1980s associated with the gasoline additive tetraethyl lead (Nriagu, 1996; Gałuszka and Wągrzei, 2019) forms a prominent event, its stratigraphic expression shaped by subsequent rapid falls following bans on this additive in the late 20th century. This overprints more regional or smaller signals from sources such as mining and coal-burning. A 20-fold Pb enrichment in Greenland snow between the 1750s and mid-1960s (Boutron et al., 1995) includes a marked 1950s upturn driven by increased coal burning, seen also in ice core records from Mt. Logan, Yukon (Osterberg et al., 2008; Fig. 10c). A prolonged mining Pb signal initiated with early lead peaks recorded in the Northern Hemisphere from about 3,000 yr BP associated with Greek, Phoenician and Roman mining (e.g., Wągrzei and Draganits, 2018), and has continued into the 20th century. Stable Pb isotope ratios may be used to distinguish anthropogenically-derived Pb from natural sources (e.g., Bindler et al., 2001).
- Deforestation, farming and urbanization have increased soil erosion and hence sediment flux over many millennia (Dearning and Jones, 2003). The changes since 1950, though, have been dramatic, with a more than 4-fold increase in a planetary sediment load which has become dominated by human action; natural/ambient processes now contribute just 6% to the global budget (Syvitski et al., 2022). In lakes, a global acceleration in sediment mass accumulation rates since ~1950 CE is linked to human population growth and land-use change (Baud et al., 2021).
- Measured rates of species extinction are now considerably higher than background levels (Barnosky et al., 2011; Pimm et al., 2014; Ceballos et al., 2015; Fig. 6) having increased dramatically since 1900 CE with a conservative estimate of about 543 (Ceballos et al. 2020) vertebrate species becoming extinct. Many terrestrial vertebrate species are now on the brink of extinction with populations smaller than 1,000 individuals (Ceballos et al., 2015, 2020; IUCN, 2021). Current mammal extinction rates are twice or more than those in the 16th century, in turn twice that of the megafaunal extinctions of the LQE (Waters et al., 2016; Fig. 6b). The 16th century probably posted unusually high extinction rates, certainly compared to previous centuries, due to the sudden expansion of intercontinental shipping and biotic exchange.

Table 2. Timing of the markers associated with the GAEA. Recovery taken to be when levels fall below those at onset of abrupt rise. Abbreviations for key event-forming processes (ordered with most important anthropogenic sources first): FFB- Fossil fuel burning, IP- Industrial Pollution from multiple sources, M/S- mining/smelting, NT- Nuclear tests, A/D- Agriculture/Deforestation, CC- Climate change, SE- Species extinctions, ST- Species translocations, and DS-Domesticated species.

| Specific event markers | Key event-forming processes | Approximate timing of key stages | | | | Key reference [relevant figure] |
|--|-----------------------------|----------------------------------|----------------------|------------------|----------|--|
| | | Onset | Acceleration (start) | Peak | Recovery | |
| Carbon dioxide | FFB, IP, A/D | ?6000 BCE; 1770 | 1955 | - | - | MacFarling Meure et al. (2006); [Fig. 10a] |
| Carbon isotope excursion $\delta^{13}\text{C}$ (CO_2) | FFB | ~1750 | 1955 | - | - | Rubino et al. (2013); [Fig. 11a] |
| Spheroidal carbonaceous particles (SCP) | FFB | mid-19 th century | 1950 | 1970s–1990s | - | Rose (2015); [Fig. 11b] |
| Spheroidal alumina-silicates & mullite | FFB | Late 19 th century | 1940–50 | 1970s–1990s | - | Smieja-Król et al. (2019) |
| Black carbon soot | FFB, A/D, IP | 1850 | 1945–55 | - | - | Novakov et al. (2003); Bond et al. (2007); [Fig. 11b] |
| High Molecular Weight polyaromatic hydrocarbons | FFB, IP, M/S, A/D | | | 1940s–1980s | - | Bigus et al. (2014) |
| Sulfur | FFB, IP | 1900 | 1934 | 9–5 | 2000 | Sigl et al. (2015); [Fig. 11c] |
| Lead | M/S, IP, FFB | 1000 BCE; 1880 | 1950 | 1960s–86 | - | Osterberg et al. (2008); [Fig. 10c] |
| Copper | M/S, IP, FFB, A/D | 500 BCE; 1770 | mid-1960s | 1960s–1980s | 1990s | Hong et al. (1996); Gałuszka and Wagreich (2019) |
| Zinc | M/S, IP, FFB | 1805 | 1920s–1980s | 1990s | - | Candelone and Hong (1995); Gałuszka and Wagreich (2019) |
| Mercury | M/S, FFB, IP | 1550 | 1870; 1950 | 1970 | - | Hylander and Meili (2002) |
| Polychlorinated biphenyls (PCBs) | IP | 1929 | 1940s–1950s | 1960s–1970s | 1990 | Gałuszka et al. (2020); Fig. 11c] |
| Microplastics | IP | Early 1950s | Early 1960s | - | - | Zalasiewicz et al. (2019c) |
| Radiocarbon | NT | 1955 | 1955 | 1964–66 | 2020 | Hua et al. (2021); [Fig. 12a] |
| Plutonium | NT | 1945 | 1952–53 | 1963–64 | 1972 | Koide et al. (1977); [Fig. 12a] |
| Iodine (^{129}I) | NT | 1945 | 1952–55 | 1963–64; 1986 | - | Bautista et al. (2016); [Fig. 12a] |
| Nitrates | A/D | 1903 | 1960 | 1990 | - | Mayewski et al. (1990) |
| Nitrogen isotope excursion | A/D | 1875 | ~1950 | 1970–2000 | - | Hastings et al. (2009); [Fig. 11d] |
| Methane | A/D, FFB | 3000 BCE ~1750 | 1850; 1955 | - | - | Meinshausen et al. (2017); [Fig. 10a] |
| Organochlorine pesticides (e.g. DDT) | A/D | 1945–50 | 1950 | 1960s–1990s | - | Li and McDonald (2005); Gałuszka and Rose (2019); [Fig. 11b] |
| Black carbon char or charcoal | A/D | 9700 BCE | 2000 BCE; 1750 CE | 200 CE; 1890 | ?1990 | Power et al (2008); Han et al. (2017); [Fig. 10b] |
| Oxygen isotope excursion | CC | 1850 | 1979 | - | - | Masson-Delmotte et al. (2015) |
| Large mammals | SE | 48ka–8ka BCE | 1540; 1900 | - | - | Williams et al. (2022) |

| | | | | | | |
|-----------------|----|------|---------|-------|---|---|
| Vascular plants | ST | | 1810 | 1970s | - | |
| Vertebrates | ST | 1850 | 1950 | - | - | Seebens et al. (2017); [Fig. 10d] |
| Invertebrates | ST | 1850 | 1960–75 | - | - | |
| Domesticates | DS | | 1950 | - | - | https://ourworldindata.org/meat-and-seafood-production-consumption |

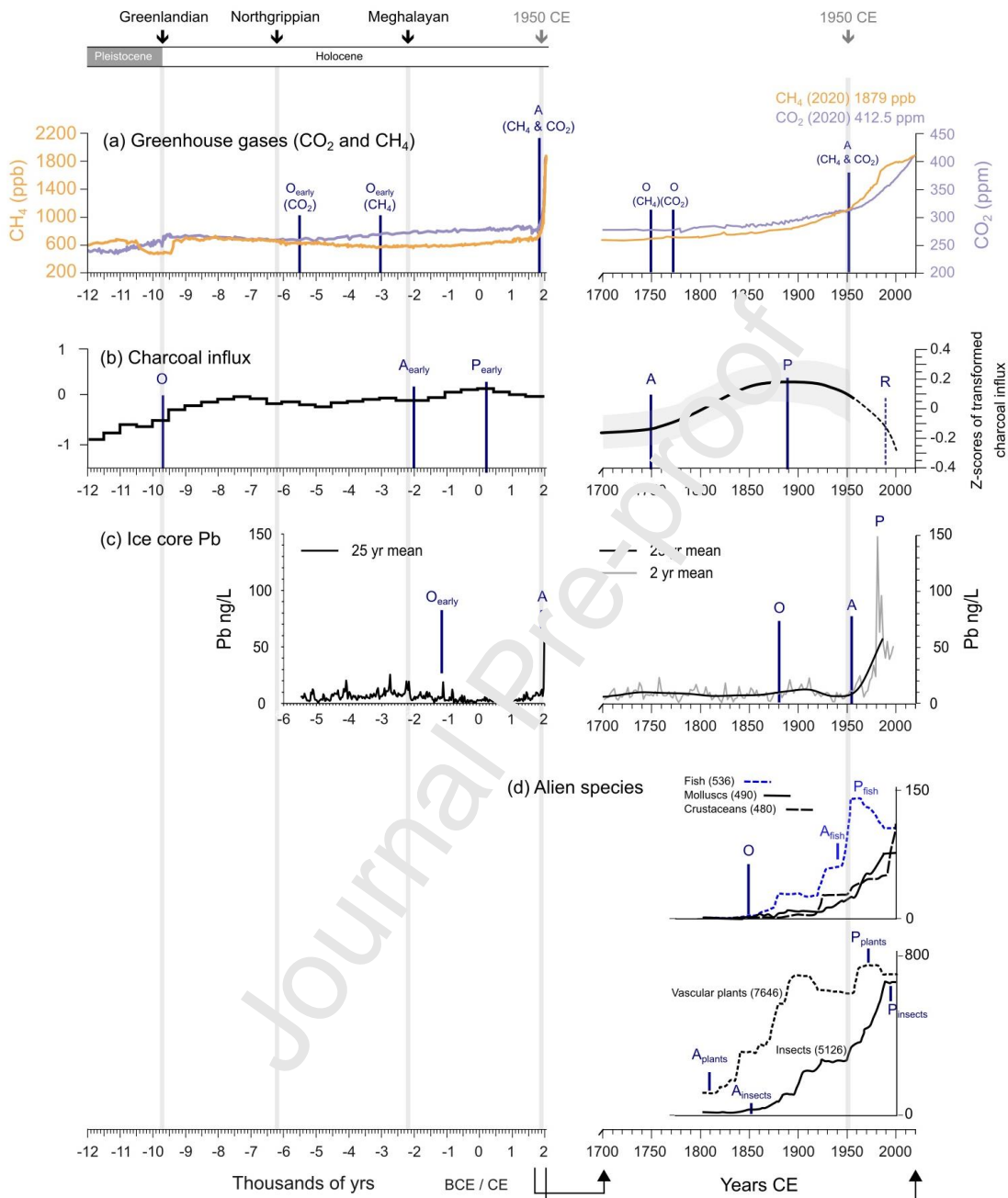


Fig. 10. Geological timelines of key GAEA (mid-20th century) events using empirical data to show the true scale and timing of different environmental changes. a) CO₂ and CH₄ data from Antarctic ice cores and atmospheric measurements from <https://ourworldindata.org/atmospheric-concentrations> and <https://www.epa.gov/climate-indicators/climate-change-indicators-atmospheric-concentrations-greenhouse-gases> respectively; b) charcoal influx (proxy for biomass combustion) data from (left panel) Power et al. (2008) and (right panel) Marlon et al. (2008); c) ice core Pb record from Mount Logan, Yukon (Osterberg et al., 2008); d) timing of first alien species introductions for all plants, fish, insects, crustaceans and molluscs, i.e., species likely to leave a stratigraphic record (from

Seebens et al., 2017). O – Onset; A – Acceleration/marked shift (and level of the event); P – Peak; R – Recovery.

- Seebens et al. (2017) report vascular plant neobiota (species translocations) peaking sharply at ~700–800 species/5 years in the late 20th century, following low introduction rates between ~1500 and 1800 CE, despite these centuries certainly posting higher rates of intercontinental biotic exchange than evident in previous millennia. Most vertebrates (except mammals) and all invertebrates show a marked 1950s upwards inflection in first records of introduction (Fig. 10d). Previous to 1800, for many millennia, species introductions and invasions had shown only gradual increase (Gibbard et al., 2021).

2) **Markers of events with prominent mid-20th century inflection, following inception during the Industrial Revolution:** These include changes in stable carbon isotope ratios, fly-ash particles, black carbon soot and polycyclic aromatic hydrocarbons (PAHs), mullite, sulfur and stable sulfur isotopes, nitrates and nitrogen isotopes, and associated rise in global temperatures and sea levels. These event markers are effectively isochronous and related to fossil-fuel burning and industrial agriculture (Fig. 11).

- Fossil fuels are depleted in ¹³C and lack ¹⁴C, hence fossil fuel combustion is diluting their proportions relative to ¹²C in atmospheric CO₂, leading to an apparent ageing of the atmosphere since the early 20th century (Suess, 1955). This ‘Suess effect’ is observed as a marked inflection event in the rate of decline in ¹³C about 1955 CE following more gradual decline from ~1750 CE (Rubino et al., 2013). The ~2‰ change in ice core carbon isotopes since pre-industrial time (Fig. 11a) is comparable to shifts observed on geological time scales (see discussion), yet occurred in a dramatically shorter time. It contrasts with a slow Early Holocene trend towards isotopically heavier carbon of <0.5‰ over ~4 kyr. This Suess effect will continue as long as fossil carbon is combusted (Graven, 2015; Graven et al., 2020). Carbon isotope recovery with climate mitigation may take at least 1,000 years under high mitigation scenarios (Solomon et al., 2009).
- Spheroidal carbonaceous fly-ash particles (SCPs) are microscopic signatures of high-temperature coal (or oil) combustion. They show an event marked by a global abundance upturn around 1950 CE, with peak signals ranging regionally from the 1970s to 1990s, with the subsequent introduction of particle-arrestor technology and increased usage of different energy sources resulting in a rapid drop in concentrations (Rose, 2015; Fig. 11b). SCPs first appeared in western Europe in the mid-19th century, appearing elsewhere at later dates.
- Mullite is a pure aluminosilicate (Al₆Si₂O₁₃) formed by the transformation of coal-hosting kaolinite, feldspars and other aluminosilicates and is commonly present (<1–59%) in fly ash worldwide (Smieja-Król et al., 2019). Mullite appearance is associated with high-temperature (>1100°C) combustion in early coal-fired power plants, initially from late 19th century sites near industrial centres. A clear 1950s–1960s event can be established with a boundary between mullite absence and presence in stratigraphic sections on every continent, even at remote sites (Fiałkiewicz-Kozieł et al., 2016, 2022).
- Black carbon soot forms as a high-temperature condensate of fossil-fuel burning, especially from motor vehicle emissions. It consequently showed marked upturns ~1950 CE and then ~1970 CE following initial late 19th century increases (Novakov et al., 2003; Bond et al., 2007; Fig. 11b). PAHs are produced from any organic combustion, so have some natural congeners from forest fires etc. More specifically, high molecular weight PAHs sourced from burning

fossil fuel have been produced since human coal-burning began, but show peak abundance in the 1940s – 1980s (Bigus et al., 2014).

- Non-sea-salt-sulfur abundance in Greenland ice cores show a prominent marked upturn in values commencing in the mid-1930s and peaking in 1975 CE, since recovering to pre-1900 CE levels (Sigl et al., 2015; Fig. 11c). Initial increases from ~1900 CE followed 900 years of near-constant background values apart from volcanic-eruption-induced peaks. Progressively lower $\delta^{34}\text{S}$ values between the 1860s and 1970s are consistent with increasing industrial sulfur emissions.
- Industrially derived nitrogen is depleted in ^{15}N , with N isotope ratios in both lake sediments and ice cores showing the main inflection event at ~1950 CE following initial downturns from ~1875 CE (Hastings et al., 2009; Holtgrieve et al., 2011). Nitrate concentrations in Greenland ice (Fig. 11d) show a similar marked 1950s–1960s upturn and a peak in the late 20th century following an initial rise from ~1890 to ~1903 CE (Mayewski et al., 1990; Hastings et al., 2009).

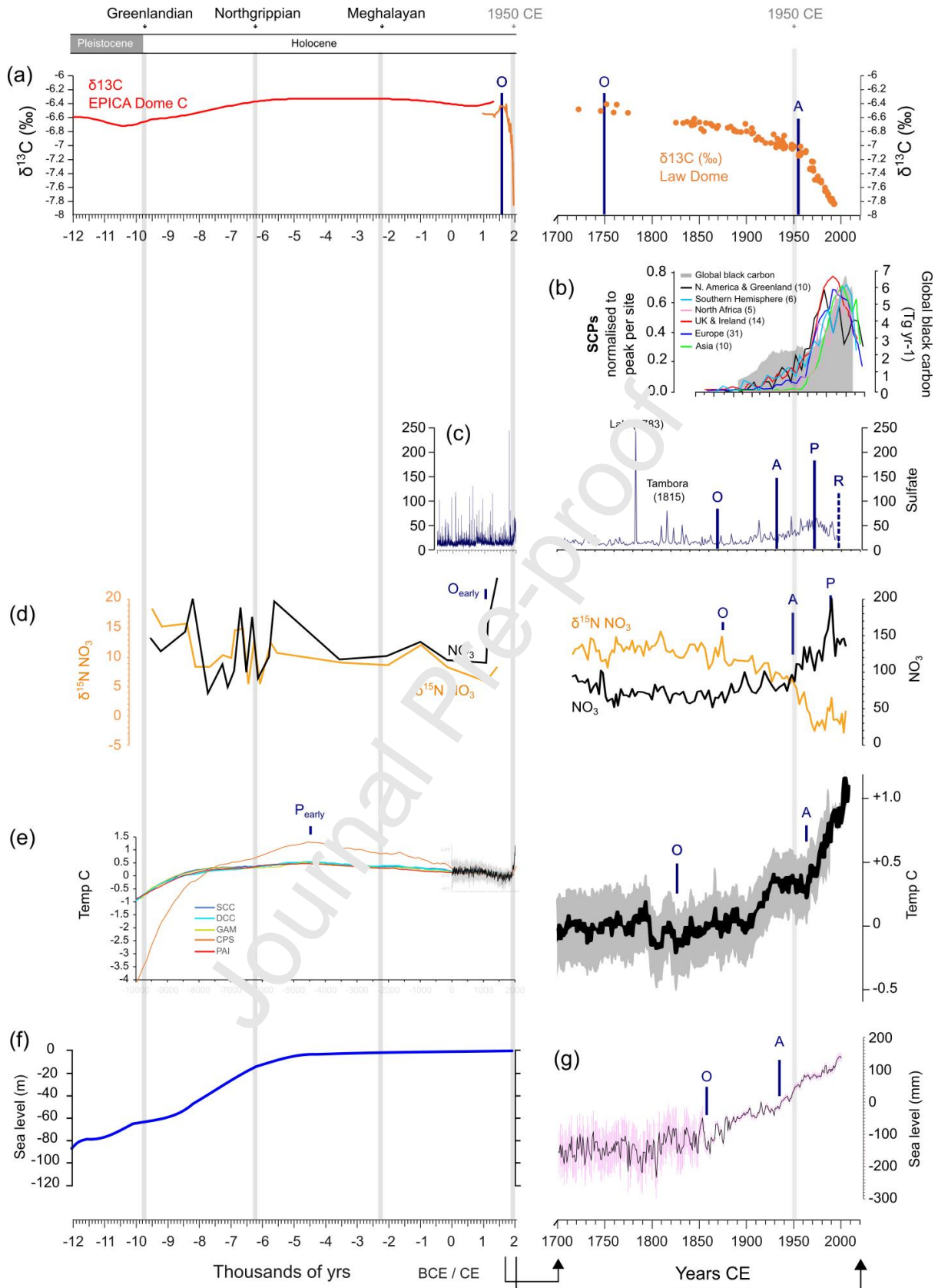


Fig. 11. Geological timelines of key GAEA (mid-20th century) events that largely initiated during the Industrial Revolution. a) ice core $\delta^{13}\text{C}$ records from Greenland (Greenland Ice Core Project [GRIP], Summit) and Antarctic (European Project for Ice Coring in Antarctica [EPICA] Dome C, Law Dome) and modern instrumental data from Rubino et al. (2013); b) regional variations in spheroidal

carbonaceous particle abundance normalized to the peak value in each lake core (derived from Rose, 2015) and global black carbon from annual fossil fuel consumption data (Novakov et al., 2003), as reproduced by Waters et al., 2016); c) non-sea-salt sulfur record from Greenland ice core with prominent peaks related to volcanic eruption events (Sigl et al., 2015 supplementary data); d) ice core nitrate and $\delta^{15}\text{N}$ data from Summit, Greenland (adapted from Head et al., 2021); e) global mean surface temperature from the Temperature 12k database using different reconstruction methods (Kaufman et al., 2020); f) Holocene global mean sea-level change relative to present day (modified from Clark et al., 2016) and g) modern sea-level curve (modified from Church et al., 2013 fig. 13.3e therein). O – Onset; A – Acceleration/marked shift (and level of the event); P – Peak; R – Recovery.

- Global mean surface temperatures have shown a rapid rise of 1.0°C from 1975 to 2020 CE, at 0.02°C/yr (Sippel et al., 2021), almost an order of magnitude faster than occurred at the Holocene onset. This contrasts with global cooling, driven by declining insolation, which characterized temperate and polar regions over the last 7,000 years (Clark et al., 2016; Kaufman et al., 2020; Fig. 11e).
- The rate of global sea-level rise has been increasing since 1970 CE (IPCC, 2021). This follows ~7,000 years of approximate stability, with the last 3,000 years showing stability to within 0.1 m (Onac et al., 2022), sea level starting to rise from the mid-19th century (Fig. 11f). Heat has been gradually penetrating to progressively greater depths since about 1950 CE with rapid acceleration in ocean warming throughout the water column since 1990 CE (Bagnell and DeVries, 2021). Over the next 2,000 years, global sea level is predicted to rise from 2–3 m to 19–22 m under differing warming scenarios and will continue to rise over subsequent millennia (IPCC, 2021).
- Greenland and Antarctica have both lost about 5 Gt of ice at slowly increasing rates since 1980 CE (Mouginot et al., 2019; King et al., 2020), with ice losses set to continue whether warming continues or stabilizes at 1.5 to 2.0°C above pre-industrial levels. An equally strong signal of Arctic sea-ice melt began in 1978 CE. This continuing Arctic trend represents a significant change in climate state, since the removal of sea ice both decreases albedo and puts more heat into the ocean, thus affecting ocean circulation at larger scales.

3) Markers of events that commenced abruptly in the mid-20th century and lasted decades: This category includes radionuclide signals dispersed in the atmosphere through testing of nuclear devices, persistent organic chemicals such as pesticides and pharmaceutical and manufacturing compounds (e.g., polychlorinated biphenyls – PCBs). These are markers of brief events which, though regional to global in extent, provide useful tools for very high-resolution correlation (Fig. 12).

- Fallout radionuclides from above-ground nuclear detonations provide a sharp bomb-spike (Fig. 12a). Plutonium isotopes and iodine-129 (^{129}I) show localised inception in 1945 CE near to early atomic detonations, a global signal commencing during 1952–1953 CE and peaking in 1963–1964 CE associated with large thermonuclear detonations (Koide et al., 1977; Bautista et al., 2016). Plutonium, exceedingly rare in nature, shows a rapid reduction in most environmental archives following cessation of the main phase of above-ground testing (with the exception of areas impacted by discharges from nuclear fuel reprocessing complexes, where discharge “pulses” provide useful local chronological markers relating to specific emission events). In contrast, ^{129}I shows a secondary peak associated with the Chernobyl accident in 1986 CE. Radiocarbon inventories doubled in response to the nuclear detonations but, with the large reservoir of natural ^{14}C , a clear upturn in that signal both

commenced and peaked later, in 1955 CE and 1964–1966 CE, respectively (Hua et al., 2021), and has only recently returned to pre-1945 CE levels.

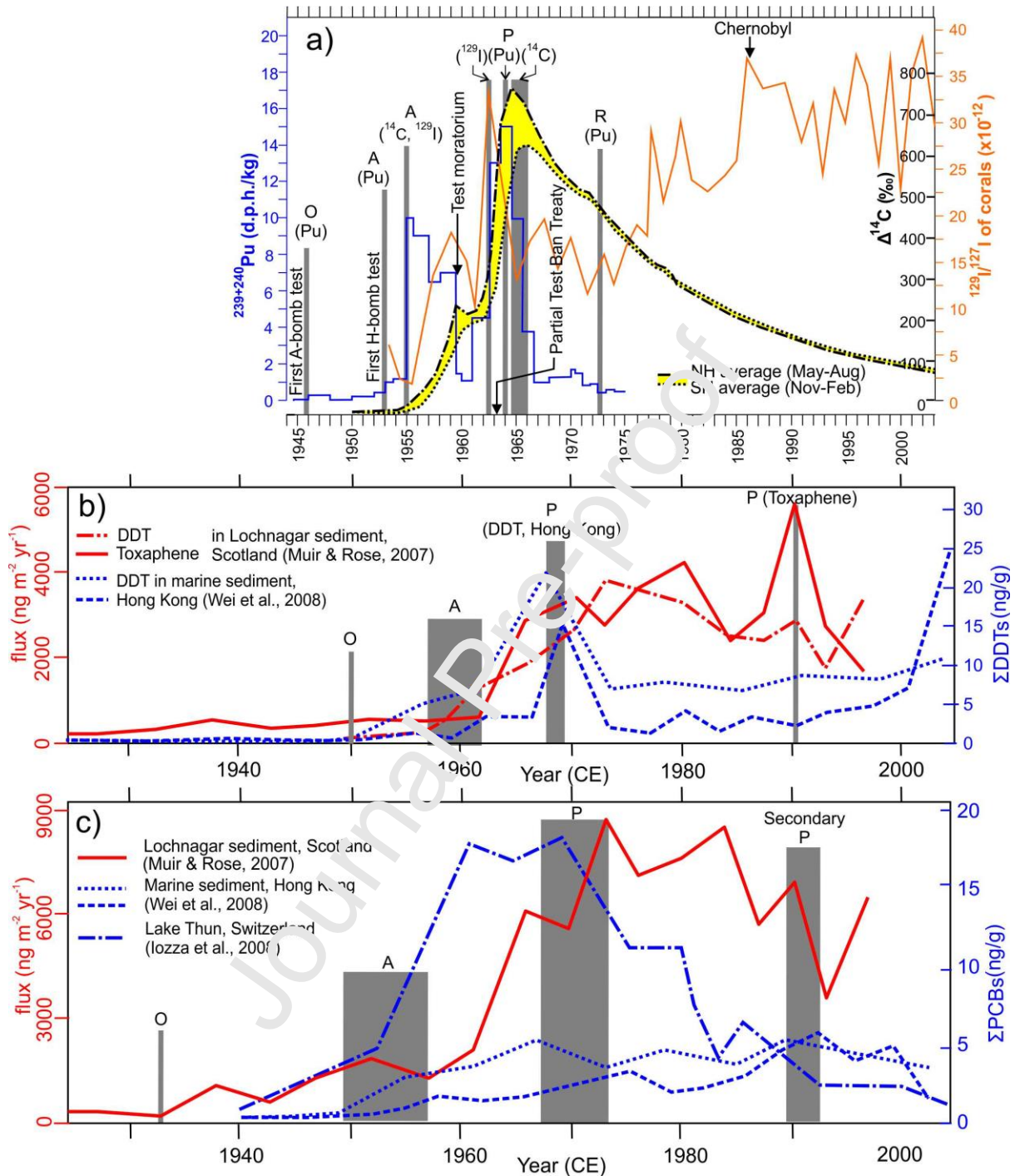


Fig. 12. Geological timelines of key GAEA events that initiated during the mid-20th century. a) radionuclides associated with fallout from above-ground nuclear detonations, including for $^{239+240}\text{Pu}$ (Koide et al., 1977), ^{14}C (Hua et al., 2021) and ^{129}I (Bautista et al., 2016); b) organochlorine pesticides DDT and toxaphene; and c) polychlorinated biphenyls. O – Onset; A – Acceleration/marked shift (and level of the event); P – Peak; R – Recovery.

- Persistent organochlorine pesticides were first commercially manufactured in the 1940s, showed a marked upturn in emissions in 1950 CE, clearly seen in the sedimentary record

(e.g., Muir and Rose, 2007; Iozza et al., 2008; Wei et al., 2008), and peaked in the 1960s–1990s. Although emissions have subsequently declined (Li and Macdonald, 2005), environmental signals have been slow to fall to pre-1950 CE levels (Fig. 12b).

- PCBs were first used in 1929 with peak environmental concentrations in the 1960s–1970s (Gałuszka et al., 2020), corresponding with production trends (Bigus et al., 2014). PCBs subsequently were banned across many developed countries in the 1970s and 1980s, leading to a rapid decrease in abundance.
- Plastics production has increased rapidly since the 1950s. Primary microplastics (e.g., synthetic textile fibres) and secondary microplastics (degradation products of macroplastics) have become ubiquitous in Anthropocene seabed, coastal and lake sediments and are even found in ice sheets (Leinfelder and Ivar do Sul, 2019; Zalasiewicz et al., 2019c). Even if emissions are successfully controlled, the large plastic reservoirs in the oceans (Pabortsava and Lampitt, 2020), together with release from legacy repositories such as eroding coastal landfill sites, will ensure their presence within the water column and deposition to the ocean floor for many centuries to come.

- 4) **Markers of events that reflect a long-lasting system change to a time interval wholly distinct from its precursors:** This includes the formation of a lower biodiversity planet with loss of faunal, fungal, floral and microbial species and homogenization through intended or accidental transfer of organisms globally, accentuated by the biotic effects of transitioning to a climate hotter than in Quaternary peak warmth (Steffen et al., 2018). This has already irreversibly reset the nature and trajectory of Earth's biosphere (Williams et al., 2015, 2022), and hence of Earth's biostratigraphical record. Another unprecedented shift in planetary state is the emergence of the technosphere, which has left a pronounced and unique stratigraphic signature (Haff, 2014, 2019). Its future is uncertain, but its influence lies behind most of the Anthropocene events that signal irreversible change to the Earth System. These processes are part of a Type 3a episode with prolonged historical precursors (described previously), but the rapidity, magnitude and novelty of change in the mid-20th century is consistent with Type 1 and 2 events. Other effects becoming apparent, and which are likely to impose long-lasting change (e.g., Tittensor et al., 2021), include:
- Thermal stress from rising temperatures is causing poleward range shifts of individual species and expansions of warm-adapted communities on all continents and most of the oceans, and severe range contractions of range-restricted species, leading to extinctions (Parmesan, 2006). Planktonic species ranges in the oceans have dramatically shifted in response to anthropogenic warming (Bryndum-Buchholz et al., 2020a; Jonkers et al., 2019). Fish and tropical coral species have also shifted their distributions, while some species have been lost to marine heat waves with more tolerant taxa forming novel ecosystems (Pandolfi, 2015; Bryndum-Buchholz et al., 2020b; Logan et al., 2021; Yamano et al., 2011). Terrestrial ecosystems have also shown substantial shifts (Loarie et al., 2009; Burrows et al., 2011).
 - Addition of CO₂ to the atmosphere, leading over time to the storage of more CO₂ in the deep ocean, is creating an ocean acidification event likely to last as long as the elevated CO₂ persists. This event will leave a long-term stratigraphic signal via rise in the Carbonate Compensation Depth (CCD) as deep-ocean carbonates progressively dissolve.

5. Discussion

The International Stratigraphic Guide clearly distinguishes geological events and episodes as two distinct concepts (Salvador, 1994, p. 73 and p. 117, respectively). In much geoscientific literature, though, the clarity in distinction between abrupt isochronous events and long diachronous episodes

is blurred or lost, in large part as these are informal terms lacking the rigorous definition of formal chronostratigraphic units. There is also a common misconception (e.g., Edgeworth et al., 2019, p. 338) that “...evidence that appears highly diachronous viewed close up will appear near-synchronous when viewed from millions of years away”. In reality, there is no simple dissolving of stratigraphical resolution with time. Many of the examples cited in this study show exceptional time-resolution even in the deep geological past (e.g., Gulick et al., 2019) that allow discrimination of isochronous events from diachronous episodes.

Our review of the extraordinary range and diversity of published deep-time ‘events’ demonstrates that following existing international stratigraphical guidance can enable more precise and effective geological analysis. We reiterate the distinction between ‘events’ and ‘episodes’ and recognise two, albeit intergradational, event categories, those with local and/or temporary effects and those with global, transformative effects.

Deep-time geological events, moreover, provide useful analogues to help investigate the Anthropocene as a chronostratigraphic unit. We show that conflicting notions of the Anthropocene may be resolved by distinguishing a long-duration, highly diachronous Anthropogenic Modification Episode (AME) from a globally isochronous array of events (the mid-20th century Great Acceleration Event Array or GAEA), markers of which locate the base of an Anthropocene chronostratigraphic unit. The contrast between, and complementarity of, the AME and GAEA helps visualize the scale and tempo of human impacts on the Earth System.

5.1 Deep-time event stratigraphy as a guide for the Anthropocene

Deep-time Type 1 Events compared with the Great Acceleration Event Array (GAEA)

The abrupt onsets or terminations of the major Proterozoic panglaciations are well marked events that provide effective guides for approved (Ediacaran) and proposed (Cryogenian) system boundaries. Both were rapid and massive state shifts as climate thresholds were crossed, in striking ‘Snowball Earth’ events that have so far not been repeated in the Phanerozoic.

The end-Cretaceous bolide impact, and resulting mass extinction, is the ultimate example of an isochronous event used to define a major chronostratigraphic boundary. Marked by a GSSP at the lowest stratigraphic signal of meteoritic debris, the K/Pg boundary was expressly defined at the moment of impact of the asteroid (Molina et al., 2006). This event is closely, but not perfectly, analogous to the signal associated with the above-ground testing of nuclear devices in the mid-20th century (Zalasiewicz et al., 2019b), where fallout radioisotopes are a potential primary guide for the base of the Anthropocene. The modern event differs in that the first nuclear detonations, in 1945 CE, led to regionally, not globally, detectable fallout. Although suggested as a GSSA boundary by Zalasiewicz et al. (2015), the global fallout from the later thermonuclear tests beginning in 1952 CE should provide a more effective and acceptable GSSP-based alternative (Waters et al., 2016); as a modification, the beginning of the calendar year identified (Head, 2019) might be adopted for closest integration with historical records.

Type 2 Events as analogues of anthropogenic markers

Type 2 events provide highly resolved correlation of individual beds across basins (e.g., tsunami deposits), across diverse environments (e.g., ash fall deposits), as regional climatic events (e.g., in the Pleistocene and Holocene), or by global palaeomagnetic reversals (e.g., Matuyama–Brunhes reversal). Note that whilst large volcanic eruptions and even super-eruptions (e.g. Toba at 74 ka) are events, large igneous provinces are sustained successions of eruptions contributing to significant climate change (e.g., the Siberian Traps implicated in the end-Permian extinction (Table 1)) and

hence represent episodes. In the Holocene, geochemical markers such as lead, copper, mercury and zinc are dispersed only locally to regionally in response to mining activity and metal processing and have different acmes in different parts of the world. Then, the upturn of burning of fossil fuels in the 20th century led to widespread aerial transport of these metals as particulates, which consequently become an important marker of the GAEA (Table 2). The radionuclide bomb-spike provides a similar, yet more isochronous and shorter-lived marker, with more precise correlatory value than the palaeomagnetic reversal that forms the primary guide for the Chibanian Stage and Middle Pleistocene Subseries; in neither case is there a resulting radical change to the Earth System.

Type 3 ‘Episodes’ as analogues of the Anthropogenic Modification Episode (AME)

At one end of the spectrum, the Great Oxidation Episode (GOE), the Great Ordovician Biodiversification Episode (GOBE), the Paleozoic Land Plant Radiation, represent protracted, complex, time-transgressive biological and chemical modifications of the planet over tens of millions of years. Although shorter in duration, Cretaceous Anoxic Oceanic Events (AOEs) and the Late Quaternary Extinction Episode (LQE), show similar multiple phases of evolution. All of these are not consistent with event stratigraphy in the sense of Ager (1973), Saito (1994, p. 117) and common usage especially for the Quaternary (Head et al., 2022a, in press). Rather, they are best viewed as episodes *sensu* NASCN (2005). Examined more closely, these episodes may include near-isochronous events, some regional and some global, and some used or promoted as guides for chronostratigraphic subdivision. The GOE, for instance, includes seemingly isochronous global events (Fig. 3) suggested as primary guides for potential revision of GTS units (Stieglitz et al., 2021). These include the radiation of oxide and hydroxide minerals, doubling terrestrial mineral species to about 4,000 (Hazen et al., 2008), which is analogous to the sudden formation by industrial synthesis of >180,000 synthetic mineral-like compounds and many thousands more anthropogenic chemicals, most since the 1950s (Hazen et al., 2017).

The GOBE is similarly a complex episode that includes regional Biotic Immigration Events (BIMEs), still diachronous but more short-lived. These are analogous to human-induced regional biotic immigrations that form the basis for the Santarosean and Santaugustinean North American Land Mammal Ages beginning ~14 ka ago and in the mid-16th century, respectively (Barnosky et al., 2014; Fig. 6b). The global carbon isotopic excursion (CIE) events present within the GOBE are apparently isochronous (Fig. 4), acting as useful guides for the recognition of (palaeontologically defined) stages. CIEs may individually show complex temporal patterns (e.g., Harper et al., 2014 on the Hirnantian HICE) but commonly include clear perturbations (typically rapid onsets) that have comparable stratigraphical utility to the Anthropocene nCIE with its sharp inflection ~1955 CE (Table 2, Fig. 11a).

The late Paleozoic Land Plant Radiation episode includes short-term global events such as chronostratigraphically significant CIEs and extinctions (Fig. 5). The proposal to define the Devonian–Carboniferous boundary using the dramatic changes associated with the Hangenberg Event (Aretz and Corradini, 2021) is comparable to the suggested use of the bomb spike onset as a global marker for the base of the Anthropocene. In both cases correlatory value is enhanced because of the approximate synchronicity with other stratally-recorded changes to the Earth System (Table 2).

Ocean Anoxic Events (OAEs), commonly associated with carbon isotopic excursions (CIEs), are widely used in global stratigraphic correlation, including some with formal chronostratigraphic expression (Fig. 7). Prominent among these is the sharp basal nCIE of the precursor phase of OAE1a, which is proposed as the primary marker for the Aptian Stage, and the OAE2 isotopic peak, proposed as a secondary marker for the Cenomanian–Turonian Stage boundary. OAE1a and OAE2 are prolonged

episodes (~1 Myr), but with CIEs that display clear onset, peak, plateau and recovery phases. This is comparable to the distinct phases of many of the event markers comprising the GAEA (Table 2), including to the sharp mid-20th century deflection in $\delta^{13}\text{C}$ values caused by fossil-fuel burning. Profound changes to biodiversity during OAE1a and OAE2 overall are consistent with Type 1 events, but although ocean-atmosphere components of the Earth System were perturbed, they eventually rebounded and recovered and hence are consistent with Type 2 events.

The Paleocene–Eocene Thermal Maximum Event (PETM) has been closely studied as an example of a brief, pronounced warming of the Earth System, and is a close analogue of a chronostratigraphic Anthropocene (Zalasiewicz et al., 2019b); both are marked by sudden negative carbon isotopic shifts (Figs. 8 and 11a) and associated global warming and ocean acidification. The Paleocene-Eocene boundary was the first Phanerozoic GSSP to be defined by chemostratigraphy. Based on the onset of the prominent nCIE, a Type 2 event, precise correlation between terrestrial and marine strata has permitted studies at high temporal resolution (e.g., Miller and Wright, 2017). The PETM and Anthropocene events differ in scale and speed. The PETM approximately doubled atmospheric CO_2 , raising global mean surface temperature by 4–8°C and sea level by ~15 m, acidified the oceans (Zachos et al., 2005, 2006; Zeebe et al., 2009, 2016) and led to geographically heterogeneous changes in precipitation (Schmitz and Pujalte, 2007; Carmichael et al., 2018; Rush et al., 2021). In comparison, since 1950 CE anthropogenic release of carbon has caused a ~45% rise in atmospheric CO_2 (Friedlingstein et al., 2020). The total amount of carbon added to the atmosphere over the last 70 years is not as large as in the PETM, but the rate of carbon release is an order of magnitude faster (Zeebe et al., 2016), and the global mean surface temperature rise of ~1°C and sea-level rise by 0.15 m are far from having equilibrated with Earth's new radiation balance (IPCC, 2021).

Some of the ground-to-air carbon transfer signals of the Anthropocene are highly distinctive compared to the PETM. Contemporary ice-sheets still directly preserve the increased CO_2 and CH_4 atmospheric contents (Fig. 10a) — such records are not available for the Eocene — while the nCIE is not yet as large for the Anthropocene as in the PETM (~2‰ vs. ~5‰), but is strikingly sharp (Figs. 8 and 11a). Additionally, high-temperature industrial burning has produced novel fly-ash and black carbon signals (Fig. 11b) that are now globally correlatable (Rose, 2015; Novakov et al., 2003). The resultant global warming and sea-level rise (Fig. 11e and f) are only beginning, but have already produced physical, chemical and biological signals in the stratigraphical record (Table 2), including rapid poleward range expansion of species, as during the PETM. The Benthic Foraminiferal Extinction (BFE) event and other dramatic biotic changes in the PETM represent Type 1 events, whereas a comparable, and more pervasive, interval of extinctions is already underway during the Anthropocene (Ceballos et al., 2015, 2020). The prolonged perturbations of the PETM over 100–200 kyr are consistent with a Type 3b episode, with a pre-onset phase equivalent to that evident prior to the GAEA.

The Late Quaternary Extinction (LQE) represents the first substantial human-caused transformation of the Earth's biota, which was followed by progressive replacement of wild-animal biomass by human and domestic animal biomass (Barnosky, 2008; Smil, 2011; Bar-On et al., 2018). In the Late Pleistocene, humans changed from acting as any other species within their ecosystem, to increasingly modifying other biota through cultural developments such as cooperative hunting and weapons. In the Holocene, ecosystems were further modified through agriculture, animal husbandry and settlements. However, the onset of those impacts was highly diachronous across an interval of more than three times the entire duration of the Holocene. These biotic transformations can neither be used as a narrative for justifying the Holocene, nor as a marker for that epoch. But, the diachronous nature of the LQE does not preclude the recognition of the Holocene as a

chronostratigraphic time unit distinct from the Pleistocene. Similarly, the diachronous accumulation of anthropogenic impacts over long time intervals — the “Anthropocene Event” of Gibbard et al. (2021, 2022) — does not preclude recognition of the Anthropocene Epoch as a chronostratigraphic unit, *sensu* Waters et al. (2016).

Events and episodes may be related to resilience theory, which states that a system subject to shock either recovers to its original state (Walker and Salt, 2006), or crosses a threshold and begins to operate in a different state. The interconnected components of Earth’s biosphere, hydrosphere, cryosphere, atmosphere, and geosphere form a resilient Earth System, able to resist considerable disturbance. But, the Earth System has also changed state when disturbance overwhelmed the existing structure. ‘Episodes’ can be either: **state shifting**, like the GOE, with its fundamental change to all components of the Earth System, and the GOBE and Paleozoic Land Plant Radiation with their sustained increase in species biodiversity; or show **resilience to change** with Earth System recovery and maintenance of its pre-existing state. Resilience examples include the Mid-Miocene Climate Optimum (MMCO) and mid-Piacenzian Warm Period (mPWP), both warm interludes in an otherwise icehouse climate induced by late Cenozoic glaciation (Fig. 9). The Cretaceous OAE1a and OAE2 show ocean anoxia and CIEs that are similarly resilient, but contain state shifts in biodiversity. Resilience dynamics also apply to Type 2 events (Fig. 1), such as the impact of a tsunami, that do not overwhelm the Earth System. But Type 1 events, notably including the bolide impact at the K-Pg boundary, are unequivocally state-shifting.

5.2 Linkages between the GAEA and AME, and their relation to the Anthropocene

We identify the long history of transformative anthropogenic alteration of the planet as an Anthropogenic Modification Episode (AME) (Fig. 13). In part analogous to a later modern human (*sensu lato*) biozone, including their fossil remains, it extends to incorporating human traces via physical and chemical modification of sediments. It fully recognizes the prolonged, diachronous, unfolding record of human–environmental interactions within a generally stable Holocene Earth System, whether they be deforestation, spread of agriculture, or urbanization as noted by, for example, Edgeworth et al. (2015), Ellis et al. (2020), Gibbard et al. (2021, 2022), Ruddiman (2018) and Ruddiman et al. (2020). But strictly speaking the long trajectory of human modification to the planet represents an episode, not a single event, or event array, as typically understood in the Quaternary.

Although loosely based on the concept that Gibbard et al. (2021, 2022) called an ‘Anthropocene Event’, the AME differs in that it is essentially geological, rather than interdisciplinary in nature. It contains many shorter-term or locally-scaled events nested within it, including local and regional events of geological and wider significance. Most notably, the AME includes the largely isochronous array of events of global reach recognised here as the Great Acceleration Event Array or GAEA (Fig. 13). Each event, with its stratigraphic marker(s), is consistent with the traditional event-stratigraphic concept. The GAEA, given its intensity, planetary significance and global isochroneity, justifies the transition from the Holocene into the Anthropocene as an epoch/series, much as do the transformative and globally-recognizable deep-time events discussed above. It also acknowledges the reality of the Anthropocene concept as proposed originally by Crutzen and Stoermer (2000) and Crutzen (2002), now widely used by the Earth System science (ESS) community and beyond, the globally isochronous geological signals of which have clear and demonstrable chronostratigraphic utility.

This chronostratigraphic Anthropocene concept, based upon a global response to focused human transformation of the planet, emphatically does not record the *first* human impact, nor does it

preclude or diminish in importance the long human record of influence extending back millennia. Rather, the proposed Anthropocene Epoch marks a point where overwhelming human impact has rapidly — essentially instantaneously in geological time— extensively and in many ways irreversibly modified the Earth System and produced globally recognizable geological signals coinciding precisely with the ESS definition (Steffen et al., 2016).

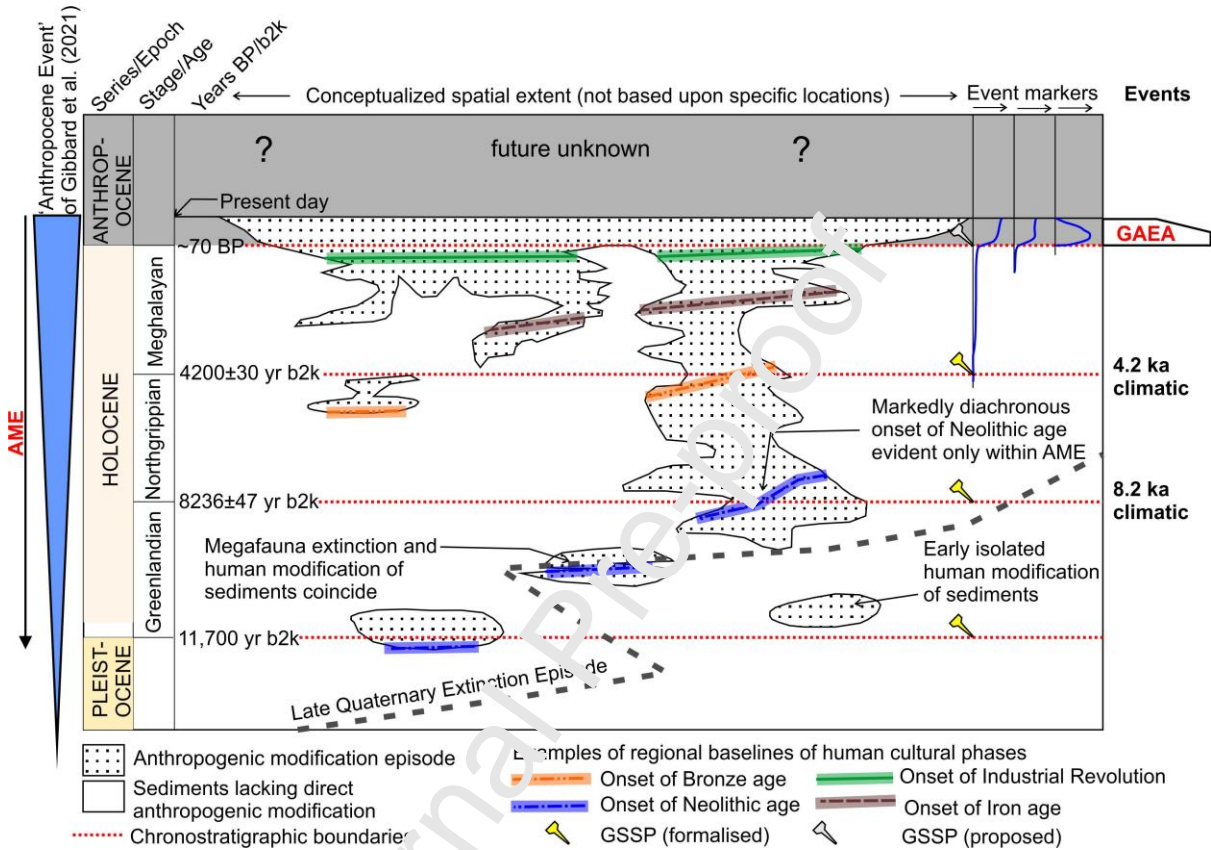


Fig. 13. Conceptualized visualisation of the relationships between chronostratigraphic units, isochronous event markers and the highly diachronous Anthropogenic Modification Episode (AME) and Late Quaternary Extinction Episode across the globe (regions schematic with no scale). The onset of archaeological ages (Neolithic, Bronze and Iron ages) and characteristics of the onset of the Industrial Revolution are diachronous and preserved within the AME.

A chronostratigraphic inception based on stratigraphic signals associated with the mid-20th century is both appropriate and practical. The array of stratigraphic markers associated with this Earth System change (Table 2), that we term the GAEA, may be used both to define and characterise the ensuing stratigraphic unit and thus should be represented in potential GSSP sections. Defining an Anthropocene epoch guided by the GAEA, as for the Northgrippian and Meghalayan stages guided by the 8.2 ka and 4.2 ka climatic events (Table 1, Fig. 13), provides an explicitly isochronous framework for temporally constraining and analyzing the scale and nature of diachronous processes on Earth.

Recognizing an Anthropogenic Modification Episode (AME) to encompass *all* of the time humans have been modifying the planet will go a long way towards improving communication by removing the ambiguity of how scientists and the general public are using the term Anthropocene. By contrast, giving the same name, Anthropocene, to both the extended diachronous episode (the

‘Anthropocene Event’ of Gibbard et al., 2021, 2022) and the chronostratigraphic unit, would be confusing, particularly given the association of the ‘cene’ suffix with series/epochs of the Cenozoic Erathem/Era and the original intent of the term. In this case, slow changes over many millennia (the AME) have precipitated, in the very recent past, a cascade of abrupt events (the GAEA). These have taken the Earth close to — or perhaps already beyond — major climatic and biospheric tipping points (Lenton et al., 2019), towards states outside of Quaternary and not just Holocene norms.

We stress the importance of differentiating between the long *process* leading to the Anthropocene, from the Late Quaternary Extinction Episode to the start of the Industrial Revolution, from the *results* of the Great Acceleration, leading to the geologically sudden onset of a different Earth System with a different sedimentary expression. Disentangling the process from the result is important, especially to help understand how the Anthropocene became reality.

Ultimately, the recognition of the Anthropocene as a chronostratigraphic unit in the GTS is justified through the planetary consequences of modern human impacts rather than its causes. The Cenozoic Era is justified by the fundamental transformation of biota across the planet, and not because of the cause of that transformation, the 66 Ma asteroid impact. An Anthropocene epoch clearly distinguishes the transformative role of technologically advanced humans from the countless previous generations of human impact that had far fewer profound effects on the Earth System. Indeed, a lower boundary for the Anthropocene series coincident with the Great Acceleration not only reflects the increasing numbers of people on the planet from 1950 onwards, but also their individually increasing rates of the consumption of raw materials, of land use, of farmed animals, of the production of multiple new products, and of their environmental impact on both planetary climate and biodiversity. It reflects the combination of people and their rapidly advancing technologies, forming a radical departure from the Holocene ‘norm’.

6. Summary and conclusions

The planetary changes driven by humans can be placed within a geological event framework, but first it is necessary to define the meaning of the term ‘event’. Significant ‘events’ have been used, or proposed, as guides for the bases of chronostratigraphic units, whereas the more protracted and complex examples, such as the Great Oxidation ‘Event’ and Great Ordovician Biodiversification ‘Event’, are more properly termed ‘episodes’, as these contain multiple diachronous ‘phases’ as well as nested ‘events’. With increasing resolution, even relatively short-term phenomena such as the ~0.2 Myr Paleocene–Eocene Thermal Maximum may be seen to include multiple briefer events, and so be better described under the term ‘episode’. In many of the cases described in this review, events are linked with, and are brief components of, much longer episodes. Events and episodes form a continuum: distinction is relatively straightforward between end-members, and is less obvious in the middle ground. At the scale of any study, ‘events’ are best reserved for those phenomena simple and brief enough to provide precise correlatory ties, as in the original definition and subsequent stratigraphic guidance, while ‘episodes’ are protracted, multifactorial and typically diachronous intervals.

Within this perspective, an Anthropogenic Modification Episode (AME) of at least ~50 ka duration may be proposed to encompass all geologically significant changes made by humans to the environment. Within that long AME are many more synchronous brief events. By far the most globally instantaneous and recognizable of these comprise the Great Acceleration Event Array (GAEA) that we recognise clustering around the mid-20th century. The signals are sufficiently strong and widespread in the geological record, and reflect planetary rearrangement of sufficient scale to be used in defining an Anthropocene at the rank of epoch/series. In applying event stratigraphy to

the Anthropocene in this more conventional way, chronostratigraphic classification is underpinned rather than replaced, via brief, relatively simple events with high, regional to global, correlation potential.

Some of these stratigraphic events are novel, with little or no precedent in Earth's geological record, such as the sedimentary dispersal of microplastics, of synthetic persistent organic pollutants, of myriad technofossil types, of fly-ash, and of artificial radionuclides. Other markers reflect state shifts in the Earth System: associated with reduced global biodiversity and the marked translocation of non-native species, global warming, sea-level rise and ocean acidification that ultimately make the Anthropocene radically distinct from the Holocene.

That the GAEA should guide the Anthropocene base is consistent with normal geological practice, such as the '8.2 ka climatic event' and '4.2 ka climatic event' used to subdivide the Holocene, the onset of the PETM hyperthermal event that defines the base of the Eocene, and the bolide impact event defining the Paleogene base.

We thus propose recognizing a long, slow-unfolding Anthropocene Modification Episode (the AME), outside of formal chronostratigraphy, leading to and incorporating the Great Acceleration Event Array (the GAEA) that signals the onset of a chronostratigraphic Anthropocene epoch/series. This proposed terminology accurately reflects the various human caused changes to the planet, while acknowledging that many Earth System parameters have, in the past 70 years, escaped the envelope of variability of the Holocene Epoch.

Acknowledgements

Contributing authors are members of the Anthropocene Working Group (AWG), of the Subcommittee on Quaternary Stratigraphy (SQC), a component body of the International Commission on Stratigraphy (ICS). The paper was inspired by a publication by Gibbard et al. (2021), which initiated our critical enquiry into the Anthropocene as a geological event.

Author contributions

All authors developed and contributed to drafts of the text as part of their voluntary AWG efforts. The concept of the study was designed by C.W. in association with J.Za., M.J.H., S.T., M.Wi., A.B., M.Wa., and W.S. Table 1 was developed by M.Wi., C.W., I.F. and M.Wa and Table 2 by C.W. in association with all authors. Fig. 1 was developed by C.W., M.Wi, S.W. and M.Wa, Figs. 2, 3, 5, 6, 7 and 12 were drafted by C.W., Fig. 4 by M.Wi., Fig. 8b by S.W., Fig. 9 by F.Mc. and M.Wi, Figs. 10 and 11 by S.T. and C.W. and Fig. 13 by R.L. and C.W. Harry Dowsett and Alan Haywood are thanked for providing original files used in the compilation of Fig. 9b, and Gabi Ogg for Fig. 8a (reproduced with permission from Elsevier).

Declaration of competing interest

The authors declare that they have no known competing financial interests or personal relationships that could have appeared to influence the work reported in this paper.

The authors declare the following financial interests/personal relationships which may be considered as potential competing interests:

Colin Waters (NB. funding is for AWG, which includes coauthors too) reports a relationship with Haus der Kulturen der Welt, Berlin that includes: funding grants.

Journal Pre-proof

References

- Ager, D.V. (1973). *The Nature of the Stratigraphical Record*, 1st ed. Chichester: John Wiley and Sons, 114 p.
- Aigner, T. (1982) Calcareous Tempestites: Storm-dominated Stratification in Upper Muschelkalk Limestones (Middle Trias, SW-Germany). In: Einsele, G. and Seilacher, A. (eds) *Cyclic and Event Stratification*. Springer, Berlin, Heidelberg, pp. 180–198. https://doi.org/10.1007/978-3-642-75829-4_13
- Alegret, L., Arreguín-Rodríguez, G.J., Trasviña-Moreno, C.A. and Thomas, E. (2021). Turnover and stability in the deep sea: Benthic foraminifera as tracers of Paleogene global change. *Global and Planetary Change*, 196, 103372. <https://doi.org/10.1016/j.gloplacha.2020.103372>.
- Aretz, M. and Corradini, C. (2021). Global review of the Devonian–Carboniferous Boundary: an introduction. *Palaeobiodiversity and Palaeoenvironments*, 101, 285–293. <https://doi.org/10.1007/s12549-021-00499-8>
- Aubry, M-P., Ouda, K., Depuis, C. et al. (2007). The Global Standard Stratotype-section and Point (GSSP) for the base of the Eocene Series in the Dababiya section (Egypt). *Episodes*, 30, 271–286. <https://doi.org/10.7916/D8BP0C85>
- AWG (2019). Announcement by the Anthropocene Working Group, 2019. <http://quaternary.stratigraphy.org/working-groups/anthropocene/>
- Bagnell, A. and DeVries, T. (2021). 20th century cooling of the deep ocean contributed to delayed acceleration of Earth's energy imbalance. *Nature Communications*, 12, 4604. <https://doi.org/10.1038/s41467-021-24472-3>
- Barnosky, A.D. (2008). Megafauna biomass tradeoff as a driver of Quaternary and future extinctions. *Proceedings of the National Academy of Sciences*, 105 (Supplement 1), 11543-11548. <https://doi.org/10.1073/pnas.0801918105>
- Barnosky, A.D., Matzke, N., Tomiya, S. et al. (2011). Has the Earth's sixth mass extinction already arrived? *Nature*, 471, 51–57. <https://doi.org/10.1038/nature09678>
- Barnosky, A.D., Holmes, M., Kirchholtes, R., et al. (2014). Prelude to the Anthropocene: Two new North American Land Mammal Ages (NALMAs). *Anthropocene Review*, 1(3), 225–242. <https://doi.org/10.1177/2053019614547433>
- Bar-On, Y.M., Phillips, R. and Milo, R. (2018). The biomass distribution on Earth. *Proceedings of the National Academy of Sciences*, 115, 6506–6511. <https://doi.org/10.1073/pnas.1711842115>
- Bartoli, G., Sarnthein, M., Weinelt, M., Erlenkeuser, H., Garbe-Schönberg, D and Lea, D.W. (2005). Final closure of Panama and the onset of northern hemisphere glaciation. *Earth and Planetary Science Letters*, 237, 33–44. <https://doi.org/10.1016/j.epsl.2005.06.020>
- Baud, A., Jenny, J.P., Francus, P. and Gregory-Eaves, I. (2021). Global acceleration of lake sediment accumulation rates associated with recent human population growth and land-use changes. *Journal of Paleolimnology*, 66(4), 453-467. <https://doi.org/10.1007/s10933-021-00217-6>
- Bautista, A.T., Matsuzaki, H. and Siringan, F.P. (2016). Historical record of nuclear activities from ¹²⁹I in corals from the northern hemisphere (Philippines). *Journal of Environmental Radioactivity*, 164, 174–181. <https://doi.org/10.1016/j.jenvrad.2016.07.022>

- Becker, R.T., Marshall, J.E.A. and Da Silva, A.-C. (2020). Chapter 22: The Devonian Period. In: Gradstein, F., Ogg, J., Schmitz, M. and Ogg, G. (eds.) *A Geologic Time Scale 2020*, Elsevier B.V. 733–810.
- Bekker A., (2022). Huronian Glaciation. In: Gargaud M. et al. (eds) *Encyclopedia of Astrobiology*. Springer, Berlin, Heidelberg. https://doi.org/10.1007/978-3-642-27833-4_742-5
- Beil, S., Kuhnt, W., Holbourn, A., Scholz, F., Oxmann, J., Wallmann, K., Lorenzen, J., Aquit, M., Chellai, E.-H. et al. (2020). Cretaceous oceanic anoxic events prolonged by phosphorous cycle feedbacks. *Climate of the Past*, 16, 757–782. <https://doi.org/10.5194/cp-16-757-2020>
- Bengtson, P., Cobban, W.A., Dodsworth, P.A.U.L. and Gale, A.S. (1996). The Turonian stage and substage boundaries. *Bulletin de l'Institut royal des Sciences naturelles de Belgique, Sciences de la Terre*, 66(69), e79.
- Bigus, P., Tobiszewski, M. and Namieśnik, J. (2014). Historical records of organic pollutants in sediment cores. *Marine Pollution Bulletin*, 78(1), 26–42. <https://doi.org/10.1016/j.marpolbul.2013.11.008>
- Bindler, R., Renberg, I., Anderson, N.J., Appleby, P.G., Emtery, O. and Boyle, J., 2001. Pb isotope ratios of lake sediments in West Greenland: inferences on pollution sources. *Atmospheric Environment*, 35(27), 4675–4685.
- Bini, M., Zanchetta, G., Perşoiu, A., Cartier, R., Catalano, F., Cacho, I., Dean, J. R., Di Rita, F., Drysdale, R. N., Finnè, M., Isola, I., Jalali, B., Lirer, F., Magri, D., Masi, A., Marks, L., Mercuri, A. M., Peyron, O., Sadori, L., Sicre, M.-A., Welc, F., Zielhofer, C. and Briquet, E. (2019). The 4.2 ka BP Event in the Mediterranean region: an overview. *Climate of the Past*, 15, 555–577. <https://doi.org/10.5194/cp-15-555-2019>, 2019.
- Bond, T.C., Bhardwaj, E., Dong, R., Jogaraj, S., Jung, S., Roden, C., Streets, D.G. and Trautmann, N.M. (2007). Historical emissions of black and organic carbon aerosol from energy-related combustion, 1850–2000. *Global Biogeochemical Cycles*, 21, GB2018. <https://doi.org/10.1029/2006GB002840>
- Björck, S., Walker, M.J.C., Cwynar, L.C., Johnsen, S., Knudsen, K.-L., Lowe, J.J., Wohlfarth, B., INTIMATE Members (1998). An event stratigraphy for the Last Termination in the North Atlantic region based on the Greenland ice-core record: a proposal by the INTIMATE group. *Journal of Quaternary Science*, 13, 273–292. [https://doi.org/10.1002/\(SICI\)1099-1417\(199807/08\)13:4<273::AID-JQS386>3.0.CO;2-A](https://doi.org/10.1002/(SICI)1099-1417(199807/08)13:4<273::AID-JQS386>3.0.CO;2-A)
- Böhme, M. (2003). The Miocene Climatic Optimum: Evidence from ectothermic vertebrates of Central Europe. *Palaeogeography, Palaeoclimatology, Palaeoecology*, 195, 389–401. [https://doi.org/10.1016/S0031-0182\(03\)00367-5](https://doi.org/10.1016/S0031-0182(03)00367-5)
- Boulila, S., Charbonnier, G., Spangenberg, J.E., Gardin, S., Galbrun, B., Briard, J. and Le Callonnec, L. (2020). Unraveling short- and long-term carbon cycle variations during the Oceanic Anoxic Event 2 from the Paris Basin Chalk. *Global and Planetary Change*, 186, 103126, <https://doi.org/10.1016/j.gloplacha.2020.103126>
- Boutron, C.F., Candelone, J.P. and Hong, S. (1995). Greenland snow and ice cores: Unique archives of large-scale pollution of the troposphere of the Northern Hemisphere by lead and other heavy metals. *Science of the Total Environment*, 160, 233–241. [https://doi.org/10.1016/0048-9697\(95\)04359-9](https://doi.org/10.1016/0048-9697(95)04359-9)

- Bowen, G.J. and Zachos, J.C. (2010). Rapid carbon sequestration at the termination of the Palaeocene–Eocene Thermal Maximum. *Nature Geoscience*, 3(12), 866–869. <https://doi.org/10.1038/ngeo1014>
- Bowen, G.J., Maibauer, B.J., Kraus, M.J. et al. (2015). Two massive, rapid releases of carbon during the Paleocene-Eocene thermal maximum. *Nature Geoscience*, 8, 44–47. <https://doi.org/10.1038/ngeo2316>
- Bowman, C.N., Young, S.A., Kaljo, D., Eriksson, M.E., Them, T.R., Hints, O., Martma, T. and Owens, J.D. (2019). Linking the progressive expansion of reducing conditions to a stepwise mass extinction event in the late Silurian oceans. *Geology*, 47, 968–972. <https://doi.org/10.1130/G46571.1>
- Brinkhuis, H., Collinson, M.E., Sluijs, A., Sinninghe-Damste, J.S. et al., (2006). Episodic fresh surface waters in the Eocene Arctic Ocean. *Nature*, 441, 606–609. <https://doi.org/10.1038/nature04692>
- Brook, B.W. and Barnosky, A.D. (2012). Quaternary extinctions and their link to climate change. In: *Saving a Million Species: Extinction Risk from Climate Change*, ed. by Hannah, Island Press, Washington, D.C. pp. 179-198.
- Bryn, P., Solheim, A., Berg, K., Lien, R., Forsberg, C.F., Hafliðsson, H., Ottesen, D. and Rise, L. (2003). The Storegga Slide Complex: repeated large scale sliding in response to climatic cyclicity, in: Locat, J., Mienert, J. (Eds.), *Submarine Mass Movements and their Consequences Advances in Natural and Technological Hazards Research*, vol. 19. Kluwer Academic Publishers, Dordrecht, pp. 215–222.
- Bryndum-Buchholz, A., Prentice, F., Tittensor, D.P., Blanchard, J.L., Cheung, W.W.L., Christensen, V., Galbraith, E.D., Maury, O. and Lotze, H.K. (2020a). Differing marine animal biomass shifts under 21st century climate change between Canada's three oceans. *Facets*, 5, 105–122. <https://doi.org/10.1139/facets-2019-0025>
- Bryndum-Buchholz, A., Boyce, D.G., Tittensor, D.P., Christensen, V., Bianchi, D. and Lotze, H.K. (2020b). Climate-change impacts and fisheries management challenges in the North Atlantic Ocean. *Marine Ecology Progress Series*, 646, 1–17. <https://doi.org/10.3354/meps13438>
- Burgess, S.D., Bowring, S.A., Shen, S.Z. et al. (2014). High-precision timeline for Earth's most severe extinction. *Proceedings of the National Academy of Sciences*, 111, 3316–3321. <https://doi.org/10.1073/pnas.1317692111>
- Burke, K.D., Williams, J.W., Chandler, M.A., Haywood, A.M., Lunt, D.J. and Otto-Bliesner, B.L. (2018). Pliocene and Eocene provide best analogs for near-future climates. *Proceedings of the National Academy of Sciences*, 115, 13288–13293. <https://doi.org/10.1073/pnas.1809600115>
- Burrows, M.T., Schoeman, D.S., Buckley, L.B. et al. (2011). The pace of shifting climate in marine and terrestrial ecosystems. *Science*, 334, 652–655. <https://doi.org/10.1126/science.1210288>.
- Calner, M. (2008). Silurian global events – at the tipping point of climate change. In: Elewa, A.M.T. (ed.), *Mass Extinction*, Springer, pp. 21–57.
- Candelone, J.P. and Hong, S. (1995). Post-Industrial Revolution changes in large-scale atmospheric pollution of the northern hemisphere by heavy metals as documented in central Greenland snow and ice. *Journal of Geophysical Research*, 100, 16605–16616. <https://doi.org/10.1029/95JD00989>
- Carmichael, M.J., Pancost, R.D. and Lunt, D.J. (2018). Changes in the occurrence of extreme precipitation events at the Paleocene–Eocene thermal maximum. *Earth and Planetary Science Letters*, 501, 24–36. <https://doi.org/10.1016/j.epsl.2018.08.005>

- Carmichael, S.K., Waters, J.A., Königshof, P., Suttner, T.J., Kido, E. et al. (2019). Paleogeography and paleoenvironments of the Late Devonian Kellwasser event: A review of its sedimentological and geochemical expression. *Global and Planetary Change*, 183, 102984. <https://doi.org/10.1016/j.gloplacha.2019.102984>
- Caruthers, A.H., Smith, P.L. and Gröcke, D.R. (2013). The Pliensbachian–Toarcian (Early Jurassic) extinction, a global multi-phased event. *Palaeogeography, Palaeoclimatology, Palaeoecology*, 386, 104–118. <https://doi.org/10.1016/j.palaeo.2013.05.010>
- Catling, D.C. and Zahnle, K.J. (2020). The Archean atmosphere. *Science Advances*, 6, eaax1420. <https://doi.org/10.1126/sciadv.aax1420>
- Ceballos, G., Ehrlich, P.R., Barnosky, A.D., et al. (2015). Accelerated modern human-induced species losses: Entering the sixth mass extinction. *Scientific Advances*, 1(5), e1400253. <https://doi.org/10.1126/sciadv.1400253>
- Ceballos, G., Ehrlich, P.R. and Raven, P.H. (2020). Vertebrates on the brink as indicators of biological annihilation and the sixth mass extinction. *Proceedings of the National Academy of Sciences*, 117, 13596–13602. <https://doi.org/10.1073/pnas.1922686117>
- Channell, J.E.T., Singer, B.S. and Jicha, B.R. (2020). Timing of Quaternary geomagnetic reversals and excursions in volcanic and sedimentary archives. *Quaternary Science Reviews*, 228, 1–29. <https://doi.org/10.1016/j.quascirev.2019.106114>
- Clark, P.U., Shakun, J.D., Marcott, S.A., et al. 2016. Consequences of twenty-first-century policy for multi-millennial climate and sea-level change. *Nature Climate Change* 6, 360–369. <https://doi.org/10.1038/nclimate2923>
- Cohen, K.M., Finney, S.C., Gibbard, P.L. and Fan, J.X. (2013). The ICS International Chronostratigraphic Chart. *Episodes*, 36(3), 199–204. <https://doi.org/10.18814/epiiugs/2013/v36i3/002>
- Collinson, M.E., Smith, S.E., van Konijnenburg-van Cittert, J.H.A., Batten, D.J., van der Burgh, J., Barke, J. and Marone, F. (2013). New observations and synthesis of Paleogene heterosporous water ferns. *International Journal of Plant Sciences*, 174, 350–363. <https://doi.org/10.1086/668249>
- Cramer, B.B. and Jarvis, I. (2020). Chapter 11: Carbon Isotope Stratigraphy. In: Gradstein, F., Ogg, J., Schmitz, M. and Ogg, G. (eds.) *A Geologic Time Scale 2020*, Elsevier B.V. 309-343.
- Cramer, B.S. and Kent, D.V. (2005). Bolide summer: The Paleocene/Eocene thermal maximum as a response to an extraterrestrial trigger. *Palaeogeography, Palaeoclimatology, Palaeoecology*, 224(1-3), 144–166. <https://doi.org/10.1016/j.palaeo.2005.03.040>
- Crouch, E.M., Heilmann-Clausen, C., Brinkhuis, H., Morgans, H.E.G., Rogers, K.M., Egger, H. and Schmitz, B. (2001). Global dinoflagellate event associated with the late Paleocene thermal maximum. *Geology* 29, 315–318. [https://doi.org/10.1130/0091-7613\(2001\)029<0315:GDEAWT>2.0.CO;2](https://doi.org/10.1130/0091-7613(2001)029<0315:GDEAWT>2.0.CO;2)
- Crutzen, P.J. (2002). Geology of mankind. *Nature*, 415, p. 23. https://doi.org/10.1007/978-3-319-27460-7_10
- Crutzen, P.J. and Stoermer, E.F. (2000). The "Anthropocene". *Global Change. IGBP Newsletter*, 41, 17–18.

- Dahl, T.W. and Arens, S.K.M. (2020). The impacts of land plant evolution on Earth's climate and oxygenation state – An interdisciplinary review. *Chemical Geology* 547, 119665. <https://doi.org/10.1016/j.chemgeo.2020.119665>
- Dansgaard, W., Johnsen, S.J., Clausen, H.B., Dahl-Jensen, D., Gundestrup, N.S., Hammer, C.U., Hvidberg, C.S., Steffensen, J.P., Sveinbjörnsdóttir, A.E., Jouzel, J. and Bond, G. (1993). Evidence for general instability of past climate from a 250-kyr ice-core record. *Nature* 364, 218–220. <https://doi.org/10.1038/364218a0>.
- Davies, N.S. and Gibling, M.R. (2010). Cambrian to Devonian evolution of alluvial systems: the sedimentological impact of the earliest land plants. *Earth-Science Reviews*, 98, 171–200. <https://doi.org/10.1016/j.earscirev.2009.11.002>
- Dearing, J.A. and Jones, R.T. (2003). Coupling temporal and spatial dimensions of global sediment flux through lake and marine sediment records. *Global and Planetary Change*, 39, 147–168. [https://doi.org/10.1016/S0921-8181\(03\)00022-5](https://doi.org/10.1016/S0921-8181(03)00022-5)
- Denison, C.N. (2021). Stratigraphic and sedimentological aspects of the worldwide distribution of *Apectodinium* in Paleocene/Eocene Thermal Maximum deposits. Geological Society, London, Special Publications, 511. <https://doi.org/10.1144/SP511-2020-46>
- Dickens, G.R., O'Neil, J.R., Rea, D.K., and Owen, R.M. (1995). Dissociation of oceanic methane hydrate as a cause of the carbon isotope excursion at the end of the Paleocene. *Paleoceanography*, 10(6), 965–971. <https://doi.org/10.1029/95PA0208>.
- Dowsett, H.J., Robinson, M.M., Stoll, D.K., Foley, K.M., Johnson, A.L.A., Williams, M. and Riesselman, C.R. (2013). The PRISM (Pliocene palaeoclimate) reconstruction: time for a paradigm shift. *Philosophical Transactions of the Royal Society A* 371, 20120524. <http://dx.doi.org/10.1098/rsta.2012.0524>
- Edgeworth, M., Richter, D.DeB., Waters, C.N., Haff, P., Neal, C. and Price, S.J. (2015). Diachronous beginnings of the Anthropocene: The lower bounding surface of anthropogenic deposits. *Anthropocene Review* 2(1), 33–58. <https://doi.org/10.1177/2053019614565394>
- Edgeworth, M., Ellis, E.C., Gibbard, P., Neal, C. and Ellis, M. (2019). The chronostratigraphic method is unsuitable for determining the start of the Anthropocene. *Progress in Physical Geography* 43(3) 334–344. <https://doi.org/10.1177/0309133319831673>
- Edwards, D., Cherns, L. and Raven, J.A. (2015). Could land-based early photosynthesizing ecosystems have bioengineered the planet in mid-Palaeozoic times? *Palaeontology*, 58(5), 803–837. <https://doi.org/10.1111/pala.12187>
- Ellis, E.C., Beusen, A.H. and Goldewijk, K.K. (2020). Anthropogenic Biomes: 10,000 BCE to 2015 CE. *Land*, 9 (5), 129. <https://doi.org/10.3390/land9050129>
- EPICA Community Members (2006). One-to-one coupling of glacial climate variability in Greenland and Antarctica. *Nature*, 444, 195–198. <https://doi.org/10.1038/nature05301>
- Fiałkiewicz-Kozieł, B., Smieja-Krol, B., Frontasyeva, M., Slowinski, M., Marcisz, K., Lapshina, E., Gilbert, D., Buttler, A., Jassey, V.E., Kaliszan, K., Laggoun-Defarge, F., Kolaczek, P. and Lamentowicz, M., (2016). Anthropogenic- and natural sources of dust in peatland during the Anthropocene. *Scientific Reports*, 6, 38731. <https://doi.org/10.1038/srep38731>

- Fiałkiewicz-Kozieł, B., Bao, K. and Smieja-Król, B. (2022). Geographical drivers of geochemical and mineralogical evolution of Motianling peatland (Northeast China) exposed to different sources of rare earth elements and Pb, Nd, and Sr isotopes. *Science of the Total Environment*, 807, 150481. <https://doi.org/10.1016/j.scitotenv.2021.150481>
- Friedlingstein, P., O'Sullivan, M., Jones, M.W. et al. (2020). Global Carbon Budget 2020. *Earth System Science Data*, 12(4), 3269–3340. <https://doi.org/10.5194/essd-2021-386>
- Frieling, J., Svensen, H.H., Planke, S., Cramwinckel, M.J., Selnes, H. and Sluijs, A. (2016). Thermogenic methane release as a cause for the long duration of the PETM. *Proceedings of the National Academy of Sciences*, 113, 12059–12064. <https://doi.org/10.1073/pnas.1603348113>
- Frieling, J., Peterse, F., Lunt, D.J., Bohaty, S.M., Sinninghe Damsté, J.S., Reichert, G.-J., and Sluijs, A., (2019). Widespread warming before and elevated barium burial during the Paleocene-Eocene Thermal Maximum: Evidence for methane hydrate release? *Paleogeography and Paleoclimatology*, 34(4), 546–566. <https://doi.org/10.1029/2018PA033425>
- Gale, A.S., Mutterlose, J. and Batenburg, S. (2020). The Cretaceous Period, Chapter 27. In: Gradstein, F., Ogg, J., Schmitz, M. and Ogg, G. (eds.) *A Geologic Time Scale 2020*, Elsevier B.V. 1023-1086.
- Gałaszka, A. and Rose, N. (2019). Organic compounds. In: Zalasiewicz, J., Waters, C., Williams, M. et al. (eds) *The Anthropocene as a Geological Time Unit: A Guide to the Scientific Evidence and Current Debate*. Cambridge: Cambridge University Press, pp. 176–192.
- Gałaszka, A. and Wagemann, M. (2019). Metals. In: Zalasiewicz, J., Waters, C., Williams, M. et al. (eds) *The Anthropocene as a Geological Time Unit: A Guide to the Scientific Evidence and Current Debate*. Cambridge: Cambridge University Press, pp. 173–186.
- Gałaszka, A., Migaszewski, Z.M. and Rose, N.L. (2020). A consideration of polychlorinated biphenyls as a chemostratigraphic marker of the Anthropocene. *The Anthropocene Review*, 7(2) 138–158. <https://doi.org/10.1177/2053019620016158>
- Garzione, C.N. (2008). Surface uplift of Tibet and Cenozoic global cooling. *Geology*. 36, 1003–1004. <https://doi.org/10.1130/focus120003.1>
- Gibbard, P.L., Bauer, A.M., Edgeworth, M., Ruddiman, W.F., Gill, J.L., Merritts, D.J., Finney, S.C., Edwards, L.E., Walker, M.J.C., Maslin, M. and Ellis, E.C. (2021). A practical solution: the Anthropocene is a geological event, not a formal epoch. *Episodes*, <https://doi.org/10.18814/epiiugs/2021/021029>
- Gibbard, P., Walker, M., Bauer, A., Edgeworth, M., Edwards, L., Ellis, E., Finney, S., Gill, J., Maslin, M., Merritts, D. and Ruddiman, W. (2022). The Anthropocene as an Event, not an Epoch. *Journal of Quaternary Science*. <https://doi.org/10.1002/jqs.3416>
- Gibbs, S.J., Bown, P.R., Sessa, J.A. et al. (2006). Nanoplankton extinction and origination across the Paleocene-Eocene Thermal Maximum. *Science*, 314(5806), 1770–1773. <https://doi.org/10.1126/science.1133902>
- Gingerich, P.D. (2006). Environment and evolution through the Paleocene–Eocene thermal maximum. *Trends in Ecology & Evolution*, 21(5), 246–253. <https://doi.org/10.1016/j.tree.2006.03.006>
- Goldman, D., Sadler, P.M. and Leslie, S.A. (2020). Chapter 20: The Ordovician Period. In: Gradstein, F., Ogg, J., Schmitz, M. and Ogg, G. (eds.) *A Geologic Time Scale 2020*, Elsevier B.V. 631-694.

- Graven, H.D. (2015). Impact of fossil fuel emissions on atmospheric radiocarbon and various applications of radiocarbon over this century. *Proceedings of the National Academy of Sciences*, 112, 9542–9545. <https://doi.org/10.1073/pnas.1504467112>
- Graven H., Keeling, R.F. and Rogelj, J. (2020). Changes to carbon isotopes in atmospheric CO₂ over the Industrial Era and into the future. *Global Biogeochemical Cycles*, 34, e2019GB006170. <https://doi.org/10.1029/2019GB006170>
- Gulick, S.P.S., Bralower, T.J., Ormö, J. et al. (2019). The first day of the Cenozoic. *Proceedings of the National Academy of Sciences*, 116(39), 19342–19351. <https://doi.org/10.1073/pnas.1909479116>
- Haff, P.K. (2014). Technology as a geological phenomenon: Implications for human well-being. In Waters, C.N., Zalasiewicz, J.A., Williams, M., Ellis, M.A. and Snelling, A.M. (Eds.), *A stratigraphical basis for the Anthropocene*. Geological Society, London, Special Publications, 395. London, UK: Geological Society, pp. 301–309. <https://doi.org/10.1144/SP395.1>
- Haff, P.K. (2019). The Technosphere and Its Relation to the Anthropocene. In: Zalasiewicz, J, Waters, C, Williams, M. et al. (eds) *The Anthropocene as a Geological Time Unit: A Guide to the Scientific Evidence and Current Debate*. Cambridge: Cambridge University Press, pp.138–143.
- Haflidason, H., Lien, R., Sjerup, H.-P., Forsberg, C.F. and Blynn, P.K. (2005). The dating and morphometry of the Storegga Slide. *Marine and Petroleum Geology*, 22, 123–36. <https://doi.org/10.1016/j.marpetgeo.2004.10.008>
- Halverson, G., Porter, S. and Shields, G. (2020). Chapter 17: The Tonian and Cryogenian Periods. In: Gradstein, F., Ogg, J., Schmitz, M. and Ogg, G. (eds.) *A Geologic Time Scale 2020*, Elsevier B.V. 495–519.
- Han, Y.M., An, Z.S. and Cao, J.J. (2017). The Anthropocene—A potential stratigraphic definition based on black carbon, char, and soot records. In: *Encyclopedia of the Anthropocene*. Reference Module in Earth Systems and Environmental Sciences. Elsevier Science, Amsterdam <https://doi.org/10.1016/B978-0-12-109548-9.10001-6>
- Harper, D.A.T., Hammarlund, E.C. and Rasmussen, C.M.Ø. (2014). End Ordovician extinctions: A coincidence of causes. *Gondwana Research*, 25, 1294–1307. <https://doi.org/10.1016/j.gr.2012.12.021>
- Harper, D.T., Hönisch, B., Zeebe, R.E., Shaffer, G., Haynes, L.L., Thomas, E. and Zachos, J.C. (2020). The magnitude of surface ocean acidification and carbon release during Eocene Thermal Maximum 2 (ETM-2) and the Paleocene-Eocene Thermal Maximum (PETM). *Paleoceanography and Paleoclimatology*, 35(2), e2019PA003699. <https://doi.org/10.1029/2019PA003699>
- Hastings, M.G., Jarvis, J.C. and Steig, E.J. (2009). Anthropogenic impacts on nitrogen isotopes of ice-core nitrate. *Science*, 324, 1288. <https://doi.org/10.1126/science.1170510>
- Haywood, A.M., Dowsett, H.J. and Dolan, A.M. (2016). Integrating geological archives and climate models for the mid-Pliocene warm period. *Nature Communications*, 7, 10646. <https://doi.org/10.1038/ncomms10646>
- Hazen, R.M., Papineau, D., Bleeker, W. et al. (2008). Mineral evolution. *American Mineralogist*, 93, 1639–1720. <https://doi.org/10.2138/am.2008.2955>

- Hazen, R. M., Grew, E. S., Origlieri, M. J., and Downs, R. T. (2017). On the mineralogy of the “Anthropocene Epoch.” *American Mineralogist*, 102, 595–611. <https://doi.org/10.2138/am-2017-5875>
- Head, M.J., (2019). Formal subdivision of the Quaternary System/Period: Present status and future directions. *Quaternary International*, 500, 32–51. <https://doi.org/10.1016/j.quaint.2019.05.018>
- Head, M.J. (2021). Review of the Early–Middle Pleistocene boundary and Marine Isotope Stage 19. *Progress in Earth and Planetary Science*, 8:50, 1–38. <https://doi.org/10.1186/s40645-021-00439-2>
- Head, M.J., Pillans, B. and Farquhar, S. (2008). The Early–Middle Pleistocene Transition: characterization and proposed guide for the defining boundary. *Episodes* 31(2), 255–259. <https://doi.org/10.18814/epiiugs/2008/v31i2/014>
- Head, M.J., Steffen, W., Fagerlind, D., Waters, C.N., Poirier, C., Syvitski, J., Zalasiewicz, J.A., Barnosky, A.D., Cearreta, A., Jeandel, C., Leinfelder, R., McNeill, J.R., Rose, N.L., Summerhayes, C., Wagnreich, M. and Zinke, J. (2021). The Great Acceleration is real and provides a quantitative basis for the proposed Anthropocene Series/Epoch. *Episodes*. <https://doi.org/10.18814/epiiugs/2021/021031>
- Head, M.J., Zalasiewicz, J.A., Waters, C.N., Turner, S.D., Williams, M., Barnosky, A.D., Steffen, W., Wagnreich, M., Haff, P.K., Syvitski, J., Leinfelder, R., McCarthy, F.M.G., Rose, N.L., Wing, Scott, L., An, Z., Cearreta, A., Cundy, A.B., Fairchild, I.J., Han, Y., Ivar do Sul, J.A., Jeandel, C., McNeill, J.R., Summerhayes, C.P. (2022a). The Anthropocene is a prospective epoch/series, not a geological event. *Episodes*, <https://doi.org/10.18814/epiiugs/2022/022022>
- Head, M.J., Aubry, M.-P., Piller, W.E. and Walker, M. (2022b). The Standard Auxiliary Boundary Stratotype: a proposed replacement for the Auxiliary Stratotype Point in supporting a Global boundary Stratotype Section and Point (GSSP). *Episodes*, <https://doi.org/10.18814/epiiugs/2022/022012>
- Head, M.J., Zalasiewicz, J., Waters, C.N., Turner, S.D., Williams, M., Barnosky, A.D., Steffen, W., Wagnreich, M., Haff, P., Syvitski, J., Leinfelder, R., McCarthy, F.M.G., Rose, N.L., Wing, S.L., An, Z., Cearreta, A., Cundy, A.B., Fairchild, I.J., Han, Y., Ivar do Sul, J.A., Jeandel, C., McNeill, J.R., Summerhayes, C.P. (in press) The proposed Anthropocene Epoch/Series is underpinned by a rich array of mid-20th century stratigraphic event signals. *Journal of Quaternary Science*.
- Heinrich, H. (1988). Origin and consequences of cyclic ice rafting in the northeast Atlantic Ocean during the past 130,000 years. *Quaternary Research*, 29(2), 142–152. [https://doi.org/10.1016/0033-5894\(88\)90057-9](https://doi.org/10.1016/0033-5894(88)90057-9)
- Henehan, M.J., Ridgwell, A., Thomas, E., Zhang, S., Alegret, L., Schmidt, D.N., Rae, J.W.B., Witts, J.D., Landman, N.H., Greene, S.E., Huber, B.T., Super, J.R., Planavsky, N.J., Hull, P.M. (2019). Rapid ocean acidification and protracted Earth system recovery followed the end-Cretaceous Chicxulub impact. *Proceedings of the National Academy of Sciences*, 116(45), 22500–22504. <https://www.pnas.org/doi/full/10.1073/pnas.1905989116>
- Hodell, D.A., Channell, J.E.T., Curtis, J.H., Romero, O.E., Röhl, U. et al. (2008). Onset of “Hudson Strait” Heinrich events in the eastern North Atlantic at the end of the middle Pleistocene transition (640 ka)? *Paleoceanography*, 23, PA4218. <https://doi.org/10.1029/2008PA001591>
- Hoffman, P.F., Abbot, D.S., Ashkenazy, Y., Benn, D.I., Cohen, P.A., Cox, G.M., Creveling, J.R., Donnadieu, Y., Erwin, D.H., Fairchild, I.J., Ferreira, D., Goodman, J.C., Halverson, G.P., Jansen, M.F., Le Hir, G., Love, G.D., Macdonald, F.A., Maloof, A.C., Ramstein, G., Rose, B.E.J., Rose, C.V.,

- Tziperman, E., Voigt, A. and Warren, S.G. (2017). Snowball Earth climate dynamics and Cryogenian geology–geobiology. *Science Advances*, 3(11), e1600983. <https://doi.org/10.1126/sciadv.1600983>
- Holbourn, A., Kuhnt, W., Schulz, M. and Erlenkeuser, H. (2005). Impacts of orbital forcing and atmospheric carbon dioxide on Miocene ice-sheet expansion. *Nature*, 438, 483–487. <https://doi.org/10.1038/nature04123>
- Holtgrieve, G.W., Schindler, D.E., Hobbs, W.O. et al. (2011). A coherent signature of anthropogenic nitrogen deposition to remote watersheds of the northern hemisphere. *Science*, 334, 1545–1548. <https://doi.org/10.1126/science.1212267>
- Hong, S., Candelone, J.-P., Patterson, C.C. and Boutron, C.F. (1996). History of ancient copper smelting pollution during Roman and Medieval times recorded in Greenland ice. *Science*, 272, 246–249. <https://doi.org/10.1126/science.272.5259.246>
- Hua, Q., Turnbull, J.C., Santos, G.M., Rakowski, A.Z., Ancapichún, S., De Pol-Holz, R., Hammer, S., Lehman, S.J., Levin, I., Miller, J.B., Palmer, J.G. and Turney, C.S.M. (2021). Atmospheric Radiocarbon for the Period 1950–2019. *Radiocarbon*, 1–23. <https://doi.org/10.1017/rdc.2021.95>
- Hutchinson, D.K., Coxall, H.K., Lunt, D.J., Steinthorsdottir, M., de Boer, A.M., Baatsen, M., von der Heydt, A., Huber, M., Kennedy-Asser, A.T., Kunzmann, L., Laurent, J.-B., Lear, C.H., Moraweck, K., Pearson, P.N., Piga, E., Pound, M.J., Salzmann, U., Scher, H.D., Sijp, W.P., Śliwińska, K.K., Wilson, P. A. and Zhang, Z. (2021). The Eocene–Oligocene transition: a review of marine and terrestrial proxy data, models and model–data comparisons, *Climate of the Past*, 17, 269–315, <https://doi.org/10.5194/cp-17-269-2021>
- Hylander, L.D. and Meili, M. (2002). 500 years of mercury production: global annual inventory by region until 2000 and associated emissions. *The Science of the Total Environment*, 304, 13–27. [https://doi.org/10.1016/S0048-9697\(02\)00513-3](https://doi.org/10.1016/S0048-9697(02)00513-3)
- Iozza, S., Müller, C.E., Schmid, P. et al. (2003). Historical profiles of chlorinated paraffins and polychlorinated biphenyls in a dated sediment core from Lake Thun (Switzerland). *Environmental Science & Technology*, 42(4), 1045–1050. <https://doi.org/10.1021/es702383t>
- IPCC (Intergovernmental Panel on Climate Change) (2021). Summary for Policymakers. In: *Climate Change 2021: The Physical Science Basis. Contribution of Working Group I to the Sixth Assessment Report of the Intergovernmental Panel on Climate Change* [Masson-Delmotte, V., Zhai, P., Pirani, A. et al. (eds.)]. Cambridge University Press, 41pp.
- IUCN 2021. The IUCN Red List of Threatened Species. Version 2021-2. <https://www.iucnredlist.org>. Downloaded on [last accessed 26th October 2021].
- Jonkers, L., Hillebrand, H. and Kucera, M. (2019). Global change drives modern plankton communities away from the pre-industrial state. *Nature* 570(7761), 372–375. <https://doi.org/10.1038/s41586-019-1230-3>
- Kasbohm, J. and Schoene, B. (2018). Rapid eruption of the Columbia River flood basalt and correlation with the mid-Miocene climate optimum. *Science Advances*, 4, eaat8223. <https://doi.org/10.1126/sciadv.aat8223>

- Kaufman, D., McKay, N., Routsos, C., Erb, M., Dätwyler, C., Sommer, P.S., Heiri, O. and Davis, B. (2020). Holocene global mean surface temperature, a multi-method reconstruction approach. *Scientific Data*, 7, 201. <https://doi.org/10.1038/s41597-020-0530-7>
- Kelly, D.C., Bralower, T.J. and Zachos, J.C. (1998). Evolutionary consequences of the latest Paleocene thermal maximum for tropical planktonic foraminifera. *Palaeogeography, Palaeoclimatology, Palaeoecology*, 141, 139–161. [https://doi.org/10.1016/S0031-0182\(98\)00017-0](https://doi.org/10.1016/S0031-0182(98)00017-0)
- Kelly, D.C., Zachos, J.C., Bralower, T.J. and Schellenberg, S.A. (2005). Enhanced terrestrial weathering/runoff and surface ocean carbonate production during the recovery stages of the Paleocene-Eocene thermal maximum. *Paleoceanography*, 20, PA4023. <https://doi.org/10.1029/2005PA001163>
- Kender, S., Bogus, K., Pedersen, G.K., Dybkjær, K., Mather, T.A., Mariani, E., Ridgwell, A., Riding, J.B., Wagner, T., Hesselbo, S.P. and Leng, M.J. (2021). Paleocene/Eocene carbon feedbacks triggered by volcanic activity. *Nature communications*, 12(1), 1–10. <https://doi.org/10.1038/s41467-021-25536-0>
- Kennett, J.P. and Stott, L.D. (1991). Abrupt deep-sea warming, paleoceanographic changes and benthic extinctions at the end of the Paleocene. *Nature*, 352(6241), 225–229. <https://doi.org/10.1038/353225a0>
- King, M.D., Howat, I.M., Candela, S.G. et al., (2020). Dynamic ice loss from the Greenland Ice Sheet driven by sustained glacier retreat. *Communications Earth and Environment*, 1(1). <https://doi.org/10.1038/s43247-020-0001-2>
- Koch, P.L., and Barnosky, A.D. (2006). Late Oligocene extinctions: State of the debate. *Annual Review of Ecology, Evolution, and Systematics*, 37, 215–250. <https://doi.org/10.1146/annurev.ecolsys.34.011802.132415>
- Koch, P.L., Zachos, J.C. and Gingerich, F.D. (1992). Correlation between isotope records in marine and continental carbon reservoirs near the Paleocene/Eocene boundary. *Nature*, 358, 319–322. <https://doi.org/10.1038/358319a0>
- Koide, M., Goldberg, E.D., Herron, M.M. and Langway, C.C. (1977). Transuranic depositional history in South Greenland firn layers. *Nature*, 269, 137–139. <https://doi.org/10.1038/269137a0>
- Knoll, A.H., Walter, M.R., Narbonne, G.M. and Christie-Blick, N. (2006). The Ediacaran Period: a new addition to the geologic time scale. *Lethaia*, 39, 13–30. <https://doi.org/10.1080/00241160500409223>
- Kring, D.A. (2007). The Chicxulub impact event and its environmental consequences at the Cretaceous-Tertiary boundary. *Palaeogeography, Palaeoclimatology, Palaeoecology*, 255, 4–21. <https://doi.org/10.1016/j.palaeo.2007.02.037>
- Kürschner, W.M., Kvaček, Z. and Dilcher, D.L. (2008). The impact of Miocene atmospheric carbon dioxide fluctuations on climate and the evolution of terrestrial ecosystems. *Proceedings of the National Academy of Sciences*, 105, 449–453. <https://doi.org/10.1073/pnas.0708588105>
- Leckie, R.M., Bralower, T.J. and Cashman, R. (2002). Oceanic anoxic events and plankton evolution: Biotic response to tectonic forcing during the mid-Cretaceous. *Paleoceanography*, 17, 13-1–13-29: <https://doi.org/10.1029/2001PA000623>
- Leinfelder, R. and Ivar do Sul, J.A. (2019). The Stratigraphy of Plastics and Their Preservation in Geological Records. In: Zalasiewicz, J., Waters, C., Williams, M. et al. (eds) *The Anthropocene as a*

Geological Time Unit: A Guide to the Scientific Evidence and Current Debate. Cambridge: Cambridge University Press, pp. 147–155.

Lenton, T.M., Rockstrom, J., Gaffney, O., Rahmstorf, S., Richardson, K., Steffen, W. and Schellnhuber, H.J. 2019. Climate tipping points – too risky to bet against. *Nature*, 575, 592–595.

LeRoy, M.A., Gill, B.C., Sperling, E.A., McKenzie, N.R., Park, T.-K.S. et al. (2021). Variable redox conditions as an evolutionary driver? A multi-basin comparison of redox in the middle and later Cambrian oceans (Drumian-Paibian). *Palaeogeography, Palaeoclimatology, Palaeoecology*, 566, 110209. <https://doi.org/10.1016/j.palaeo.2020.110209>

Lewis, A.R., Marchant, D.R., Ashworth, A.C., Hedenäs, L., Hemming, S.R., Johnson, J.V., Leng, M.J., Machlus, M.L., Newton, A.E., Raine, J.I., Willenbring, J.K., Williams, M. and Wolfe, A.P. (2008). Mid-Miocene cooling and the extinction of tundra in continental Antarctica. *Proceedings of the National Academy of Sciences*, 105, 10676–10680. <https://doi.org/10.1073/pnas.0802501105>

Li, Y.F. and Macdonald, R.W. (2005). Sources and pathways of selected organochlorine pesticides to the Arctic and the effect of pathway divergence on HCH trends in biota: a review. *Science of the Total Environment*, 342, 87–106. <https://doi.org/10.1016/j.scitotenv.2004.12.027>

Lindström, S., van de Schootbrugge, B., Hansen, K.H., Pedersen, G.K., Alsen, P., Thibault, N., Dybkjær, K., Bjerrum, C.J. and Nielsen, L.H. (2017). A new correlation of Triassic–Jurassic boundary successions in NW Europe, Nevada and Peru, and the Central Atlantic Magmatic Province: A time-line for the end-Triassic mass extinction. *Palaeogeography, Palaeoclimatology, Palaeoecology*, 478, 80–102. <https://doi.org/10.1016/j.palaeo.2016.12.025>

Lisiecki, L.E. and Raymo, M.E. (2005). A Pliocene–Pleistocene stack of 57 globally distributed benthic $\delta^{18}\text{O}$ records. *Paleoceanography*, 20, PA1003. <https://doi.org/10.1029/2004PA001071>

Loarie, S.R., Duffy, P.B., Hamilton, H. et al. (2009). The velocity of climate change. *Nature*, 462, 1052–1055. <https://doi.org/10.1038/nature08019>

Logan, C.A., Dunne, J.P., Ryan, J.S. et al. (2021). Quantifying global potential for coral evolutionary response to climate change. *Nature Climate Change*, 11, 537–542. <https://doi.org/10.1038/s41558-021-01037-2>

Lowe, J.J., Birks, H.H., Bond, G.S.J. et al. (1999). The chronology of palaeoenvironmental changes during the last Glacial–Holocene transition: Towards an event stratigraphy for the British Isles. *Journal of the Geological Society*, 156, 397–410. <https://doi.org/10.1144/gsjgs.156.2.0397>

Lyons, S.L., Baczynski, A.A., Babila, T.L., Bralower, T.J., Hajek, E.A., Kump, L.R., et al. (2019). Palaeocene–Eocene thermal maximum prolonged by fossil carbon oxidation. *Nature Geoscience*, 12(1), 54–60. <https://doi.org/10.1038/s41561-018-0277-3>

MacFarling Meure, C., Etheridge, D.E., Trudinger, C. et al. (2006). Law Dome CO_2 , CH_4 and N_2O ice core records extended to 2000 years BP. *Geophysical Research Letters*, 33(14), L14810. <https://doi.org/10.1029/2006GL026152>

Marlon, J.R., Bartlein, P.J., Carcaillet, C., Gavin, D.G., Harrison, S.P., Higuera, P.E., Joos, F., Power, M.J. and Prentice, I.C. (2008). Climate and human influences on global biomass burning over the past two millennia. *Nature Geoscience*, 1(10), 697–702. <https://doi.org/10.1038/ngeo313>

Masson-Delmotte, V., Steen-Larsen, H.C., Ortega, P., Swingedouw, D., Popp, T., Vinther, B.M., Oerter, H., Sveinbjornsdottir, A.E., Gudlaugsdottir, H., Box, J.E., Falourd, S., Fettweis, X., Gallée, H.,

- Garnier, E., Gkinis, V., Jouzel, J., Landais, A., Minster, B., Paradis, N., Orsi, A., Risi, C., Werner M., White, J.W.C. (2015). Recent changes in north-west Greenland climate documented by NEEM shallow ice core data and simulations, and implications for past-temperature reconstructions. *The Cryosphere*, 9, 1481–1504. <https://doi.org/10.5194/tc-9-1481-2015>
- Mayewski, P.A., Lyons, W.B., Spencer, M.J., Twickler, M.S., Buck, C.F. and Whitlow, S. (1990). An ice-core record of atmospheric response to anthropogenic sulphate and nitrate. *Nature*, 346, 554–556. <https://doi.org/10.1038/346554a0>
- Meinshausen, M., Vogel, E., Nauels, A. et al. (2017). Historical greenhouse gas concentrations for climate modelling (CMIP6). *Geoscientific Model Development*, 10, 2057–2116. <https://doi.org/10.5194/gmd-10-2057-2017>
- Melchin, M.J., Sadler, P.M. and Cramer, B.D. (2020). Chapter 21: The Silurian Period. In: Gradstein, F., Ogg, J., Schmitz, M. and Ogg, G. (eds.) *A Geologic Time Scale 2020*. Elsevier B.V. 695–732.
- Methner, K., Campani, M., Fiebig, J., Löffler, N., Kempf, O. and Much, A. (2020). Middle Miocene long-term continental temperature change in and out of pace with marine climate records. *Scientific Reports*, 10, 7989. <https://doi.org/10.1038/s41598-020-64743-5>
- Miller, K.D. and Wright, J.D. (2017). Success and failure in Cenozoic global correlations using golden spikes: A geochemical and magnetostratigraphic perspective. *Episodes*, March 2017. <https://doi.org/10.18814/epiugs/2017/v40i1/017002>
- Molina, E., Alegret, L., Arenillas, I. et al., (2006). The Global Boundary Stratotype Section and Point for the base of the Danian Stage (Paleocene/Palaeogene, “Tertiary”, Cenozoic) at El Kef, Tunisia - Original definition and revision. *Episodes*, 29(1), 263–273. <https://doi.org/10.18814/epiugs/2006/v29i4/004>
- Moore, E.A., and Kurtz, A.C. (2008). Black carbon in Paleocene–Eocene boundary sediments: A test of biomass combustion as the PETM trigger. *Palaeogeography, Palaeoclimatology, Palaeoecology*, 267(1-2), 147–152. <https://doi.org/10.1016/j.palaeo.2008.06.010>
- Mosbrugger, V., Utescher, T., and Dicher, D.L. (2005). Cenozoic continental climatic evolution of Central Europe. *Proceedings of the National Academy of Sciences*, 102, 14964–14969. <https://doi.org/10.1073/pnas.0505267102>
- Mouginot, J., Rignot, E., Bjørk, A.A. et al. (2019). Forty-six years of Greenland Ice Sheet mass balance from 1972 to 2018. *Proceedings of the National Academy of Sciences*, 116, 9239–9244. <https://doi.org/10.1073/pnas.1904242116>
- Muir, D.C.G. and Rose, N.L. (2007). Persistent organic pollutants in the sediments of Lochnagar. In: (Rose, N.L., Ed.) *Lochnagar: The Natural History of a Mountain Lake*, *Developments in Paleoenvironmental Research*. Dordrecht: Springer, 375–402.
- Murphy, B.H., Farley, K.A. and Zachos, J.C. (2010). An extraterrestrial ³He-based timescale for the Paleocene-Eocene thermal maximum (PETM) from Walvis Ridge, IODP Site 1266. *Geochimica et Cosmochimica Acta*, 74, 5098–5108. <https://doi.org/10.1016/j.gca.2010.03.039>
- North American Commission on Stratigraphic Nomenclature (NACSN) (2005). *North American Stratigraphic Code*. *American Association of Petroleum Geologists Bulletin*, 89, 1547–1591. <https://doi.org/10.1306/07050504129>

- Novakov, T., Ramanathan, V., Hansen, J.E. et al. (2003). Large historical changes of fossil-fuel black carbon aerosols. *Geophysical Research Letters*, 30(6), 1324, 57-1–57-4. <https://doi.org/10.1029/2002GL016345>
- Nriagu, J.O. (1996). A history of global metal pollution. *Science*, 272, 5259, 223–224. <https://doi.org/10.1126/science.272.5259.223>
- Ogg, J.G. (2020). Geomagnetic Polarity Time Scale. Chapter 5. In Gradstein, F.M., Ogg, J.G., Schmitz, M. and Ogg, G. (eds) *A Geological Time Scale 2012*. Elsevier, p. 159–192.
- Onac, B.C., Mitrovica, J.X., Jinés, J., Asmerom, Y., Polyak, V.J., Tuccimei, P., Ashe, E.L., Fornós, J.J., Hoggard, M.J., Couson, S., Ginés, A., Soligo, M. and Villa, I.M. (2022). Exceptionally stable preindustrial sea level inferred from the western Mediterranean Sea. *Science Advances*, 8, eabm6185. <https://doi.org/10.1126/sciadv.abm6185>
- Osterberg, E., Mayewski, P., Kreutz, K., Fisher, D., Handley, M., Sneed, S., Zdanowicz, C., Zheng, J., Demuth, M., Waskiewicz, M. and Bourgeois, J. (2008). Ice core record of rising lead pollution in the North Pacific atmosphere. *Geophysical Research Letters*, 35, L03817. <https://doi.org/10.1029/2007GL032680>
- Pabortsava, K. and Lampitt, R.S. (2020). High concentrations of plastic hidden beneath the surface of the Atlantic Ocean. *Nature Communications*, 11, 4073. <https://doi.org/10.1038/s41467-020-17932-9>
- Pandolfi, J.M. (2015). Incorporating uncertainty in predicting the future response of coral reefs to climate change. *Annual Review of Ecology, Evolution, and Systematics*, 46, 281–303. <https://doi.org/10.1146/annurev-ecolsys-12-02-2015-091811>
- Parmesan, C. (2006). Ecological and evolutionary responses to recent climate change. *Annual Review of Ecology, Evolution, and Systematics*, 37, 637–669. <https://doi.org/10.1146/annurev.ecolsys.37.091305.110100>
- Pawlik, L., Buma, B., Šamonil, P., Kvíček, I., Gałazka, A., Kohout, P., and Malik, I. (2020). Impact of trees and forests on the Devonian landscape and weathering processes with implications to the global Earth's system properties – A critical review. *Earth-Science Reviews*, 205, 103200. <https://doi.org/10.1016/j.earscirev.2020.103200>
- Pedro, J.B., Jochum, M., Rutter, C., He, F., Barker, S., and Rasmussen, S.O. (2018). Beyond the bipolar seesaw: Toward a process understanding of interhemispheric coupling. *Quaternary Science Reviews*, 192, 27–46. <https://doi.org/10.1016/j.quascirev.2018.05.005>
- Peng, S.C., Babcock, L.E. and Ahlberg, P. (2020). Chapter 19: The Cambrian Period. In: Gradstein, F., Ogg, J., Schmitz, M. and Ogg, G. (eds.) *A Geologic Time Scale 2020*, Elsevier B.V. 565–629.
- Penman, D.E. and Zachos, J.C. (2018). New constraints on massive carbon release and recovery processes during the Paleocene-Eocene Thermal Maximum. *Environmental Research Letters*, 13(10), 105008. <https://doi.org/10.1088/1748-9326/aae285>
- Penman, D.E., Hönisch, B., Zeebe, R.E. et al. (2014). Rapid and sustained ocean acidification during the Paleocene-Eocene Thermal Maximum. *Paleoceanography*, 29, 357–369. <https://doi.org/10.1002/2014PA002621>
- Pimm, S.L., Jenkins, C.N., Abell, R., Brooks, T.M., Gittleman, J.L., Joppa, L.N., Raven, P.H., Roberts, C.M. and Sexton, J.O. (2014). The biodiversity of species and their rates of extinction, distribution, and protection. *Science*, 344, 1246752. <https://doi.org/10.1126/science.1246752>

- Poulton, S.W., Bekker, A., Cumming, V.M., Zerkle, A.L., Canfield, D.E. and Johnston, D.T. (2021). A 200-million-year delay in permanent atmospheric oxygenation. *Nature*, 592, 232–236. <https://doi.org/10.1038/s41586-021-03393-7>
- Power, M.J., Marlon, J., Ortiz, N., Bartlein, P.J., Harrison, S.P., Mayle, F.E., Ballouche, A., Bradshaw, R.H., Carcaillet, C., Cordova, C. and Mooney, S. (2008). Changes in fire regimes since the Last Glacial Maximum: an assessment based on a global synthesis and analysis of charcoal data. *Climate dynamics*, 30(7-8), 887–907. <https://doi.org/10.1007/s00382-007-0334-x>
- Prave, A.R. Kirsimäe, K., Lepland, A., Fallick, A.E., Kreitsmann, T., Deines, Y.E., Romashkin, A.E., Rychanchik, D.V., Medvedev, P.V., Moussavou, M., Bakakas, K. and Hodgskiss, M.S.W. (2022). The grandest of them all: the Lomagundi–Jatuli Event and Earth's oxygenation. *Journal of the Geological Society*, 179(1):jgs2021-036. <http://dx.doi.org/10.1144/jgs2021-036>
- Rae, J.W.B., Zhang, Y.G., Liu, X., Foster, G.L., Stoll, H.M. and Whiteford, R.D.M. (2021). Atmospheric CO₂ over the Past 66 Million Years from Marine Archives. *Annual Review of Earth and Planetary Sciences*, 49, 609–641. <https://doi.org/10.1146/annurev-earth-082120-063026>
- Rasmussen, S.O., Bigler, M., Blockley, S.P., Blunier, T., Buchardt, S.L., Clausen, H.B., Cvijanovic, I., Dahl-Jensen, D., Johnsen, S.J., Fischer, H., Gkinis, V., Guillevic, L., Hoek, W.Z., Lowe, J.J., Pedro, J.B., Popp, T., Seierstad, I.K., Steffensen, J.P., Svensson, A.M., Vallelonga, P., Vinther, B.M., Walker, M.J.C., Wheatley, J.J. and Winstrup, M. (2014). A stratigraphic framework for abrupt climatic changes during the Last Glacial period based on three synchronized Greenland ice-core records: refining and extending the INTIMATE event stratigraphy. *Quaternary Science Review*, 106, 14–28. <https://doi.org/10.1016/j.quascirev.2014.09.001>
- Rawson, P.F., Allen, P.M., Bevins, R.E., Brenckle, P.J., Cope, J.C.W., Evans, J.A., Gale, A.S., Gibbard, P.L., Gregory, F.J., Hesselbo, S.P., Marshall, J.E.A., Knox, R.W.O.B., Oates, M.J., Riley, N.J., Rushton, A.W.A., Smith, A.G., Trewin, N.H. and Zalasiewicz, J.A. (2002). *Stratigraphical Procedure*. Geological Society, London, Professional Handbook, pp. 57.
- Renne, P.R., Deino, A.L., Hilgen, F.J., Kiper, K.F., Mark, D.F., Mitchell III, W.S., Morgan, L.E., Mundil, R., Smit, J., 2013. Time scales of critical events around the Cretaceous–Paleogene boundary. *Science*, 339, 684–687. <http://dx.doi.org/10.1126/science.1230492>
- Robinson, M.M., and Spivey, W.E. (2019). Environmental and geomorphological changes on the eastern North American continental shelf across the Paleocene–Eocene boundary. *Paleoceanography and Paleoclimatology*, 34(4), 715–732. <https://doi.org/10.1029/2018PA003357>
- Rohde, R.A. and Muller, R.A. (2005). Cycles in fossil diversity. *Nature*, 434, 208–210. <https://doi.org/10.1038/nature03339>
- Röhl, U., Westerhold, T., Bralower, T.J. and Zachos J.C. (2007). On the duration of the Paleocene–Eocene thermal maximum (PETM). *Geochemistry, Geophysics, Geosystems*, 8(12), Q12002. <https://doi.org/10.1029/2007GC001784>
- Rose, N.L. (2015). Spheroidal carbonaceous fly-ash particles provide a globally synchronous stratigraphic marker for the Anthropocene. *Environmental Science & Technology*, 49, 4155–4162. <https://doi.org/10.1021/acs.est.5b00543>
- Rubino, M., Etheridge, D.M., Trudinger, C.M. et al. (2013). A revised 1000 year atmospheric $\delta^{13}\text{C}$ -CO₂ record from Law Dome and South Pole, Antarctica. *Journal of Geophysical Research*, 118, 8482–8499. <https://doi.org/10.1002/jgrd.50668>

- Ruddiman, W.F., He, F., Vavrus, S.J. and Kutzbach, J.E. (2020). The early anthropogenic hypothesis: A review. *Quaternary Science Reviews*, 240, 106386. <https://doi.org/10.1016/j.quascirev.2020.106386>
- Ruddiman, W.F. (2018). Three flaws in defining a formal 'Anthropocene'. *Progress in Physical Geography: Earth and Environment*, 42(4), 451–461. <https://doi.org/10.1177/0309133318783142>
- Rush, W.D., Kiehl, J.T., Shields, C.A. and Zachos, J.C. (2021). Increased frequency of extreme precipitation events in the North Atlantic during the PETM: Observations and theory. *Palaeogeography, Palaeoclimatology, Palaeoecology*, 568, 110289. <https://doi.org/10.1016/j.palaeo.2021.110289>
- Salvador, A. (1994). *International Stratigraphic Guide. A Guide to Stratigraphic classification, terminology, and Procedure*. The International Union of Geological Sciences and the Geological Society of America. 2nd Edition.
- Sandom, C., Faurby, S., Sandel, B. and Svenning, J.-C. (2014). Global late Quaternary megafauna extinctions linked to humans, not climate change. *Proceedings of the Royal Society*, B281, 20133254. <https://doi.org/10.1098/rspb.2013.3254>
- Sano, S. (2003). Cretaceous oceanic anoxic events and their relations to carbonate platform drowning episodes. *Fossils*, 74, 20-26. [in Japanese].
- Schlanger, S.O. and Jenkyns, H.C. (1976). Cretaceous oceanic anoxic events: causes and consequences. *Geologie en Mijnbouw*, 55, 179–184
- Schmitz, B. and Pujalte, V. (2007). Abrupt increase in seasonal extreme precipitation at the Paleocene-Eocene boundary. *Geology*, 35(3), 215–218. <https://doi.org/10.1130/G23261A.1>
- Schulte, P., Alegret, L., Arenillas, I. et al. (2010). The Chicxulub asteroid impact and mass extinction at the Cretaceous-Paleogene boundary. *Science*, 327, 1214–1218. <https://doi.org/10.1126/science.1177261>
- Secord, R., Bloch, J.I., Chester, S.G., Dwyer, D.M., Wood, A.R., Wing, S.L., Kraus, M.J., McInerney, F.A. and Krigbaum, J. (2012). Evolution of the earliest horses driven by climate change in the Paleocene-Eocene Thermal Maximum. *Science*, 335(6071), 959–962. <https://doi.org/10.1126/science.1213859>
- Seebens, H., Blackburn, T.M., Dyer, E.E., Genovesi, P., Hulme, P.E., Jeschke, J.M., Pagad, S. and 38 others (2018). No saturation in the accumulation of alien species worldwide. *Nature Communications*, 8, 14435. <https://doi.org/10.1038/ncomms14435>
- Servais, T. and Harper, D.A.T. (2018). The Great Ordovician Biodiversification Event (GOBE): definition, concept and duration. *Lethaia*, 51, 151–164. <https://doi.org/10.1111/let.12259>
- Servais, T., Cascales-Miñana, B. and Harper, D.A.T. (2021). The Great Ordovician Biodiversification Event (GOBE) is not a single event. *Paleontological Research*, 25(4), 315–328. <https://doi.org/10.2517/2021PR001>
- Shevenell, A.E. (2016). Drilling and modelling studies expose Antarctica's Miocene secrets. *Proceedings of the National Academy of Sciences*, 113, 3419–3421. <https://doi.org/10.1073/pnas.1601789113>
- Shields, G.A., Strachan, R.A., Porter, S.M. et al. (2021). A template for an improved rock-based subdivision of the pre-Cryogenian timescale. *Journal of the Geological Society*, 179. <https://doi.org/10.1144/jgs2020-222>

Formal ratification of the Global Boundary Stratotype Section and Point (GSSP) for the Chibanian Stage and Middle Pleistocene Subseries of the Quaternary System: the Chiba Section, Japan. *Episodes* 44(3), 317–347. <https://doi.org/10.18814/epiiugs/2020/020080>

Syvitski, J., Waters, C.N., Day, J., Milliman, J.D., Summerhayes, C., Steffen, W., Zalasiewicz, J., Cearreta, A., Gałuszka, A., Hajdas, I., Head, M.J., Leinfelder, R., McNeill, J.R., Poirier, C., Rose, N.L., Shotyk, W., Wagnreich, M. and Williams, M., (2020). Extraordinary human energy consumption and resultant geological impacts beginning around 1950 CE initiated the proposed Anthropocene Epoch. *Communications Earth & Environment*, 1, 32, <https://doi.org/10.1038/s43247-020-00029-y>

Syvitski, J., Restrepo Angel, J., Saito, Y., Overeem, I., Vörösmarty, C., Wang, H. and Olago, D. (2022). Earth's sediment budget during the Anthropocene. *Nature Reviews Earth & Environment*, 3, 179–196. <https://www.nature.com/articles/s43017-021-00253-w>

Thomas, E. (1989). Development of Cenozoic deep-sea benthic foraminiferal faunas in Antarctic waters. In: Crame, J.A., ed., *Origins and Evolution of the Antarctic Flora*. Geological Society Special Publication, 47, 283–296. <https://doi.org/10.1144/GSL.SP.1989.047.01.21>

Thomas, E. (2003). Benthic foraminiferal record across the Initial Eocene Thermal Maximum, Southern Ocean Site 690. Causes and consequences of globally warm climates in the Early Paleogene. *Geological Society of America Special Paper*, 369, 19–331.

Tittensor, D.P., Novaglio, C., Harrison, C.S. et al. (2021). Next-generation ensemble projections reveal higher climate risks for marine ecosystems. *Natural Climate Change*, 11, 973–981. <https://doi.org/10.1038/s41558-021-01173-9>

Vandenbergh, N., Hilgen, F.J. and Speijer, R. (2012). The Paleogene Period. Chapter 28. In Gradstein, F.M., Ogg, J.G., Schmitz, M. and Ogg, G. (eds) *A Geological Time Scale 2012*. Elsevier, p. 853–922.

van der Meulen, B., Gingerich, P.D., Leirich, L.J., Meijer, N., van Broekhuizen, S., van Ginneken, S., and Abels, H.A. (2020). Carbon isotope and mammal recovery from extreme greenhouse warming at the Paleocene–Eocene boundary in astronomically-calibrated fluvial strata, Bighorn Basin, Wyoming, USA. *Earth and Planetary Science Letters*, 534, 116044. <https://doi.org/10.1016/j.epsl.2019.116044>

Van Kranendonk, M.J., Alt, J.M., et al. (2012). A chronostratigraphic division of the Precambrian: possibilities and challenges. In: Gradstein, F.M., Ogg, J.G., Schmitz, M. and Ogg, G. (eds). *The Geologic Time Scale 2012*. Elsevier, 299–392.

Viglietti, P.A., Benson, R.E.J., Smith, R.M.H., Botha, J., Kammerer, C.F., Skosan, Z. and 17 others. (2021). Evidence from South Africa for a protracted end-Permian extinction on land. *Proceedings of the National Academy of Sciences*, 118, e2017045118. <https://doi.org/10.1073/pnas.2017045118>

Vinther, B., Clausen, H.B., Johnsen, S.J., Rasmussen, S.O., Andersen, K.K., Buchardt, S.L., Dahl-Jensen, D., Seierstad, I.K., Siggard-Andersen, M.-L., Steffensen, J.P., Svensson, A., Olsen, J. and Heinemeier, J. (2006). A synchronised dating of three Greenland ice cores throughout the Holocene. *Journal of Geophysical Research*, v. 111, D13102. <https://doi.org/10.1029/2005JD006921>

Wagnreich, M. and Draganits, E. (2018). Early mining and smelting lead anomalies in geological archives as potential stratigraphic markers for the base of an early Anthropocene. *The Anthropocene Review*, 5(2), 177–201. <https://doi.org/10.1177/2053019618756682>

Walker, B. and Salt, D. (2006). Resilience thinking: Sustaining ecosystems and people in a changing world. Island Press: Washington, Covelo, London, pp. 174.

Walker, M.J.C., Björck, S., Lowe, J.J., Cwynar, L.C., Johnsen, S., Knudsen, K.-L., Wohlfarth, B., INTIMATE group (1999). Isotopic 'events' in the GRIP ice core: a stratotype for the Late Pleistocene. *Quaternary Science Reviews*, 18, 1143–1150. [https://doi.org/10.1016/S0277-3791\(99\)00023-2](https://doi.org/10.1016/S0277-3791(99)00023-2)

Walker, M., Johnsen, S., Rasmussen, S.O., Popp, T., Steffensen, J.-P., Gibbard, P., Hoek, W., Lowe, J., Andrews, J., Björck, S., Cwynar, L.C., Hughen, K., Kershaw, P., Kromer, B., Litt, T., Lowe, D.J., Nakagawa, T., Newnham, R. and Schwander, J. (2009). Formal definition and dating of the GSSP (Global Stratotype Section and Point) for the base of the Holocene using the Greenland NGRIP ice core, and selected auxiliary records. *Journal of Quaternary Science*, 24, 3–17. <https://doi.org/10.1002/jqs.1227>

Walker, M., Head, M.J., Berkelhammer, M., Björck, S., Cheng, H., Cwynar, L., Fisher, D., Gkinis, V., Long, A., Lowe, J., Newnham, R., Rasmussen, S. and Weiss, H. (2015). Formal ratification of the subdivision of the Holocene Series/Epoch (Quaternary System/Period): two new Global Boundary Stratotype Sections and Points (GSSPs) and three new stages/subseries. *Episodes*, 41(4), 213–223. <https://doi.org/10.18814/epiiugs/2018/018016>

Walker, M., Head, M.J., Berkelhammer, M., Björck, S., Cheng, H., Cwynar, L., Fisher, D., Gkinis, V., Long, A., Lowe, J., Newnham, R., Rasmussen, S. and Weiss, H. (2019). Subdividing the Holocene Series/Epoch: formalisation of stages/ages and subseries/subepochs, and designation of GSSPs and auxiliary stratotypes. *Journal of Quaternary Science*, 34, 173–186. <https://doi.org/10.1002/jqs.3097>

Waters, C.N., Zalasiewicz, J., Summerhayes, C., Farnosky, A.D., Poirier, C., Gałuszka, A., Cearreta, A., Edgeworth, M., Ellis, E.C., Ellis, M., Jeandel, C., Leinfelder, R., McNeill, J.R., Richter, D. deB., Steffen, W., Syvitski, J., Vidas, D., Wagreich, M., Williams, M., An Zhisheng, Grinevald, J., Odada, E., Oreskes, N. and Wolfe, A.P., (2016). The Anthropocene is functionally and stratigraphically distinct from the Holocene. *Science*. 351(6269), 137. <http://doi.org/10.1126/science.aad2622>

Waters, C.N., Zalasiewicz, J., Summerhayes, C., Fairchild, I.J., Rose, N.L., Loader, N.J., Shotyk, W., Cearreta, A., Head, M.J., Syvitski, J.P.M., Williams, M., Wagreich, M., Barnosky, A.D., An, Z., Leinfelder, R., Jeandel, C., Gałuszka, A., Ivar do Sul, J., Gradstein, F., Steffen, W., McNeill, J.R., Wing, S., Poirier, C. and Edgeworth, M., (2018). Global Boundary Stratotype Section and Point (GSSP) for the Anthropocene Series. Where and how to look for potential candidates. *Earth-Science Reviews*, 178, 379-429. <https://doi.org/10.1016/j.earscirev.2017.12.016>

Webby, B.D. (2004). Introduction. In Webby, B.D., Paris, F., Droser, M.L. and Percival, I.G. (eds): *The Great Ordovician Biodiversification Event*, 1–37. Columbia University Press, New York.

Wei, S., Wang, Y., Lam, J.C. et al. (2008). Historical trends of organic pollutants in sediment cores from Hong Kong. *Marine Pollution Bulletin*, 57(6), 758–766. <https://doi.org/10.1016/j.marpolbul.2008.03.008>

Wellman, C.H. 2010. The invasion of the land by plants: when and where? *New Phytologist*, 188, 306–309. <https://www.jstor.org/stable/40927865>

Willeit, M., Ganopolski, A., Calov, R., Robinson, A. and Maslin, M. (2015). The role of CO₂ decline for the onset of Northern Hemisphere glaciation. *Quaternary Science Reviews*, 119, 22–34. <https://doi.org/10.1016/j.quascirev.2015.04.015>

- Williams, M., Zalasiewicz, J., Waters, C.N. et al. (2016). The Anthropocene: a conspicuous stratigraphical signal of anthropogenic changes in production and consumption across the biosphere. *Earth's Future*, 4, 34–53. <https://doi.org/10.1002/2015EF000339>
- Williams, M., Leinfelder, R., Barnosky, A.D., Head, M.J., McCarthy, F.M.G., Cearreta, A., Himson, S., Holmes, R., Waters, C.N., Zalasiewicz, J., Turner, S., McGann, M., Hadly, E.A., Stegner, M.A., Pilkington, P.M., Kaiser, J., Berrio, J.C., Wilkinson, I.P., Zinke, J. and DeLong, K.L. (2022). Planetary-scale change to the biosphere signalled by global species translocations can be used to identify the Anthropocene. *Palaeontology*, e12618.
- Wing, S.L. and Currano, E.D. (2013). Plant response to a global greenhouse 56 million years ago. *American Journal of Botany*, 100, 1234–1254. <https://doi.org/10.3732/ajb.1200554>
- WWF 2020. Living Planet Report 2020. <https://www.worldwildlife.org/publications/living-planet-report-2020>
- Yamano, H., Sugihara, K. and Nomura, K. (2011). Rapid poleward range expansion of tropical reef corals in response to rising sea surface temperatures. *Geophysical Research Letters*, 38, L04601, <https://doi.org/10.1029/2010GL046474>
- Yang, X.-Q., Li, Z., Gao, B. and Zhou, Y.-Q. (2021). The Carbonium Drumian carbon isotope excursion (DICE) in the Keping area of the northwestern Tarim Basin, NW China. *Palaeogeography, Palaeoclimatology, Palaeoecology*, 571, 110385. <https://doi.org/10.1016/j.palaeo.2021.110385>
- Zachos, J.C., Lohmann, K.C., Walker, J.C.G. and Wise, S.W. (1993). Abrupt climate change and transient climates during the Paleogene: A marine perspective. *The Journal of Geology*, 101(2), 100th Anniversary Symposium: Evolution of the Earth's Surface, 191–213. <http://www.jstor.org/stable/30081147>
- Zachos, J.C., Röhl, U., Schellenberg, S.A. et al. (2005). Rapid acidification of the ocean during the Paleocene–Eocene thermal maximum. *Science*, 308, 1611–1611. <https://doi.org/10.1126/science.1119004>
- Zachos, J.C., Schouten, S., Bohaty, S., Quattlebaum, T., Sluijs, A., Brinkhuis, H., Gibbs, S.J., and Bralower, T.J. (2006). Extreme warming of mid-latitude coastal ocean during the Paleocene-Eocene Thermal Maximum: Inferences from TEX₈₆ and isotope data. *Geology*, 34, 737–740. <https://doi.org/10.1130/G22522.1>
- Zachos, J.C., Dickens, G.R. and Zeebe, R.E. (2008). An early Cenozoic perspective on greenhouse warming and carbon-cycle dynamics. *Nature*, 451, 279–283. <https://doi.org/10.1038/nature06588>
- Zalasiewicz, J., Waters, C.N., Williams, M., Barnosky, A., Cearreta, A., Crutzen, P., Ellis, E., Ellis, M.A., Fairchild, I.J., Grinevald, J., Haff, P.K., Hajdas, I., Leinfelder, R., McNeill, J., Odada, E.O., Poirier, C., Richter, D., Steffen, W., Summerhayes, C., Syvitski, J.P.M., Vidas, D., Wagemann, M., Wing, S.L., Wolfe, A.P., Zhisheng, A. and Oreskes, N., (2015). When did the Anthropocene begin? A mid-twentieth century boundary level is stratigraphically optimal. *Quaternary International*. 383, 196–203. <https://doi.org/10.1016/j.quaint.2014.11.045>
- Zalasiewicz, J., Waters, C.N., Summerhayes, C., Wolfe, A.P., Barnosky, A.D., Cearreta, A., Crutzen, P., Ellis, E.C., Fairchild, I.J., Gąsuzka, A., Haff, P., Hajdas, I., Head, M.J., Ivar do Sul, J., Jeandel, C., Leinfelder, R., McNeill, J.R., Neal, C., Odada, E., Oreskes, N., Steffen, W., Syvitski, J.P.M., Wagemann, M., Williams, M., (2017). The Working Group on the 'Anthropocene': Summary of evidence and recommendations. *Anthropocene*. 19, 55–60. <https://doi.org/10.1016/j.ancene.2017.09.001>

Zalasiewicz, J., Waters, C.N., Head, M.J., Poirier, C., Summerhayes, C.P., Leinfelder, R., Grinevald, J., Steffen, W., Syvitski, J.P.M., Haff, P., McNeill, J.R., Wagnreich, M., Fairchild, I.J., Richter, D.D., Vidas, D., Williams, M., Barnosky, A.D., Cearreta, A. (2019a). A formal Anthropocene is compatible with but distinct from its diachronous anthropogenic counterparts: a response to WF Ruddiman's 'three flaws in defining a formal Anthropocene'. *Progress in Physical Geography*, 43(3), 319–333. <https://doi.org/10.1177/0309133319832607>

Zalasiewicz, J., Summerhayes, C.P., Head, M.J. et al. (2019b). Stratigraphy and the Geological Time Scale. In: Zalasiewicz, J., Waters, C.N., Williams, M., Summerhayes, C. (editors). *The Anthropocene as a Geological Time Unit: A Guide to the Scientific Evidence and Current Debate*. Cambridge University Press, 11–31.

Zalasiewicz, J., Gabbott, S.E. and Waters C.N. (2019c). Chapter 23: Plastic Waste: how plastic has become part of the Earth's geological cycle. In: Letcher, T.M. and Valero, D.A. (eds.) *Waste: A Handbook for Management*, 2nd edition. Elsevier, New York, 443–452. ISBN: 9780128150603.

Zalasiewicz, J., Waters, C. and Williams, M. (2020). Chapter 31: The Anthropocene. In: Gradstein, F., Ogg, J., Schmitz, M. and Ogg, G. (eds.) *A Geologic Time Scale 2020*, Elsevier B.V. 1257–1280.

Zeebe, R.E., Zachos, J.C. and Dickens, G.R. (2009). Carbon dioxide forcing alone insufficient to explain Palaeocene–Eocene Thermal Maximum warming. *Nature Geoscience*, 2(8), 576–580. <https://doi.org/10.1038/ngeo578>

Zeebe, R.E., Dickens, G.R., Ridgwell, A. et al. (2014). Onset of carbon isotope excursion at the Paleocene-Eocene thermal maximum took millennia, not 13 years. *Proceedings of the National Academy of Sciences*, 111, E1062–E1063. <https://doi.org/10.1073/pnas.1321177111>

Zeebe, R.E., Ridgwell, A., and Zachos, J. C. (2016). Anthropogenic carbon release rate unprecedented during the past 66 million years. *Nature Geoscience*, 9, 325–329. <https://doi.org/10.1038/ngeo2681>

Zhou, C., Huyskens, M.H., Lang, X., Xiao, S. and Yin, Q.-Z. (2019). Calibrating the terminations of Cryogenian global glaciations. *Geology*, 47, 251–254. <https://doi.org/10.1130/G45719.1>